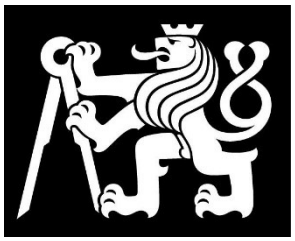

CZECH TECHNICAL UNIVERSITY IN PRAGUE

Faculty of Mechanical Engineering

Department of Automotive, Combustion Engine and Railway Engineering

Dog Clutch Without Angular Backlash

DISSERTATION THESIS
2023

Ing. Michal JASNÝ

Program:	P2301 Mechanical Engineering
Specialization:	2302V004 Machines and Equipment for Transportation
Supervisor:	doc. Dr. Ing. Gabriela Achtenová

Abstract

Dog clutches are simple and inexpensive mechanisms for shifting gears. However, their usage in automotive gearboxes was limited due to angular backlash in the engaged state and the resulting discomfort.

Based on a thorough research of existing solutions, a new and unique design of a dog clutch without angular backlash was developed and later patented. The angular backlash is minimized due to the purely mechanical blocking mechanism. The new dog clutch is interchangeable with conventional gearshift mechanisms without additional modifications and requires an external synchronization system.

The design of the new dog clutch with blocking mechanism is described in detail with a focus on the innovative parts – gearshift dogs and the blocking mechanism. Adaptation for sequential shifting was carried out and the clutch was complemented by a design and simulation program.

Two prototypes of the clutch were manufactured in cooperation with an industrial partner and verified on the test bench inside a gearbox. These prototypes were tested for functionality, service life, and comfort during gearshift. The test bench had to be significantly modified and updated to make these tests possible.

The verification was judged successful. The dog clutch with blocking mechanism is suitable for shifting gears in automotive gearboxes, in particular of hybrid and electric vehicles equipped with electric motor. It is able to eliminate some shortcomings of conventional dog clutches, as described in the research part.

Keywords

Dog clutch; Angular backlash; Blocking mechanism; Gearbox; External synchronization; Gearshift; Prototype; Test bench.

Declaration

I declare that this thesis has been composed solely by myself and that it has not been submitted, in whole or in part, to any previous application for a degree. Except where stated otherwise by reference or acknowledgment, the work presented is entirely my own.

Prague, April 2023

……

Ing. Michal Jasný

Acknowledgment

I would like to express my gratitude to the following institutions and projects that generously supported my research:

- **Grant Agency of the Czech Technical University in Prague**, grant No. SGS19/160/OHK2/3T/
- **Technological Agency, Czech Republic**, program Centres of Competence, project No. TE01020020 Josef Bozek Competence Centre for Automotive Industry and program National Competence Centres, project No. TN01000026 Josef Bozek National Center of Competence for Surface Vehicles
- **Ministry of Education, Youth and Sports,** program NPU I (LO), project No. LO1311 Development of Vehicle Centre of Sustainable Mobility
- **ŠKODA AUTO a.s.**, for the provided gearboxes and components for testing, technical consultation regarding the dog clutch design and financing the prototypes.
- **University of West Bohemia, Faculty of Applied Sciences**, for cooperation on the gearshift simulation model.

I also would like to thank sincerely all my superiors and colleagues who helped me during my work and studies, especially:

- **doc. Dr. Ing. Gabriela Achtenová** – my supervisor, for supporting me during my studies at CTU in Prague whenever necessary and supervising my bachelors, diploma, and dissertation theses.
- **Ing. Jiří Pakosta, Ph.D.** – my colleague and consultant at CTU in Prague, for extensive help with measurements in laboratories and willingness to answer all my questions.
- **Ing. Bohuslav Novotný** – former head of the Department of Gearbox Development at ŠKODA AUTO a.s., for countless consultations and valuable advice regarding the dog clutch design and manufacturing.
- **Ing. Martin Kovář** – my former student and later colleague at CTU in Prague, for productive and successful cooperation on development of the LabVIEW control system for inertia test bench.

A huge thanks also goes to my mom for regularly baking the best cookies in the world for me and my dad for performing the food delivery service, my friends for occasionally asking me when will I finish my studies and, therefore, pushing me into proceeding with my work even in situations I was generally not feeling as willing to do so, and finally my flat-mates in our community for nodding their head in approval whenever I proudly announced further progress in writing the thesis.

Table of Contents

Abstract ..... **III**
Keywords ..... **III**
Declaration ..... **IV**
Acknowledgment ..... **V**
Table of Contents ..... **VI**
Abbreviations and Nomenclature ..... **VIII**
1 Introduction and Motivation **1**
2 Current State of Knowledge **3**
2.1 Gearshift Mechanisms 3
2.1.1 Sliding Gear *3*
2.1.2 Synchronizer *4*
2.1.3 Dog Clutch *8*
2.1.4 Hollow Shaft Gearshift Mechanism *12*
2.2 Dog Clutch Design Examples 14
2.2.1 Dog Clutch without Backlash – 1930 Patent *14*
2.2.2 Aisin Dog Clutch *16*
2.2.3 Zeroshift *16*
2.2.4 Dog Clutch with Rectangular Dogs – 2012 Patent *18*
2.2.5 Dog Clutch with Cradles – 2015 Patent *19*
2.2.6 Dog Clutches Developed or Tested at CTU in Prague *20*
2.3 Dog Clutches in Passenger Car Gearboxes 29
2.3.1 Dedicated Hybrid Transmissions *29*
2.3.2 Transmissions for EVs *32*
2.3.3 Automatic Transmissions *33*
3 Objectives **34**
4 Solution **35**
4.1 Initial Design of Dog Clutch With Blocking Mechanism 35
4.1.1 Improvement Potential in Design *36*
4.1.2 Improvement Potential in Testing *37*
4.2 Final Design of Dog Clutch With Blocking Mechanism 37
4.2.1 Dog Clutch Design and Improvements *38*
4.2.2 Program for Parametric Design *42*
4.2.3 Gearshift Dogs *43*
4.2.4 Blocking Ring *52*
4.2.5 Prototypes of the Clutch *59*
4.2.6 Gearshift Simulation Model *60*
4.3 Adaptation for Sequential Shifting 63
4.3.1 Additional Flexible Elements *63*
4.3.2 Gearshift Simulation *66*

5 Verification 68
5.1 Inertia Test Bench 68
5.1.1 Initial State of the Test Bench 68
5.1.2 Adding External Synchronization 69
5.1.3 New Control System 71
5.2 Functionality 74
5.2.1 Assembly 74
5.2.2 Gearshift Force 75
5.2.3 Shifting Gears 76
5.2.4 Torque Load 78
5.3 Service Life 79
5.4 NVH and Comfort 81
5.4.1 Test Bench Setup 81
5.4.2 Vibration Measurement 84
5.4.3 Noise Measurement 86
5.4.4 Determining Input Parameters Range 86
5.4.5 Results 90
6 Consequences for Science and Industry 94
6.1 Gearbox Test Bench with External Synchronization and Clutch Control 94
6.2 Gearshift Mechanism without Angular Backlash 94
6.3 Gearshift Mechanism for Gearboxes with External Synchronization 95
6.4 Tools for Design and Simulation of the Gearshift Mechanism 95
7 Conclusion and Future Work 96
8 Bibliography 98
8.1 Sources Cited in the Thesis 98
8.2 Author's Patents and Publications Cited in the Thesis 103
8.3 Other Author's Publications 104
List of Figures 104
List of Tables 107
List of Attachments 108
List of Used Software 108
Download Links 108

Abbreviations and Nomenclature

All the abbreviations and symbols used in the thesis are listed below.

Table 1: Abbreviations used in the thesis

AMT	Automated Manual Transmission	HAMT	Hybrid Automated Manual Transmission
AT	Automatic Transmission	HEV	Hybrid Electric Vehicle
CV	Constant Velocity	ICE	Internal Combustion Engine
CAD	Computer Aided Design	MHEV	Mild Hybrid Electric Vehicle
CVT	Continuously Variable Transmission	MT	Manual Transmission
DCT	Dual Clutch Transmission	NI	National Instruments
DHT	Dedicated Hybrid Transmission	NVH	Noise, Vibration, Harshness
DMF	Dual Mass Flywheel	PHEV	Plug-in Hybrid Electric Vehicle
DOF	Degree of Freedom	RMS	Root Mean Square
EM	Electric Motor	RPM	Revolutions per Minute
EV	Electric Vehicle	SPL	Sound Pressure Level
FCEV	Fuel Cell Electric Vehicle	VI	LabVIEW Virtual Instrument
FEM	Finite Element Method		

Table 2: Latin nomenclature used In the thesis

A	Area [m^2]	k	Safety factor [1]
d	Diameter [m]	n	Quantity [1]
D	Fatigue damage [1]		Revolutions [min^{-1}]
E	Young's modulus [MPa]	N	Breaking point of S-N curve [1]
f	Friction coefficient [1]	p	Pressure [MPa]
F	Force [N]	r	Radius [m]
h	Height [m]	R	Coefficient of cycle asymmetry [1]
	Exponent for S-N curve [1]	s	Distance [m]
i	Gear ratio [1]	t	Thickness [m]
	Running index		Time [s]
I	Area moment of inertia [m^4]	T	Torque [Nm]
j	Running index	q	Exponent for S-N curve [1]
J	Moment of inertia [$kg*m^2$]	w	Width [m]

Table 3: Greek nomenclature used In the thesis

α	Side angle [°]	τ	Shear stress [$N*mm^{-2}$]
β	Face angle [°]	ϕ	Angular backlash [°]
Δ	Difference	ψ	Coefficient of uneven distribution [1]
η	Efficiency [1]	ω	Angular speed [s^{-1}]
σ	Bending stress [$N*mm^{-2}$]		

1 Introduction and Motivation

Greenhouse gases, regulation of CO_2 emissions, alternative fuels, sustainable mobility, vehicle electrification. You, the reader of this thesis, are almost certainly familiar with these concepts and their consequences. Therefore, let me skip a lengthy introduction and take the rising market share of hybrid (HEV) and electric vehicles (EV) as an undisputable fact. Furthermore, forecasts for the coming years claim that this trend will continue (Figure 1). This presents new challenges in automotive engineering and requires innovative technical solutions.

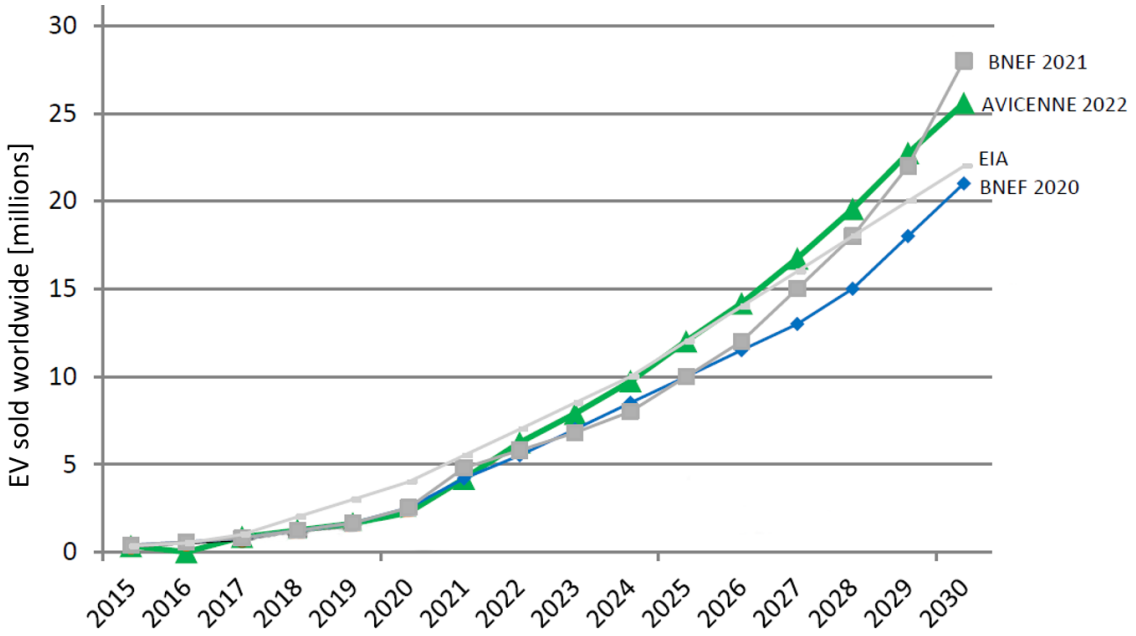

Figure 1: EV sales forecasts regarding to international organizations (2021 data) [1]
BNEF = Bloomberg New Energy Finance; EIA = U.S. Energy Information Administration

The technical requirements for HEVs or EVs (safety, comfort, durability, usability, availability, etc.) are the same as those for conventional vehicles with an internal combustion engine; [2]. However, this shift from vehicles powered exclusively by ICE to vehicles combining ICE with an electric motor or vehicles powered solely by the electric motor brings new demands on the construction of their powertrains and gearboxes. The main requirement for the development of HEVs and EVs is therefore to realize these objectives at reasonable cost; [3]. My research focuses on developing a new gearshift mechanism for these vehicles. The following paragraphs explain the motivation for the research and requirements for this gearshift mechanism.

The electric motor of the HEVs and EVs can usually be used as an external synchronization for the gearbox without additional costs. The largest potential for cost savings with respect to the gearshift mechanism have parallel hybrids – their ICE needs to be connected to the wheels using a gearbox with a wide range of gear ratios; [4]. The simplest and cheapest type of gearbox is the manual parallel shaft gearbox (MT), respectively, its automated variant (AMT);

[5]. These gearboxes generally use the most widespread gearshift mechanism in passenger cars, the synchronizer; [3].

The aim of my research is to replace the synchronizer with a new, simple and inexpensive gearshift mechanism, which would omit the ability of synchronization, redundant function for these vehicles. However, it must fulfill or improve all the other important functions of the synchronizer. Since parallel hybrid architecture is one of the less complicated and expensive, combining it with the cheapest gearbox type and a simple purpose-built and cheap-to-make gearshift mechanism could help spread this hybrid technology into affordable and mass-produced passenger cars. One example of a 7-speed AMT gearbox designed for hybrid vehicles is described in the paper [6].

The new gearshift mechanism must also be suitable for purely electric vehicles. Various investigations show that multiple gear ratios (mostly two) provided by a gearbox help improve the efficiency and driving range of EVs; [7]. This is mainly a consequence of the lower EM efficiency under certain operating conditions. A gearshift mechanism is required for such a gearbox.

Generally, the simplest gearshift mechanism for constant mesh gears is a dog clutch. However, the main reason why this solution never fully spread to passenger car gearboxes is related to driving comfort and NVH. Furthermore, the main source of NVH in passenger cars has traditionally been ICE. For an electric powertrain, the following sources become crucial: electric motor, inverter, and gearbox; [3] and [8]. In the gearbox, the main NVH issues are gear whine and gearshift mechanisms.

Gearshift mechanisms can cause vibrations and noise not only during the gearshift process, but also when the torque direction changes. This is generally caused by an angular backlash. Efforts to minimize this backlash of dog clutches can be traced back at least to the 1930s; [9]. Nevertheless, no universally applicable solution was invented. Minimizing angular backlash is therefore one of the key properties of the new gearshift mechanism while being as cheap and as compact as possible. More compact gearboxes can be stiffer, further reducing the NVH; [10].

2 Current State of Knowledge

This chapter briefly describes the most common gearshift mechanisms used to shift gears in mechanical gearboxes of passenger cars. Subsequently, it focuses on the existing dog clutch solutions, their advantages and disadvantages, examples of use in mass-produced gearboxes and concepts.

2.1 Gearshift Mechanisms

Mechanical gearboxes with parallel shafts (MT, AMT, and DCT) require an internal gearshift mechanism to shift gears. During the gearshift, the torque transmission must be briefly interrupted – the gearshift mechanism cannot be loaded. Dedicated hybrid transmissions (DHT) usually utilize the structure of mechanical gearboxes and their internal gearshift mechanisms; [11]. These gearboxes offer high efficiency and low cost compared to automatic gearboxes with planetary gearsets (AT) and continuously variable transmissions (CVT); [5]. This chapter provides a summary of the gearshift mechanisms commonly used in these mechanical gearboxes.

2.1.1 Sliding Gear

Sliding gear is the simplest gear shifting mechanism. The pair of spur gears is not in constant mesh. Engaging is realized through axial movement of one of the gears using the shift fork. This mechanism cannot be used for helical gears, only for spur gears which are significantly louder under load. Therefore, this mechanism is nowadays used in cheaper passenger car gearboxes for the reverse gear only.

Engaging of the reverse gear must in this case be done while stationary, angular speed synchronization is not present. Otherwise, the teeth wear out much faster or can be damaged eventually. The teeth must have appropriately chamfered faces to ensure engagement regardless of the initial angular position of both gears.

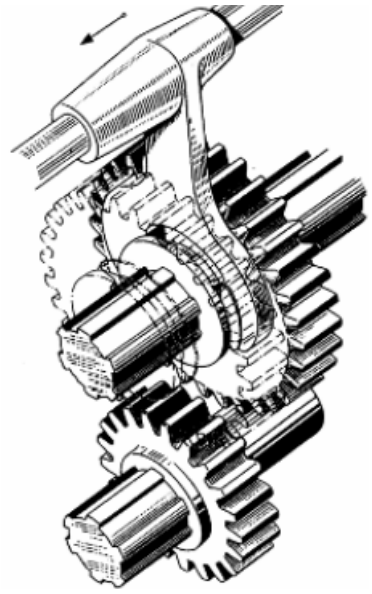

Figure 2: Sliding gear mechanism [5]

2.1.2 Synchronizer

The replacement of the spur gears with helical gears significantly reduces the noise under load, but it does not allow relative axial movement of both gears. Helical gears must be in constant mesh, one of the gear wheels in each pair is therefore running free on its shaft. During the gearshift this gear wheel needs to be connected to the shaft by the gearshift mechanism positioned next to it.

Various gearshift mechanisms can deal with the task – for example the dog clutch, as shall be further demonstrated. However, the synchronizer is able to first match the angular speed of the shaft with the angular speed of the shifted gear wheel. Originally, this task needed to be performed by the driver. The synchronizer helped shorten the duration of shifting compared to non-synchronized gearshift and improved service life; [12].

Fundamentally, the synchronizer incorporates two clutch principles in one unit. There are friction surfaces that are responsible for matching the angular speed (analogy with general friction clutch design) and toothing responsible for torque transfer in the engaged state (analogy with general dog clutch design). Nowadays a synchronizer always contains an additional mechanism which prevents the dogs from engaging before the angular speed is synchronized. This effect is called blocking synchronization and prevents excessive wear of the toothing whenever the driver performs the gearshift too ferociously. It also helps minimizing the angular backlash.

2.1.2.1 Borg-Warner synchronizer

The Borg-Warner synchronizer is the most widely used design amongst gearshift mechanisms used in passenger car gearboxes; [13]. It has been used since the 1950s and its reliability has been proved over long years of service; [14].

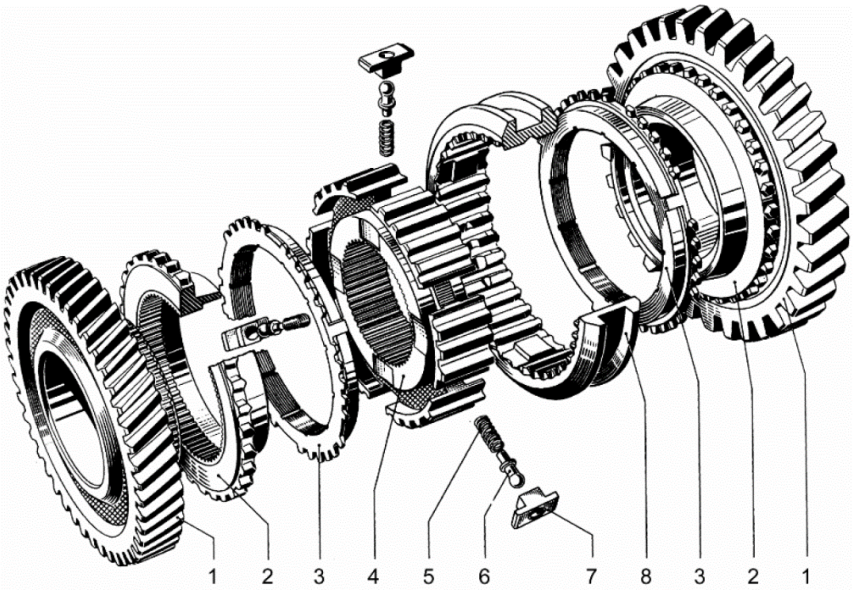

Figure 3: Borg-Warner single-cone synchronizer (ZF-B) [5]
1 – idler gear; 2 – synchronizer hub with toothing and friction cone;
3 – synchronizer ring with counter-cone and locking toothing; 4 – synchronizer body with internal toothing for positive locking with the gearbox shaft and external toothing for the gearshift sleeve;
5 – compression spring; 6 – ball pin; 7 – thrust piece; 8 – gearshift sleeve with internal toothing

It belongs to the group of gearshift mechanisms with blocking synchronization. The synchronizer body (4) is fixed to the shaft using internal toothing. The synchronizer ring (3) is angularly guided in the synchronizer body by stop bosses. These are narrower than the grooves in the synchronizer body. That allows only limited rotation of the synchronizer ring – half of the pitch. Before the shifting process starts, the gearshift sleeve (8) is held in the middle position by a detent.

In the first phase, the gearshift force *F* triggers the axial movement of the gearshift sleeve. This causes the ball pins (6) to act on the thrust pieces (7) to press the synchronizing ring (3) with its counter-cone against the friction cone of the synchronizer hub (2). The angular speed difference Δω between the gearshift sleeve (8) and the synchronizer ring (3) relative to the idler gear (1) causes the synchronizer ring to turn until the teeth contact the groove walls. This first phase of the synchronizing process is called ’asynchronizing’.

In the second phase, the gearshift sleeve is moved further. This brings the bevels of the internal toothing of the gearshift sleeve (8) and the external toothing of the synchronizer ring (3) into contact. The main synchronization process starts. The gearshift force is applied to the synchronizer ring via the thrust pieces (7) and the dogs (8), the force being divided between them. The gearing torque T_Z arising at the bevels acts in the way of opening the locking device. However, the gearing torque T_Z is smaller than the friction torque T_R that acts to close the locking device. In this slipping phase the gearshift sleeve cannot be shifted further – this is the principle of blocking synchronization.

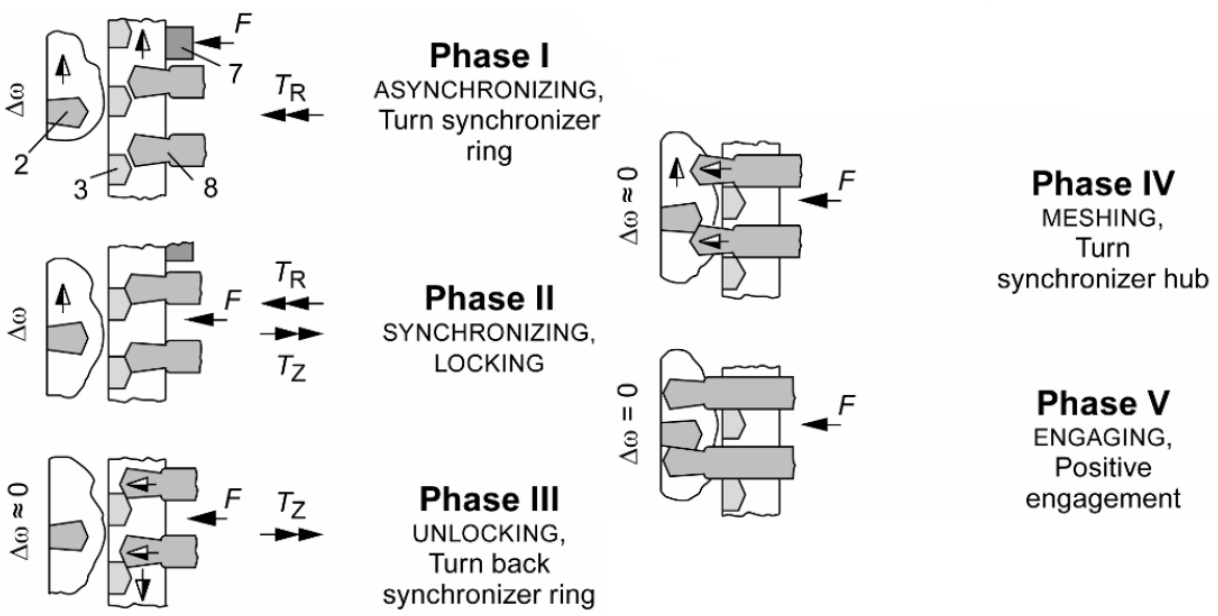

Figure 4: The synchronizing process of Borg-Warner synchronizer [5]
double arrows – torques; simple arrows – forces; half-filled arrows – movement direction

When the angular speed synchronization has been achieved, the friction torque tends towards zero – the third phase (the unlocking process) begins. The gearing torque becomes greater than the friction torque and acts via the bevels to turn back the synchronizer ring. The gearshift force decreases rapidly in this phase. Throughout the axial movement of the

gearshift sleeve, the spring-loaded ball pin slides along the inclined grooved surface. This presses it against the spring (5) into the thrust piece, until it is covered by the gearshift sleeve.

During shifting, the gearshift sleeve toothing encounters the bevels of the selector teeth of the synchronizer hub (2). In this fourth phase, the ball pin is covered. The synchronizer ring is pressed against the friction cone of the synchronizer hub only by residual pressure via the thrust pieces. This residual pressure arises from friction between the moving gearshift sleeve and the thrust pieces (with ball pins). The gearshift sleeve toothing twists the synchronizer hub relative to the synchronizer ring. Shift movement is enabled. The gearshift sleeve positively engages the power flow between the gear pair and the gearbox shaft – fifth phase; [5].

2.1.2.2 Multi-cone synchronizer

In manual gearboxes, the design aims to make the gearshift effort equal for all gears. The added cone ring increases the performance of the clutch due to the larger friction surface area. However, the parallel multi-cone design requires closer manufacturing tolerances and therefore entails higher production costs; [5]. Multi-cone synchronizers are therefore used especially for low gears. Shifting lower gears is more demanding due to higher gear ratios and therefore higher moments of inertia and due to larger spreads between the lower gears. Most common usage of the double-cone synchronizer is for the first and second gear.

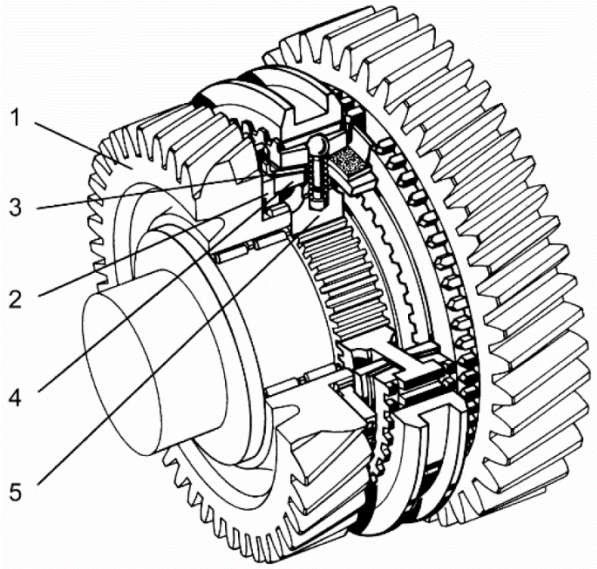

Figure 5: Double-cone synchronizer (ZF-D) [5]
1 – idler gear; 2 – synchronizer hu; 3 – double-cone ring; 4 – counter-cone ring; 5 – synchronizer body

Multi-cone synchronizers are mostly based on the Borg-Warner design. Further information, guidelines about synchronizer design and alternative synchronizer solutions can be found in the literature [5], [15] or [16].

2.1.2.3 Porsche synchronizer

Porsche developed its own blocking synchronizer that was used not only in Porsche vehicles but also by other manufacturers. It features a strong self-reinforcing locking effect for relatively low gearshift effort. However, the manufacturing costs are higher; [5].

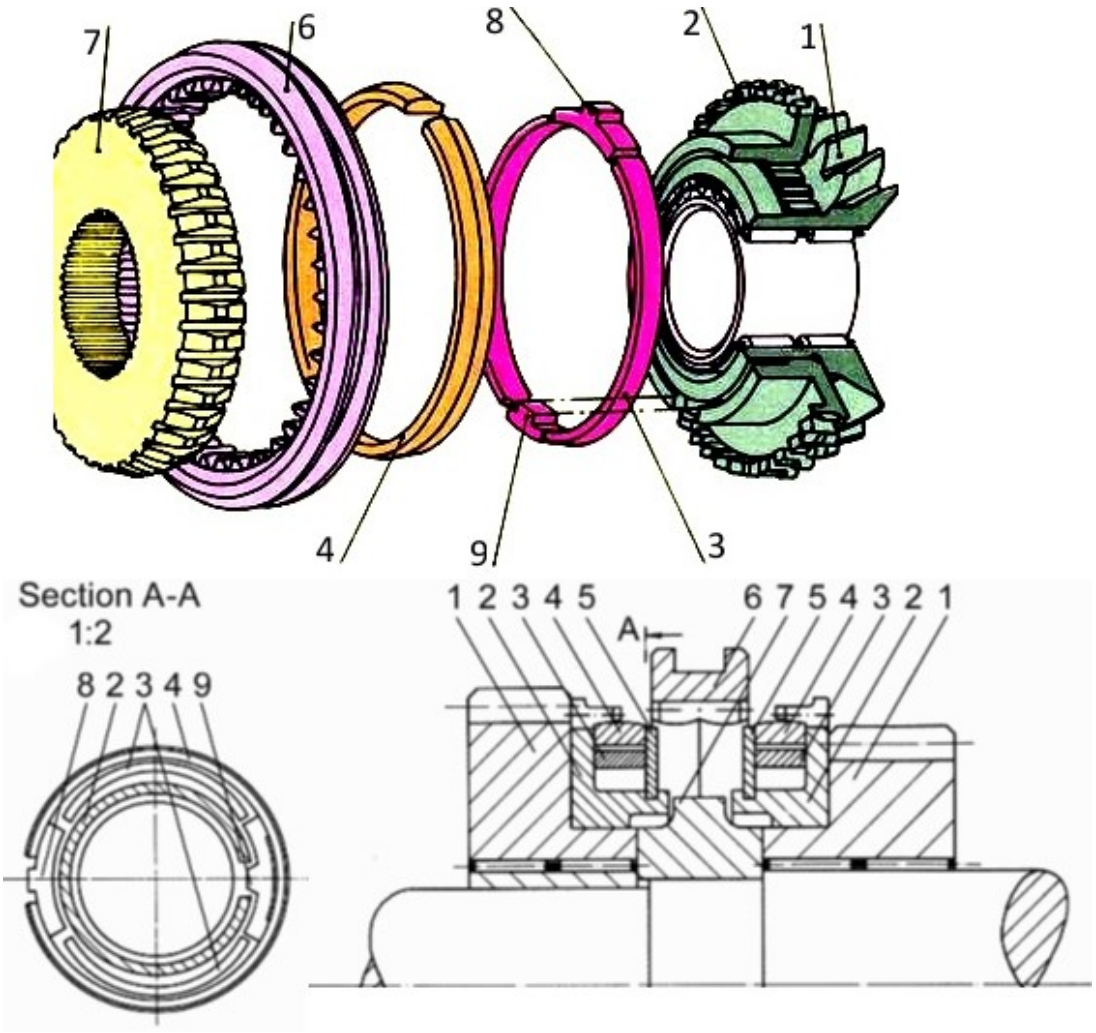

Figure 6: Porsche synchronizer [5], [17]
1 – idler gear; 2 – synchronizer hub with toothing; 3 – locking belt; 4 – synchronizer ring; 5 – circlip; 6 – gearshift sleeve; 7 –hub; 8 – blocking stone; 9 –stop stone

The gearshift sleeve (6) is axially guided by the hub (7). When the sleeve starts moving in the direction of the shifted gear wheel (1), it starts pushing on the outer rounded surface of the synchronizer ring (4). The C-shaped synchronizer ring must be compressed to a smaller diameter to allow the sleeve to slide further. When there is an angular speed difference, the synchronizer ring is twisted by the friction torque until it rests on the stop stone (9) by means of the blocking stone (8) and the locking belt (3). This gives rise to radial forces that press the locking belts outwards and prevent the synchronizer ring from being compressed. The greater the axial shifting force acting on the gearshift sleeve, the more strongly the synchronizer ring is pressed outward by the locking belts. When the synchronization is finished there is no more effective blocking force, and the synchronizer ring can then be compressed. The gearshift sleeve slides over it and engages into the toothing of synchronizer hub (2); [5].

2.1.3 Dog Clutch

The dog clutch is a suitable candidate to replace the synchronizer in the case of using external synchronization, as mentioned in the introduction. In the default configuration, dog clutches cannot offer the same qualities as the synchronizer, but the dimension and weight savings are significant; [18]. Gearboxes must be equipped with the same number of synchronizers as they have synchronized gears, even though adjacent gears usually have their pair of clutches merged into one, which operates them both. Another advantage of the dog clutch is the ability to shorten the gearshift duration when using sufficiently powerful external synchronization system, especially for lower gears (i.e., gears with high ratio).

Dog clutches without synchronization are not widely used in passenger car gearboxes. However, there exist some other applications, where they are used; [19]:

- **Racing cars.** The power flow between the engine and the wheels is interrupted during the gearshift, which is highly undesirable. Racing cars focus on the shortest gearshift time possible. Gearbox service life and ride comfort are therefore compromised. Weight savings are also very important – dog clutches offer short axial length of the gearbox (see Figure 7).
- **Motorbikes.** Due to package limitations, synchronizers are usually not an option. Dog clutches can be used due to the low moments of inertia of the entire powertrain without significant impact on ride comfort or service life.
- **Heavy commercial vehicles.** Synchronizers are not capable of providing a service life long enough within the common power-to-weight ratios of these vehicles. They are usually fitted with automated mechanical gearboxes combined with external synchronization.

Figure 7: Six-speed sequential gearbox with dog clutches of a Subaru racing car [20]

2.1.3.1 Properties and geometry

The simplest face dog clutch design (Figure 8) consists of a clutch body (1) fixed to the gearbox shaft. Then there is a sliding dog (2) – the main engaging element (Figure 9). It cannot

rotate freely but can be displaced axially through the corresponding shift fork. The second engaging element is generally integrated into the gear wheel (3). The locking or engagement is realized through the mesh of the dogs when the sliding dog is in the engaged axial position.

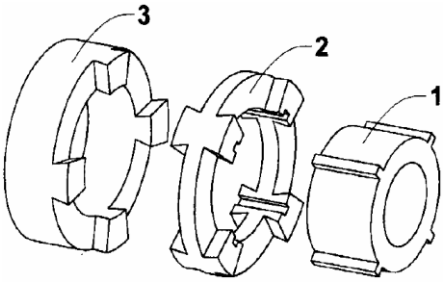

Figure 8: Face dog clutch components [21]

Figure 9: Sliding dog used in Formula 1 gearbox [22]

One of the important design aspects of a face dog clutch is the side angle of the dogs. Based on this criterion, we distinguish the following three types (see Figure 10):

a) **Negative angle.** Used especially in vehicle gearboxes; [19]. Its main advantage is the axial force which acts on the dogs in engaged state while transmitting torque as a result of the negative angle. This force points into the mesh and holds the engaged sliding dog and the gear wheel together. Generally, this means that the clutch cannot be spontaneously disengaged, and it also helps during the engagement process. However, for specific conditions (for example, high level of vibrations), the risk of unwanted disengagement may be present even for the negative angle – for example, patent [23] presents a dog clutch with additional centering components between the sliding gear and gearshift sleeve to prevent unwanted disengagement of a dog clutch with negative angles of the dogs' sides. The main disadvantage of this solution is the angular backlash that is present due to the shape of the dogs. It is necessary for successful engagement but reduces ride comfort due to torsional vibrations when the torque direction changes.

b) **Zero angle.** Equals rectangular dogs. Non-zero backlash ϕ is still necessary for successful engagement. Even though theoretically ideal, in real operation this variant suffers from the negative aspects of both others. Consequently, it is rarely used.

c) **Positive angle.** Used for specific applications, e.g., gearboxes of dragsters or differential locks of heavy-duty vehicles; [24]. Its advantage lies in the possibility of minimizing the angular backlash ϕ, which is desirable especially for vehicles with higher moments of inertia. The main disadvantage is the axial force, which in this case points out of the mesh. If the side angle of the dog is larger than the angle of self-locking for the dogs' materials, the clutch cannot stay in the mesh under load without an external detent or blocking device. Unwanted disengagement can also occur with smaller side angles due to vibrations as mentioned above.

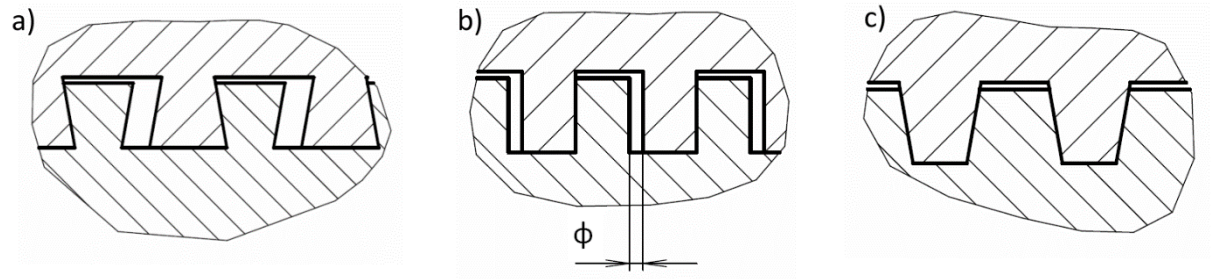

Figure 10: Types of face dog dogs regarding to the side angle of the dogs

2.1.3.2 The engagement process

The engagement process will be demonstrated for the face dog clutch with rectangular dogs and can be divided into multiple phases. It begins with the actuation of the sliding dog at time t_0. The initial mismatch speed of sliding dog and gear wheel has a value of $\Delta\omega_0$. The dog clutch transmits no torque, and the engagement phase is called free fly, lasting until the sliding dog reaches the gear wheel at t_1 time. Due to possible minor changes in vehicle speed and, more importantly, due to the friction losses and the eventual countershaft brake torque acting on the gear wheel, the mismatch speed changes to $\Delta\omega_1$ by that time. For this case, it would usually be the dogs' faces that first come in contact, resulting in an impact.

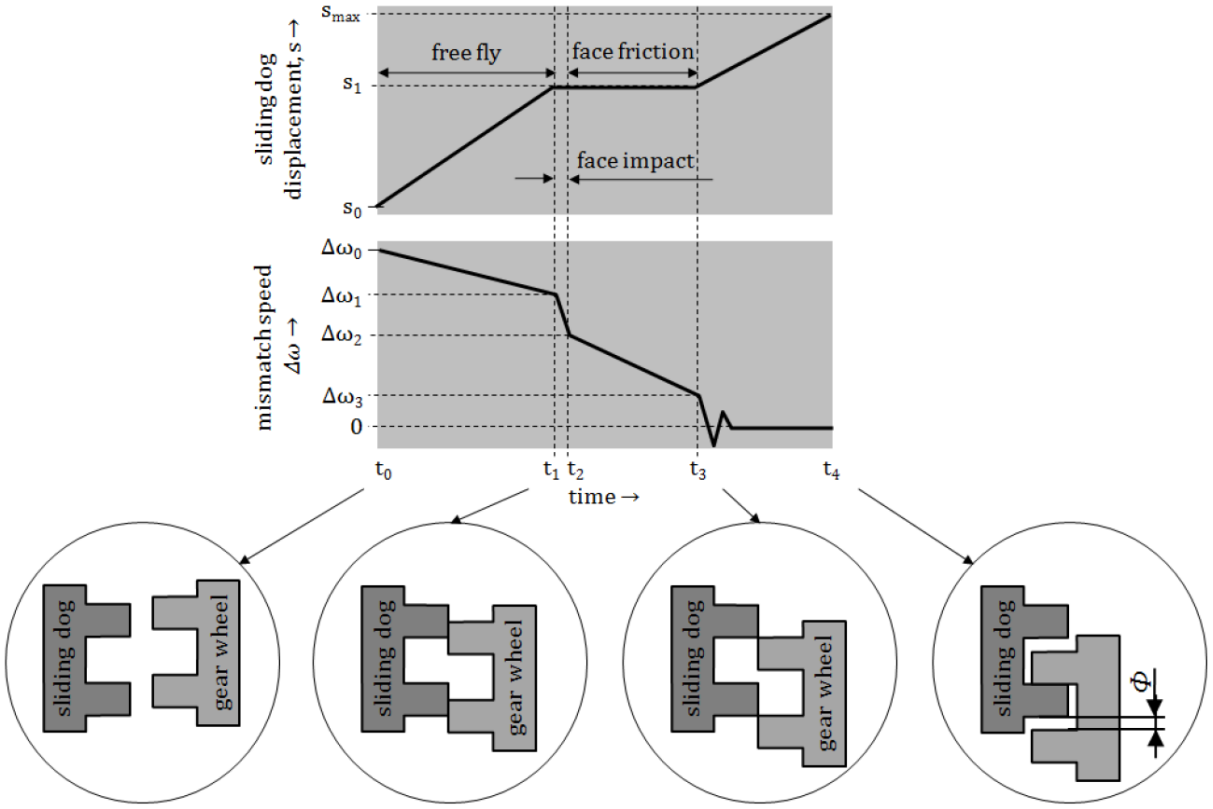

Figure 11: Engagement process of a face dog clutch with rectangular dogs [19]

The high impact force peak stops the axial movement of the sliding dog by consuming the motion energy of the whole actuation mechanism attached to it. The normal force between the sliding dog and the gear wheel and the relative turning of them imply a face friction torque acting against the relative turning. As the peak in the normal force also results

in a peak in the face friction torque, the mismatch speed reduces to $\Delta\omega_2$ in the negligible time range of the face impact.

After the impact, the face areas slide on each other, until the dogs turn against the slots at time t_3. This phase is called the face friction phase, and the face friction torque still acts against the relative turning further reduces the mismatch speed to $\Delta\omega_3$. As the dogs of the sliding dog are now free to enter the slots in the gear wheel, the dog clutch engages, and the mismatch speed quickly reduces from $\Delta\omega_3$ to zero, provoking heavily damped torsional vibrations in the driveline lasting only a few cycles. Then the process becomes steady again and the gearshift is finished at time t_4, the clutch is engaged; [19] and [25].

2.1.3.3 Successful and unsuccessful engagement

The peak value of the torsional vibrations is proportional to the torsional stiffness of the gearbox and other driveline components and their moments of inertia. Another crucial factor is the mismatch speed $\Delta\omega_3$. To minimize torsional vibrations and maximize driveline service life, the value $\Delta\omega_3$ should be kept as low as possible. This also reduces the noise during gearshift. However, for low values of mismatch speed, there is a risk of the engagement being unsuccessful. As the mismatch speed is reasonably reduced in the disengaged state of the dog clutch and is further decreased by the face friction torque, it may completely vanish during the face friction phase before engagement. The result is a permanent face-to-face situation when face contact is not resolved. The gearshift cannot be completed (Figure 12 right).

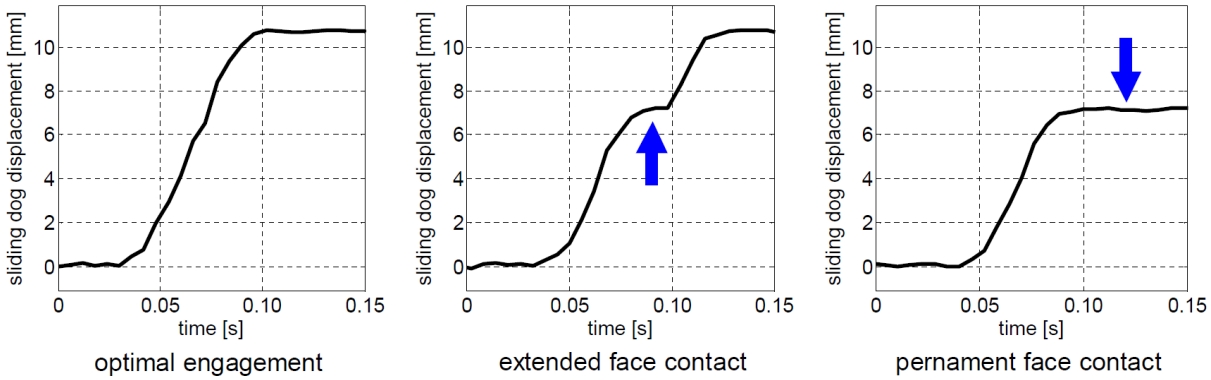

Figure 12: Possible gearshift scenarios of sliding dog [26]

The face friction phase can be skipped in the special case where the dogs of the sliding dog move into the slots of the gear wheel immediately (Figure 12 left). The probability of this phenomenon depends on the number of dogs and the width ratio of dogs and slots. This ratio can be described using the angular backlash ϕ measured in the distance s_1 of the sliding dog axial displacement (Figure 11). Further details of this phenomenon can be found in the article [26].

Problems can also be caused by another phenomenon called bounce-back. This means that at time t_1 the impact is so hard that the sliding dog is bounced back, and its dogs miss the corresponding slots in the gear wheel because of the high remaining mismatch speed. This makes the gearshift longer and increases the probability of unsuccessful engagement

described in the previous paragraph (Figure 12 middle). The choice of appropriate initial mismatch speed and gearshift force is crucial; [19].

Successful engagement, regardless of current mismatch speed, can be secured by using tapered faces of the dogs. If the taper angle is bigger than the self-locking angle, the engagement is theoretically successful even with zero mismatch speed. The disadvantage of this modification is reducing the contact height and therefore the contact surface of the dogs in mesh. To preserve the strength of the dogs, it might be necessary to make them higher, consequently the clutch becomes axially longer. Furthermore, the clutch becomes sensitive to the initial mismatch speed direction. In other words, the probability of bounce-back is determined by which one of the two parts rotates faster.

Dog clutch design basis are considered the most suitable for the new gearshift mechanism. Examples of dog clutch designs are presented in Chapter 2.2, usage in passenger car gearboxes in Chapter 2.3.

2.1.3.4 Summary

In summary, dog clutches used for shifting gears in automotive gearboxes can be generally characterized by the following properties:

- Torque transmission in the engaged state never causes spontaneous unwanted disengagement.
- The packaging is smaller compared to synchronizer thanks to omitting the synchronizing functionality. Savings in axial length are especially favorable.
- Engagement and disengagement occur without delay to the control signal – movement of the gear selector mechanism.
- Engagement is successful regardless of the initial relative angular position of the two shifted elements.
- The gearshift is as quick as possible.
- The neutral position is secured independently on the gear selector mechanism.
- The gearshift mechanism is scalable for different applications according to torque requirements.
- The gearshift mechanism is compatible with sequential gear selector mechanism.

2.1.4 Hollow Shaft Gearshift Mechanism

This system is rarely used in passenger car gearboxes. However, there have been some efforts to use it and it was also researched and considered as a design basis for the new gearshift mechanism. Therefore, a general overview is presented.

These gearshift mechanisms are incorporated into one of the gearbox shafts. The shifted wheel is mechanically connected to the shaft via an additional part that transmits the torque between them. The greatest advantage of this solution is the very compact packaging due to the absence of shift forks, levers, and other parts of the internal gear mechanism in the space between the gear wheels. Therefore, the wheels can be placed adjacent to each other and the gearbox dimensions (especially the length) are considerably reduced.

On the other hand, the rigidity and load-bearing capacity of the shaft stressed at the same time by bending and torsion is reduced due to the holes and cavities for the additional parts to move or extend. To avoid the shaft from weakening too much, the smallest possible number of elements is used. However, these may be overloaded by contact pressures while transmitting the torque at a small radius. Another limitation is the impossibility of direct shifting into another than adjacent lower or upper gear (skipping gears). This solution is therefore suitable especially for sequential gearboxes of low-performance motorcycles.

Efforts to make this solution usable in automotive were carried out; [27]. However, scalability for higher torque demands due to load capacity and service life is very limited. Examples are shown in Figure 13 (passenger car) and Figure 14 (motorcycle).

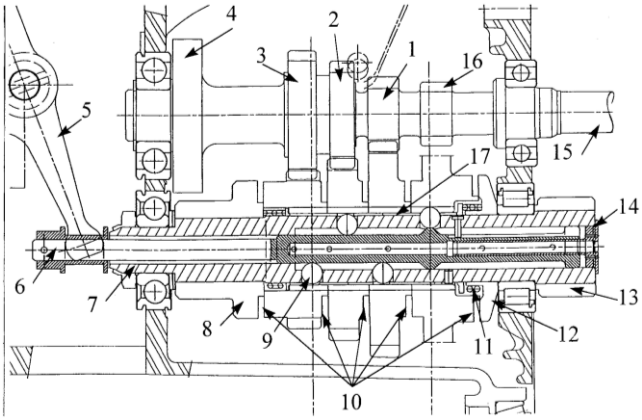

Figure 13: Prototype of a ball shift mechanism for a 3+R-speed automotive gearbox [27]

Figure 14: Internals of Vespa motorcycle gearbox with cruciform gearshift element [28]

Some gearshift mechanisms utilize the ratchet principle that allows for rotary motion in only one direction while preventing motion in the opposite direction. Their primary objective is to reduce the torque gap during shifting. Generally speaking, two gears can be at least partially shifted simultaneously. Due to the different gear ratio and ratchet mechanisms, only one of them transfers the torque. Shifting from one gear to the other means that they switch their role and the shifted gear starts transmitting the torque almost instantaneously. Similarities can be observed with Zeroshift and Bous clutches (Chapters 2.2.3 and 2.2.6.5).

The main usage can be found in gearboxes of racing motorcycles. The first implementation was done in the MotoGP season 2011 by Honda. Two pairs of pawls under each shifted gear wheel pivot on axes parallel to this gear wheel (see Figure 15). The pairs face opposite directions to transfer torque during accelerating and engine braking. Pawls' noses engage to recesses on the inner gear wheel diameter. The pawls are fully retracted in neutral.

The angle of the pawls is controlled by the gearshift mechanism through sliding rods and pins. When shifting the gear, the pin moves inward into a detent in the sliding rod. The pawls do not all engage simultaneously. When shifting upper gear, at first the sliding rods disengage the pair of pawls for engine braking at the current gear and only engage the pair of pawls for acceleration on the shifted gear. Due to the different gear ratios, the angular speed difference at the shifted gear wheel engages this wheel with the pawls. The previous gear is immediately disengaged when the torque is no longer transmitted through its pawl pair due

to the sliding rod geometry and the spring preload; [29]. Further details can be found in patent [30]. The gearbox proved its functionality on racetracks. However, its complexity, cost, and limited service life is not suitable for public roads.

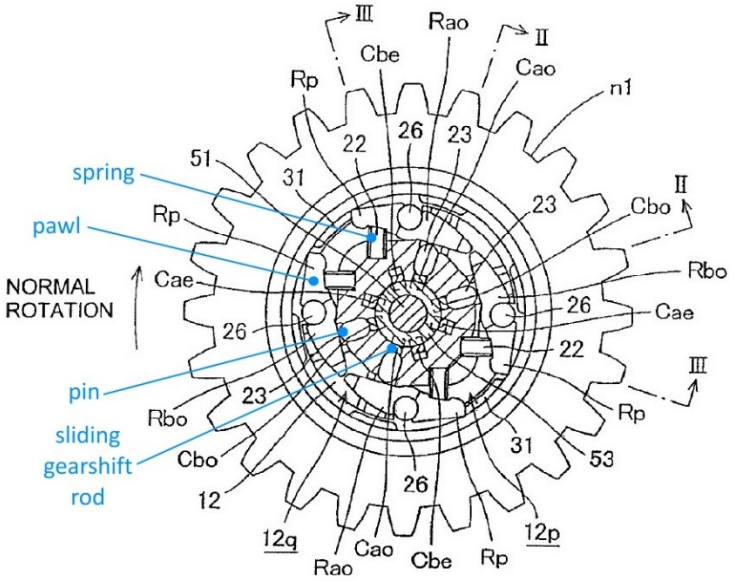

Figure 15: Honda RC212V ratchet gearshift mechanism [30]

A similar mechanism was patented even earlier and later used by Xtrac; [31]. Yamaha was the first to patent their solution for a road motorcycle; [32]. However, mass-production of this gearshift mechanism has not yet been launched. Interestingly, a 2015 Borg-Warner patent can be found, which combines a synchronizer with the ratchet mechanism and a dual clutch gearbox; [33].

2.2 Dog Clutch Design Examples

This chapter presents various patents and designs of dog clutches that the author used as an inspiration and to gain as much insight into the process as possible. Only selected solutions are presented to illustrate the wide spectrum of possibilities on the one hand and keep the thesis length in reasonable range on the other.

2.2.1 Dog Clutch without Backlash – 1930 Patent

This is the oldest effort regarding a dog clutch without angular backlash the author has found. In 1930, Harald R. Morgan patented in the United Kingdom an 'Improved Gearshift Mechanism'; [9]. It was basically a proposal of a dog clutch with additional parts responsible for minimizing the backlash in engaged state. This is proof that efforts to minimize angular backlash date back to the early days of automotive gearboxes and gearshift clutches. Quoted from the patent. '*This invention relates to dog-clutches for transmitting effort in two directions and has for its object to provide means whereby their engagement may be facilitated without introducing an undesired extent of backlash*'.

The sides of the dogs which come into contact during engagement have negative angles of the sides. The patent presents two solution examples where bolts C1 (Figure 16) or

bolts C3 (Figure 17) are responsible for minimizing the angular backlash. In both cases, the bolts engage after successful engagement of the clutch and transmit the torque in one of the two directions.

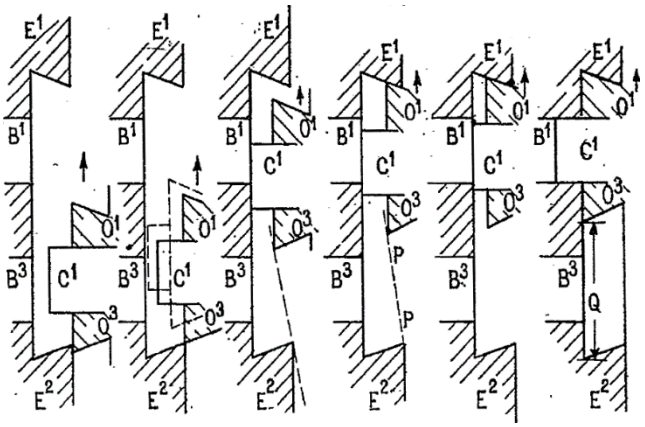

Figure 16: Dog clutch patented in 1930 – bolts C1 minimize the angular backlash [9]

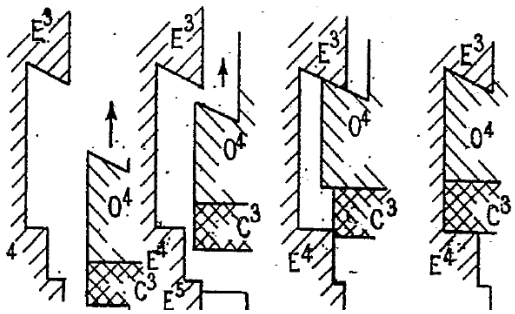

Figure 17: Dog clutch patented in 1930 – bolts C3 minimize the angular backlash [9]

The disadvantage of this solution is its complexity – it requires a relatively large number of parts including the system of bolts and springs to preload them (see Figure 18). It may be also difficult to tune the geometry and spring stiffnesses for proper functionality of the clutch not only during engagement but also disengagement. The axial length of the clutch is greater due to the additional components, especially torsional springs. Disengaging the clutch under load is not possible.

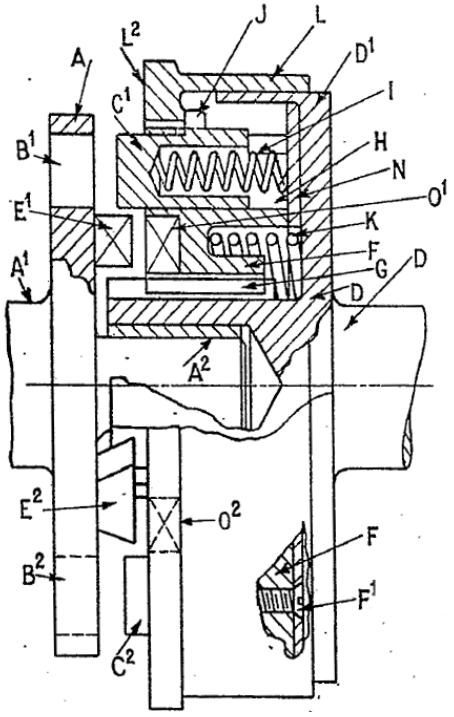

Figure 18: Dog clutch without backlash regarding to 1930 patent [9]

2.2.2 Aisin Dog Clutch

The Aisin dog clutch (see Figure 19) consists of a hub fixed to the gearbox shaft and sits between the pair of gear wheels. The sleeve is controlled by the gearshift fork and engages by sliding along the hub. The clutch is fitted by two dog types on the sleeve and the gear wheels. During the gearshift, first the synchronization dogs mesh to minimize the mismatch speed and face-to-face probability, then the torque dogs mesh and transfer the torque.

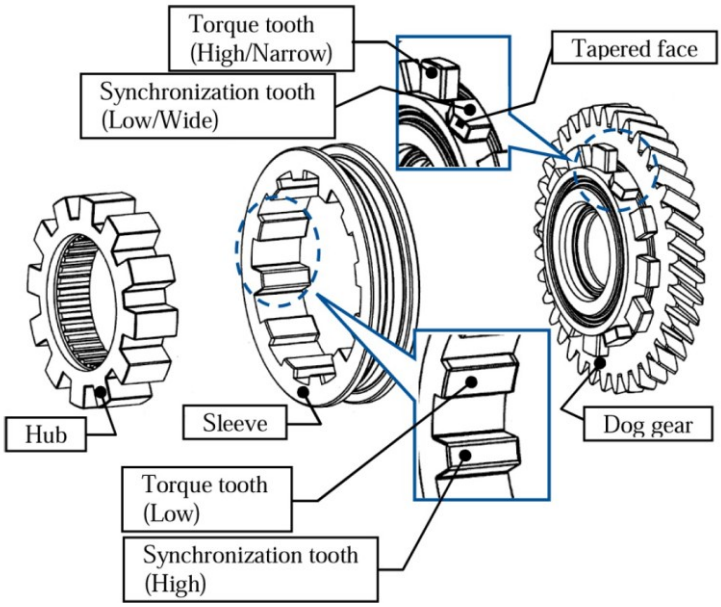

Figure 19: Aisin dog clutch – exploded view [34]

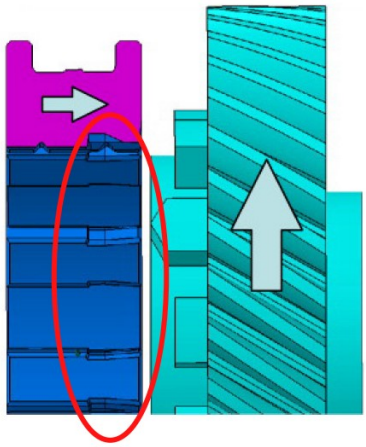

Figure 20: Negative side angle visible at the inner dogs of the sleeve [34]

Despite the two dog types and their different shapes, there is still quite a high probability of bounce-back to occur. This happens when the synchronization dogs come into contact on their tapered faces. Bounce-back probability depends on the number of synchronization and torque dogs and also on mismatch speed. For 12 dogs in total (3 of them synchronization dogs) and mismatch speed 100 min^{-1}, the measured probability of bounce-back was 15,8%; [34].

This dog clutch has very little components but requires manufacturing of two different dog shapes. The paper [34] does not describe how is the clutch secured in the engaged position. The dogs are mainly shown in plain rectangular shapes. However, in Figure 20 we can see undercut dogs (negative side angles) on the inner sleeve diameter. The backlash in engaged state will therefore be present.

2.2.3 Zeroshift

The Zeroshift system (see Figure 21) consists of a hub (2) which is fixed to the gearbox shaft and sits between the pair of idler gear wheels (1). Gear wheels have face dogs manufactured on their sides. These dogs have negative sides angle to prevent unwanted disengagement. Two sliding dogs (3) are present and therefore two gearshift sleeves (4) as well. Precisely shaped face dogs designed to transfer torque are manufactured on the sides of the sliding dogs.

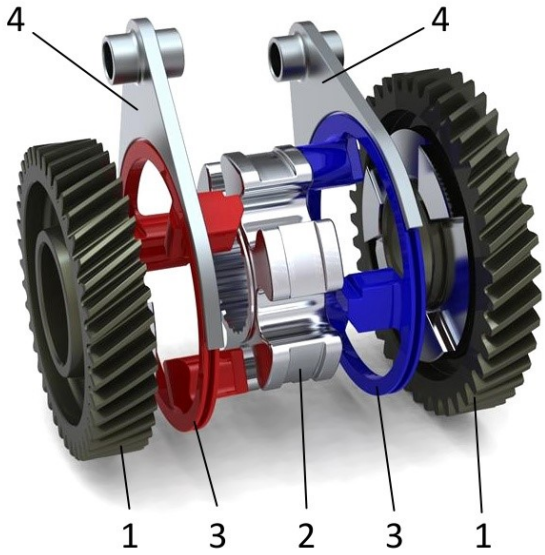

Figure 21: Zeroshift – exploded view [20]
1 – gear wheel with face dogs; 2 – hub; 3 – sliding dogs; 4 – gearshift sleeves

In neutral position, the sliding dogs are hidden in the grooves of the hub and the gearshift wheels are rotating freely – Figure 22 a). Gearshift is initiated by sliding one of the sliding dogs in selected direction. This sliding dog must be chosen carefully considering mismatch speed between sliding dogs and shifted gear wheel – the first contact of dogs must occur on their sides with negative angle – Figure 22 b). Otherwise bounce-back may easily occur. Immediately after correct engagement of the first sliding dog, the second sliding dog can move in the same direction. When both sliding dogs are engaged, the angular backlash is minimized – Figure 22 c). Nevertheless, a small backlash is still present because of the negative angle of the dogs' sides.

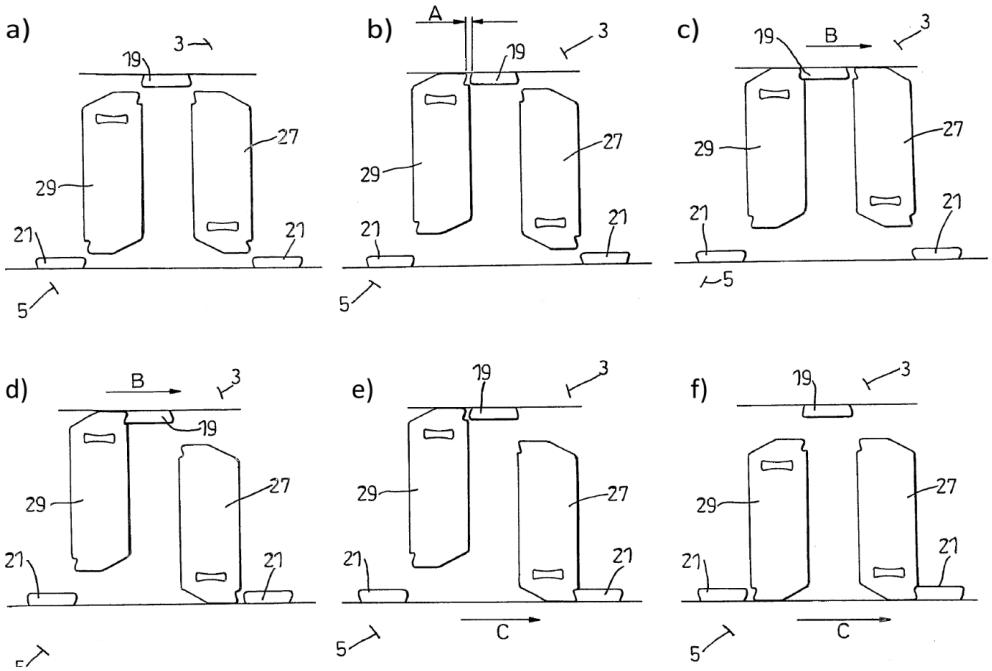

Figure 22: Zeroshift – detailed view of the gearshift process [35]
3 – gear wheel of the lower gear; 5 – gear wheel of the higher gear;
19, 21 – dogs at the gear wheels; 27, 29 – dogs at the sliding dogs

Shifting to higher gear begins in the same manner as shifting a gear from neutral – regarding mismatch speed, one sliding dog is chosen and slid towards the gear wheel of the higher gear – Figure 22 d). In the moment it engages and comes into contact with this gear wheel it is forced to slow down and rotate the same angular speed as the gear wheel. Therefore, the second sliding dogs start to rotate slower as well and after a while it is kicked out of the mesh by the dogs of the faster gear wheel. This kick is supported by positive angle of the dogs' sides which do not transfer the torque – Figure 22 e). The higher gear is engaged, backlash minimized – Figure 22 f). The whole process is actively controlled by one gearshift sleeve only; [35].

The gearshift up is very quick, and backlash is somehow minimized. However, it is accompanied by high values of NVH. Gearshift down is more complicated – the previously described system does not work and the gearshift down must be precisely and actively controlled by both gearshift sleeves to prevent damage caused by incorrect movement of the sliding dogs into mesh. A gearbox equipped with the Zeroshift system therefore must include twice as many gearshift sleeves, forks, shafts etc. compared to regular gearbox with dog clutches. The whole system must be controlled electronically by software. All these factors make the gearbox more complicated. Zeroshift was designed for racing cars due to the quick upshifts.

2.2.4 Dog Clutch with Rectangular Dogs – 2012 Patent

This solution is unique thanks to the rectangular dogs. These were mentioned in Chapter 2.1.3.1 as impractical and rarely used. Author of patent [21] suggests using rectangular dogs (5) and (7) on the sliding gear (2) and shifted gear wheel (3). Protection against spontaneous disengagement is realized by means of protrusions (9) in the axial grooves (14) of the hub (1). In the engaged state and during torque transmission, the sides of the sliding gear dogs (11) are in contact with the sides of the grooves in the hub. Therefore, the edges (13) of the sliding gear rest against the edges (12) of the protrusions. In order to disengage the clutch in this situation, it would be necessary to overcome the axial force arising in this contact. This solution simplifies sliding gear production – it can have simple rectangular dogs. However, due to the protrusions, the angular backlash is not eliminated.

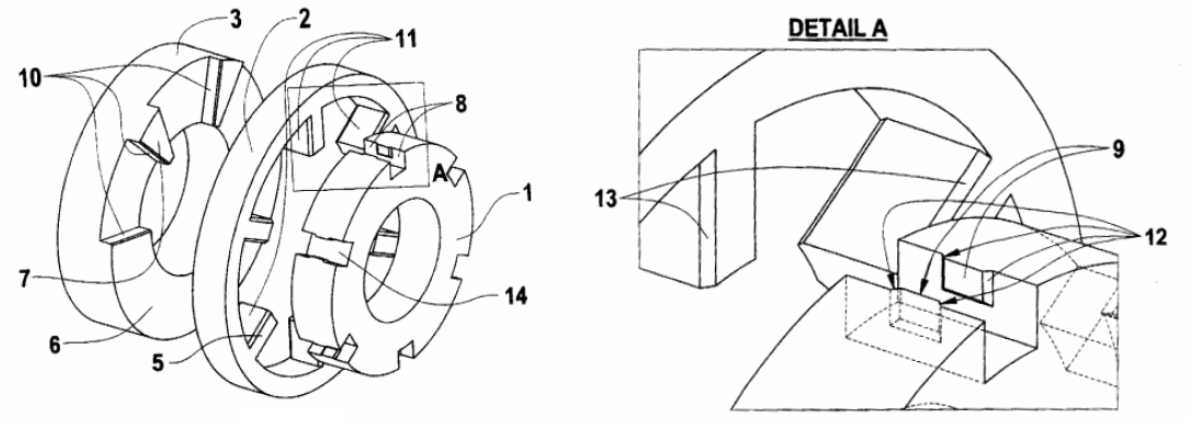

Figure 23: Dog clutch with rectangular dogs – exploded and detailed view [21]

2.2.5 Dog Clutch with Cradles – 2015 Patent

This clutch uses outer dogs and unique cradles instead of conventional face dogs. No sliding dogs are needed. Engagement is provided by gearshift stones (cradles) (4). These are positioned on the cylindrical supports in the grooves of the hub (1). In neutral position, these cradles are parallel with the axis of rotation of the clutch. Their position is secured from the outside by the gearshift sleeve (3). The gearshift is realized through this sleeve. The movement of the sleeve forces the cradles to tilt. Thus, their one side lifts and the other goes down into mesh with the corresponding dogs at the crown (2). This crown is connected to the shifted gear wheel. The stones cannot disengage unless the sleeve slides back to the neutral position; [36]. However, the patent [36] does not describe how to prevent the situation of 'face-to-face' contact and the risk of unsuccessful engagement.

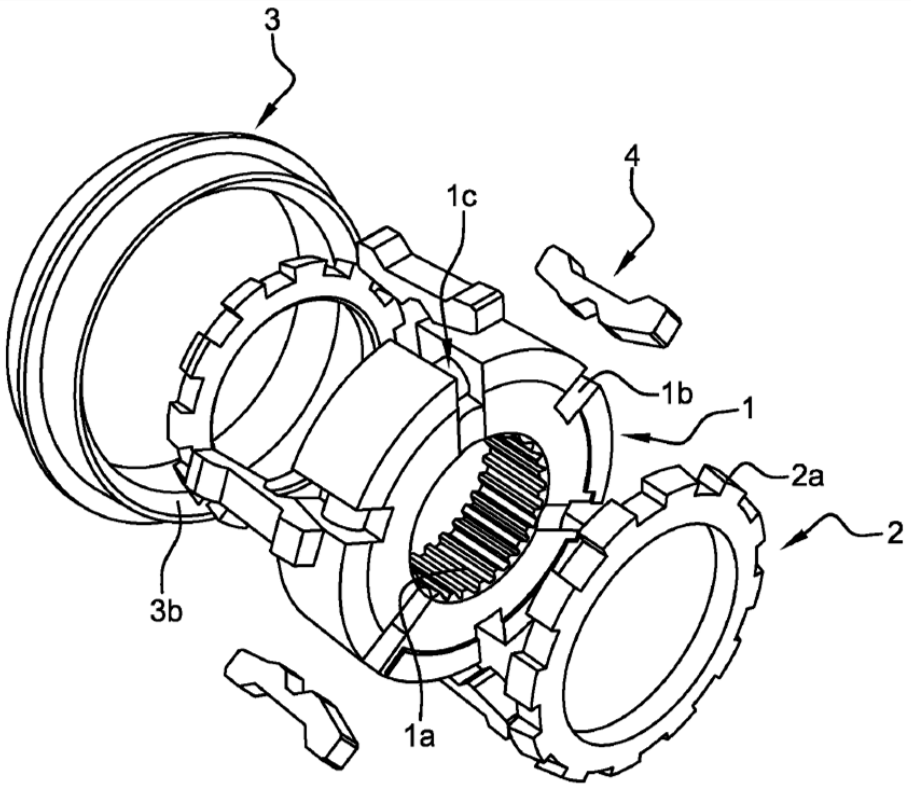

Figure 24: Dog clutch with cradles – exploded view [36]
1 – hub; 2 – crowns with dogs; 3 – gearshift sleeve; 4 – gearshift stones (cradles)

2.2.6 Dog Clutches Developed or Tested at CTU in Prague

The Czech Technical University in Prague has been active for several years in the field of design and testing of shift mechanisms, as well as in the design of new gearshift clutches. The prototype design and ultimately the testing of all the clutches mentioned in this chapter was carried out with the support of ŠKODA AUTO, a.s. and its MQ200 gearbox, specifically as a replacement for the 3rd and 4th gear synchronizer. The gearbox is manufactured in 5-speed (Figure 25) and 6-speed variants. All forward gears are synchronized and shifted by Borg-Warner synchronizers; reverse gear is a sliding gear [37].

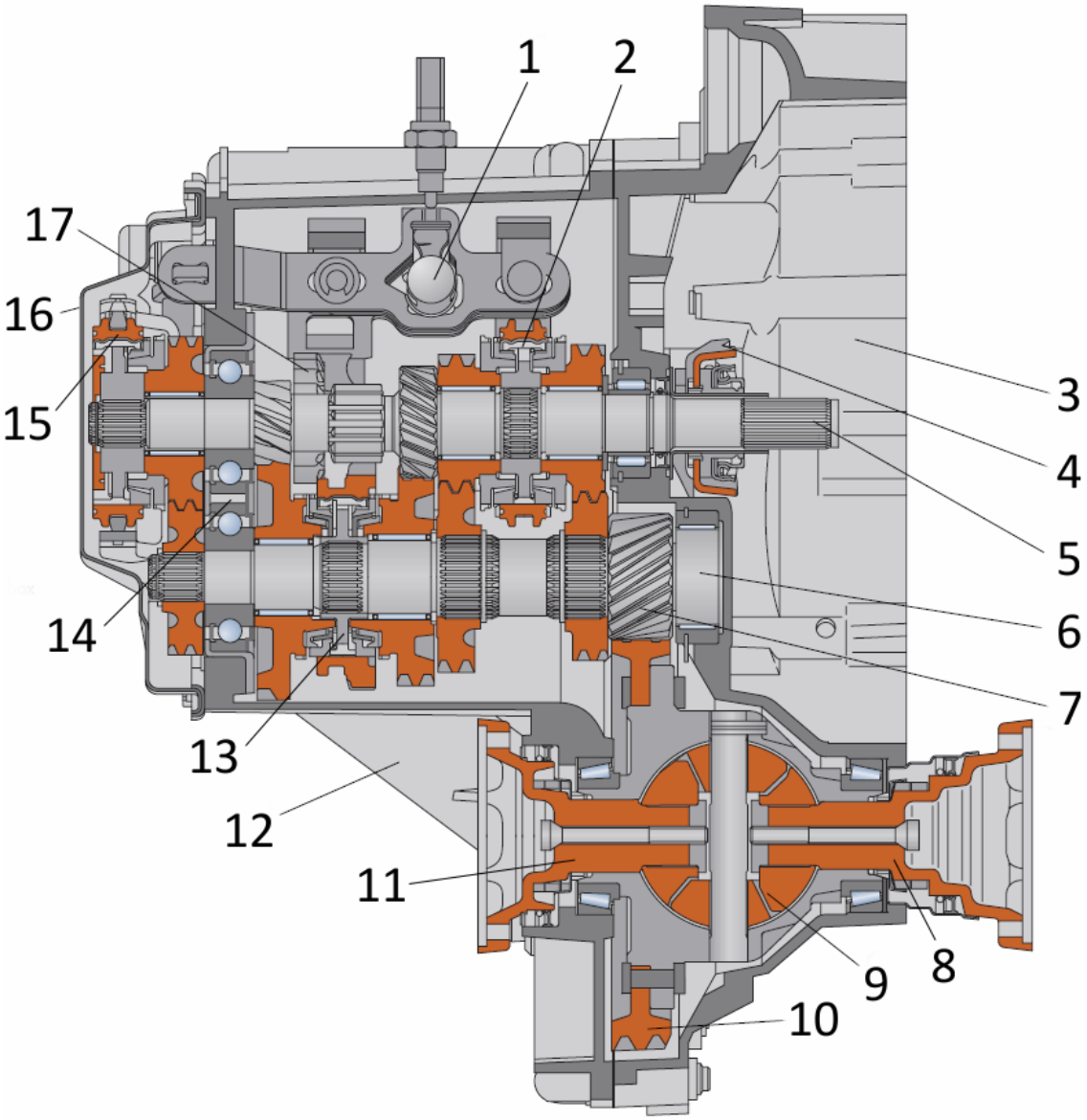

Figure 25: Section view of the 5-speed MQ200 gearbox [37]

1 – gear selector mechanism; 2 – synchronizer 3rd/4th gear; 3 – clutch housing; 4 – clutch lever; 5 – input shaft; 6 – output shaft; 7 – input wheel of final drive; 8 – output shaft to right wheel; 9 – differential; 10 – output wheel of final drive; 11 – output shaft to left wheel; 12 – gearbox housing; 13 – synchronizer 1st/2nd gear; 14 – bearing unit; 15 – synchronizer 5th gear; 16 – 5th gear cover; 17 – sliding reverse gear

2.2.6.1 Dog clutch with Maybach dogs

This clutch was presented in 2007 Ing. Miller's diploma thesis. It consists of hub (2) that is fixed to the gearbox shaft – radially using internal splines and axially sitting between the pair of idler gear wheels (1). Gear wheels have face dogs manufactured on their sides. These dogs mesh with the sliding dog (4) when engaged. The blocking ring (3) secures the sliding dog in the neutral position; [38].

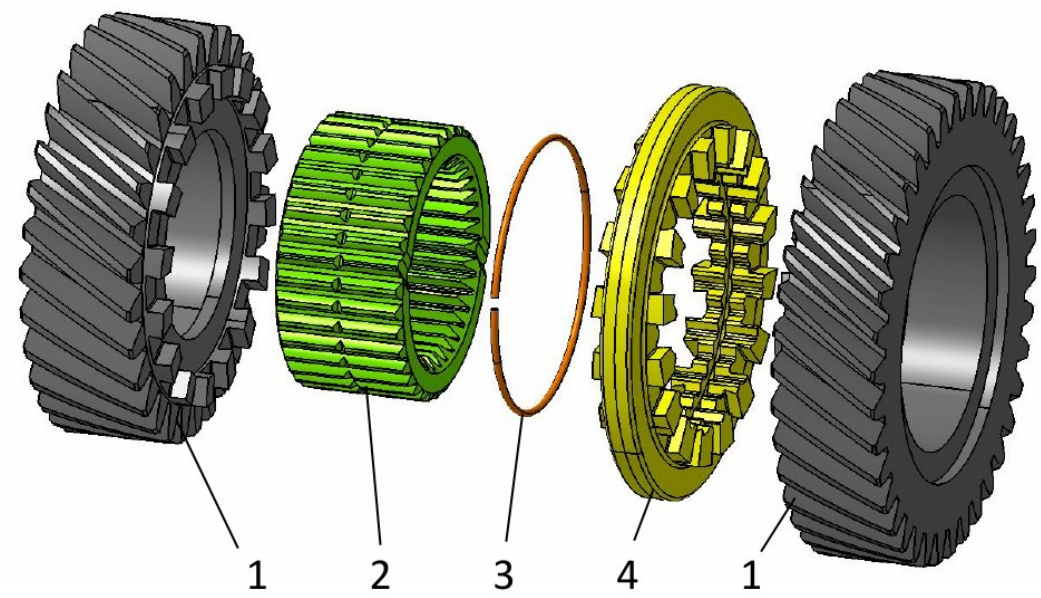

Figure 26: Maybach dog clutch – exploded view [38]
1 – gear wheel with face dogs; 2 – hub; 3 – blocking ring; 4 – sliding dog

All dogs have negative side angles to prevent unwanted disengagement. Figure 27 shows detail of the dogs' shape. No other blocking mechanism in the engaged state is present, the angular backlash is very high. The dogs' faces are tapered to fasten the shifting. The prototype was manufactured particularly to test NVH during engagement and wear of the dogs.

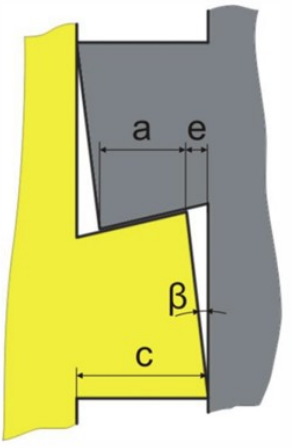

Figure 27: Geometry of the Maybach dogs [38]

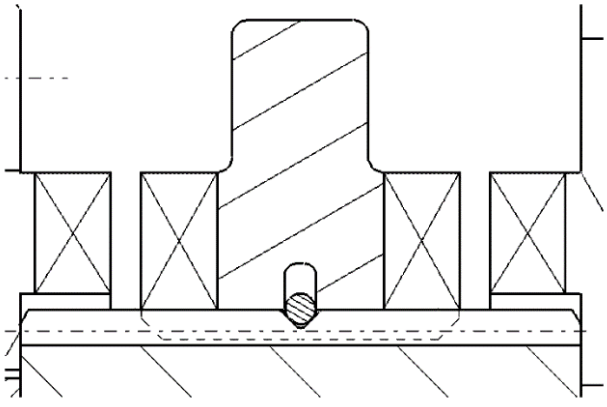

Figure 28: Sliding dog neutral blocking mechanism [38]

The measured maximum and RMS values of radial and axial acceleration during gearshifts for mismatch speeds lower than 500 min^{-1} were comparable with standard

synchronizer (measured at higher mismatch speed). This result was considered as very promising for further development; [39].

Figure 28 shows a section cut of the neutral blocking mechanism consisting of a C-shaped spring and grooves in the hub and the sliding dog. This idea served as an inspiration for the dog clutch with blocking mechanism.

2.2.6.2 Dog clutch with cylindrical dogs

This clutch was presented in 2011 Ing. Sikora's diploma thesis. It consists of hub (5) which is fixed to the gearbox shaft – radially using internal splines and axially sitting between the pair of idler gear wheels (1). Gear wheels have crowns with cylindrical face dogs connected to their sides. These dogs mesh with the sliding dog (3) when engaged. The clutch is operated by the gearshift sleeve (4). Blocking stones (7) and secure the sliding dog in the neutral and engaged positions under the pressure from coil springs (8); [40].

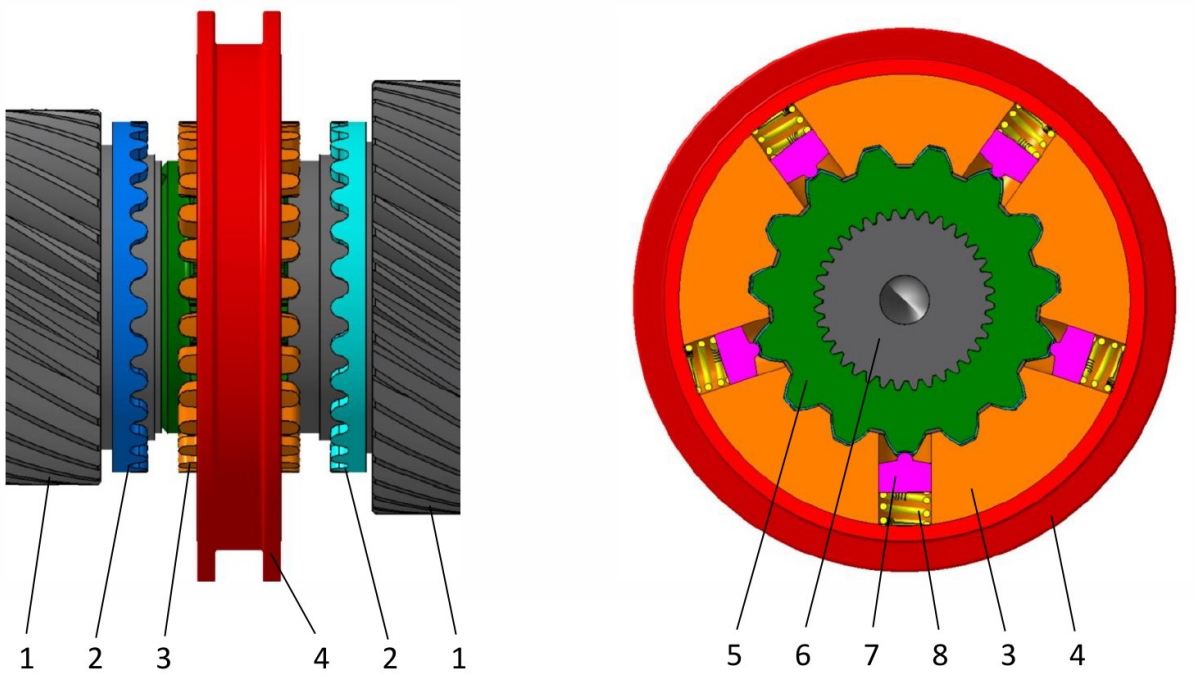

Figure 29: Dog clutch with cylindrical dogs [40]
1 – gear wheels; 2 – crowns with cylindrical dogs; 3 – sliding dog; 4 – gearshift sleeve; 5 – hub; 6 – gearbox input shaft; 7 – blocking stone; 8 – coil spring

The cylindrical shape of the dogs (see Figure 30) is very unusual. It is very favorable to minimize the angular backlash – in the engaged state, the backlash is almost eliminated. Details about transition surfaces between cylindrical dogs and their manufacturability are not described in the text. The shape is also favorable in terms of the probability of successful gearshifts. However, the risk of unsuccessful engagement (ending stuck in 'face-to face' contact) and bounce-back still exists due to the variable angle between the dogs at the moment of first contact.

The engaged position is secured by the blocking stones. These are pushed into the dents in the hub by coil springs. The force from coil springs must be large enough to secure the sliding dog in place even under the maximum transmitted torque. Considering a

reasonable safety factor (vibrations, wear of the contact surfaces, etc.), the springs and therefore the whole clutch packaging end up being quite large. Also, this means that for each disengagement the force acting on the sleeve must be larger than the blocking force which must be taken into account during gearshift actuators design.

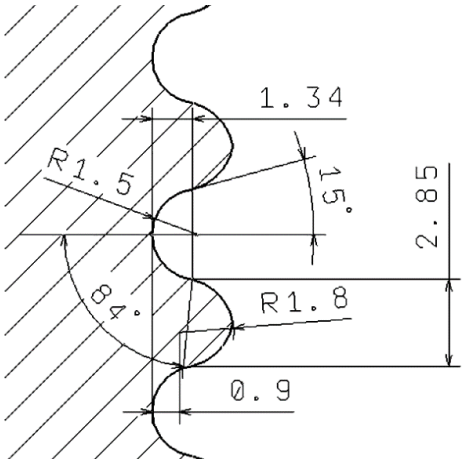

Figure 30: Geometry of the cylindrical dogs [40]

2.2.6.3 Pakoshift

This clutch is a result of Dr. Pakosta's idea implemented and presented in 2016 Ing. Lipčak's diploma thesis. It consists of hub (3) that is fixed to the gearbox shaft – radially using internal splines and axially sitting between the pair of idler gear wheels (5) and (6). Gear wheels have crowns with two dog types connected to their sides. These dogs mesh with the sliding dog (1) and the gearshift sleeve (2) when engaged; [41] and [42].

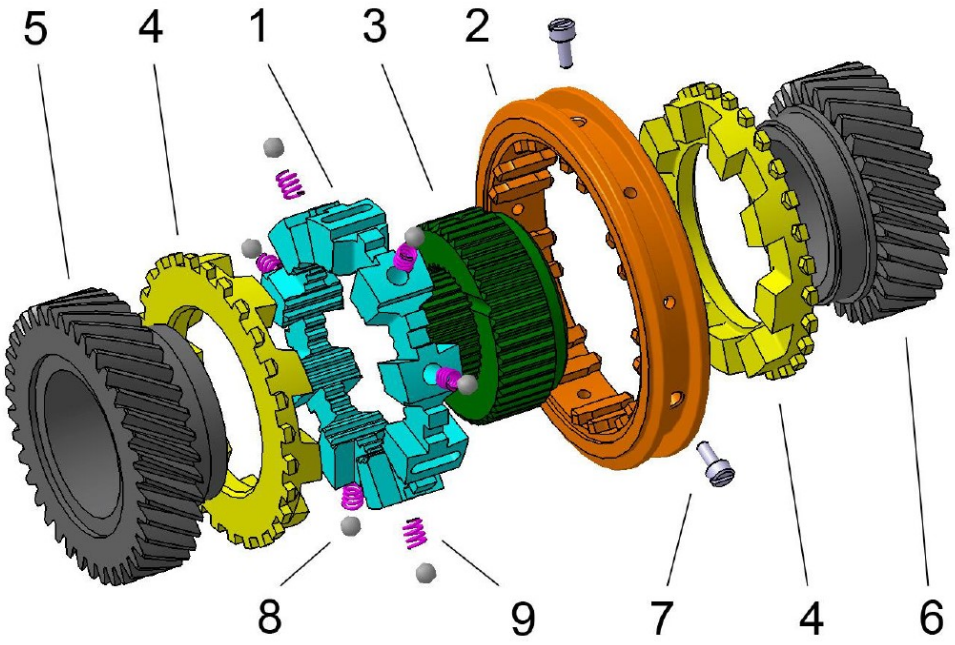

Figure 31: Pakoshift – exploded view [41]

1 – sliding dog; 2 – gearshift sleeve; 3 – hub; 4 – crown with dogs; 5 – gear wheel of 4th gear; 6 – gear wheel of 3rd gear; 7 – gearshift pins; 8 – blocking ball; 9 – coil spring

The engagement from the neutral position is started by the axial movement of the sleeve. Sliding dog moves with the sleeve due to the blocking balls (8) being pressed by the coil springs (9) into detents in the sleeve inner diameter. Bigger face dogs come first into contact and two scenarios can occur. The favorable one (see Figure 32) means that these face dogs mesh directly into the corresponding slots. Face dogs have a negative side angle and are pulled into mesh. Note that the faces of dogs are tapered, and therefore the direction of mismatch speed is important. In case of an unfavorable gearshift (see Figure 32), face-to-face contact occurs which results into axial force with opposite direction. This force can make the blocking balls skip out of the detents, which allows the sleeve move forward without the sliding dog. However, the sleeve can only move as far as the gearshift pins (7) allow. Gearshift pins provide another connection between the sleeve and the sliding dog. Unless the face dogs are in mesh, the gearshift pins do not allow the gearshift sleeve mesh with the smaller outer blocking dogs. Only when the face dogs are fully in mesh, the sleeve can move further and mesh with the blocking dogs to complete the engagement.

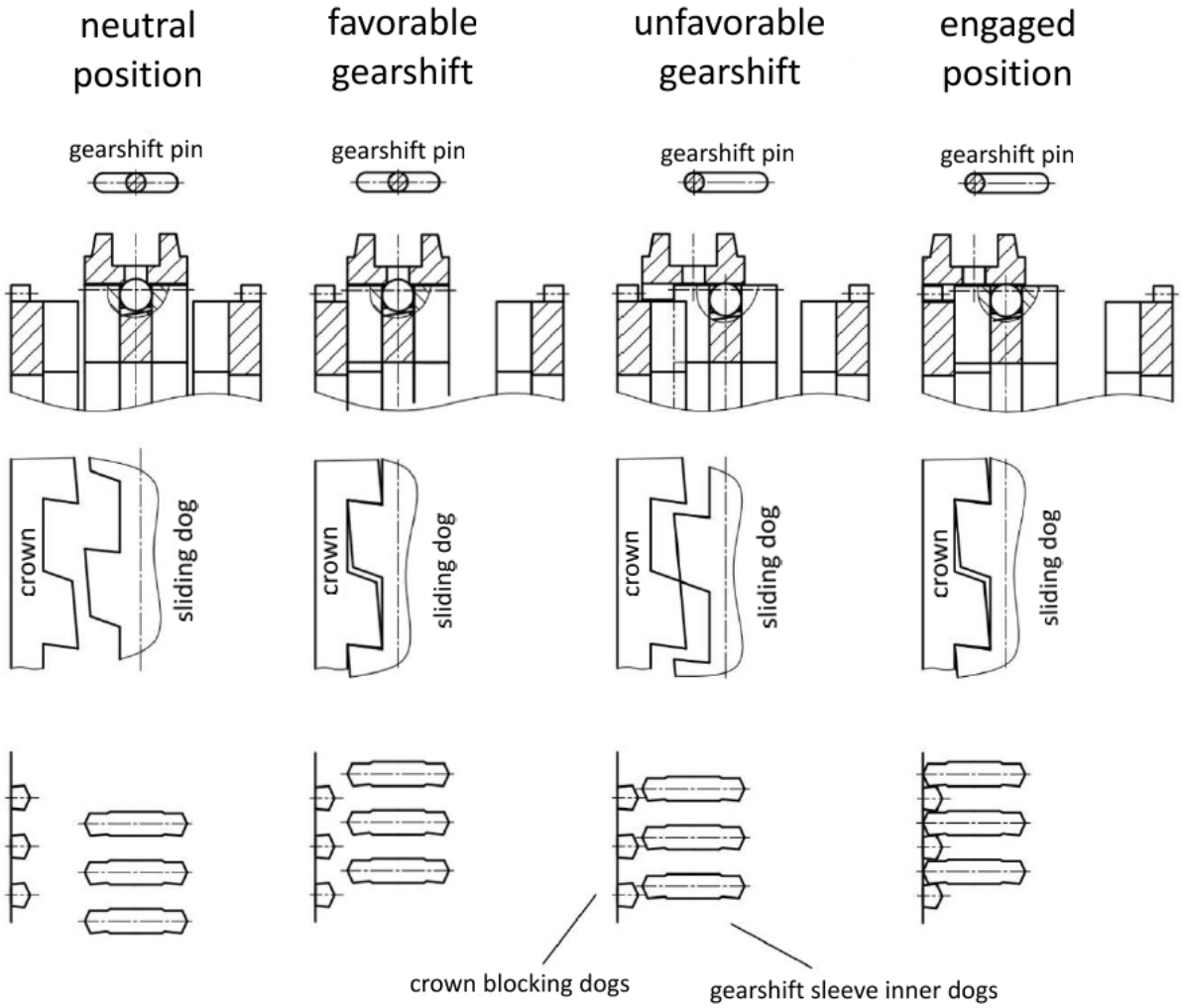

Figure 32: Engagement process of face dogs and blocking dogs [41]

The combination of negative and positive side angle of the face dogs allows variable backlash during engagement. In the beginning of the mesh, this backlash is bigger to maximize the size of slots and improve successful gearshift probability. In the engaged state, it is smaller

to secure the correct position of the crown and sleeve for smooth engagement of the blocking dogs.

Blocking dogs are very similar to synchronizer dogs. The biggest difference is that the negative angle ψ is one side only. This side transmits the brake torque of the engine. The main torque is transmitted by the larger face dogs. The primary purpose of blocking dogs is to minimize the backlash in the engaged state.

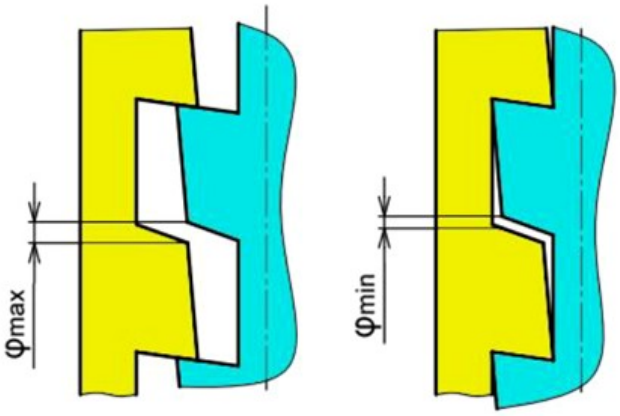

Figure 33: Backlash during engagement [41]

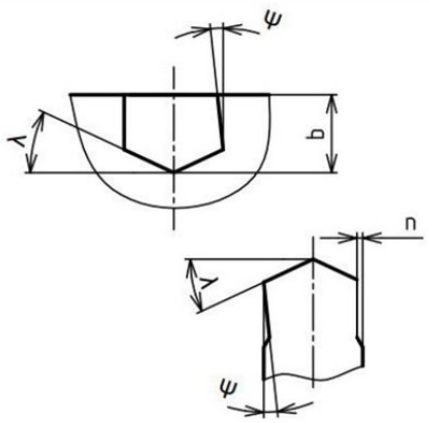

Figure 34: Geometry of blocking dogs [41]

Due to the double dogs the face dogs taper angle can be bigger than usual. This minimizes the face-to-face contact probability and bounce-back probability even for quite big mismatch speeds.

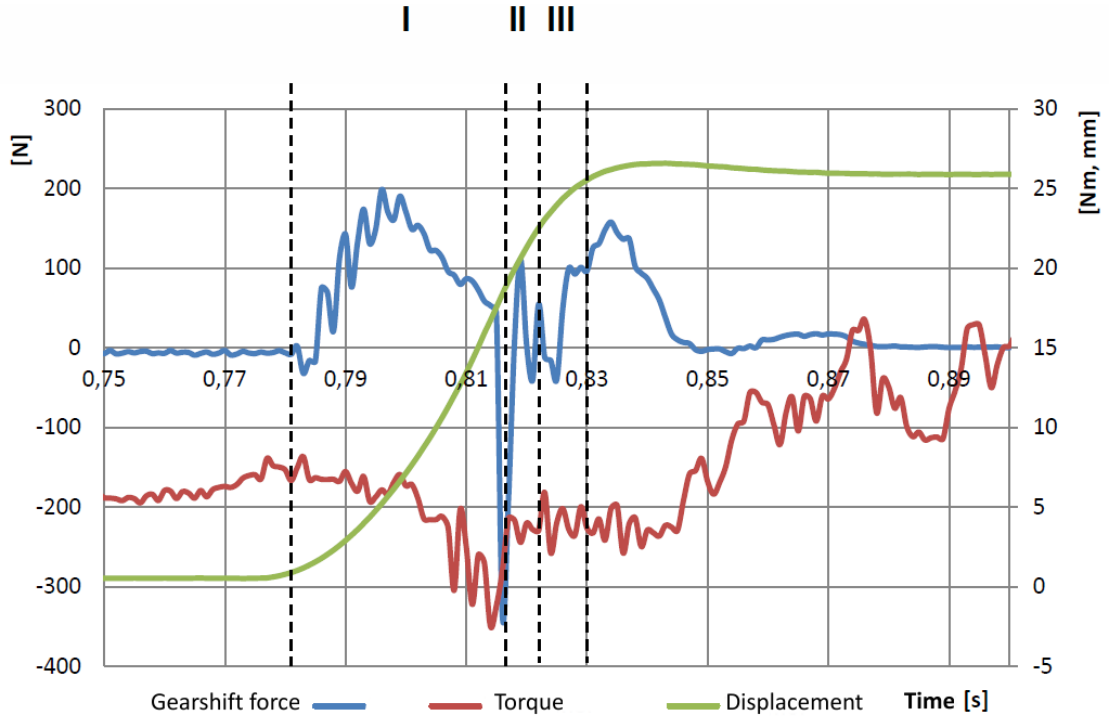

Figure 35: Example of Pakoshift behavior during gearshift [41]

The disadvantages of Pakoshift are the large number of parts, the manufacturing costs of all the dogs and the absence of a neutral position blocking mechanism – there was no space

left to incorporate it into the clutch body. Neutral is therefore secured by the gearshift fork, only resulting in quicker wear of gearshift stones. Furthermore, it may not be compatible with electric motors because it is designed for lower maximum torque in one direction.

Pakoshift prototype was tested at the inertia test bench. Figure 35 shows typical behavior of the Pakoshift clutch when engaged from neutral to 3rd gear with mismatch speed 110 min^{-1}. The displacement curve is smooth, there is no face-to-face contact. High negative force values are caused by face dogs coming into contact and pulling each other into mesh. Overall, the gearshift time is very short – in this case around 50 ms.

2.2.6.4 Dog clutch with blocking mechanism

This design was proposed by the author of this dissertation thesis as a result of his diploma thesis [43]. Standard dog clutch with positive angle of the dogs is complemented by a unique blocking mechanism. The shape of the dogs minimizes angular backlash in engaged state, and the purely mechanical blocking mechanism prevents unwanted disengagement under load. Disengagement is possible under all operating conditions, even under load, the force needed for disengagement stays constant.

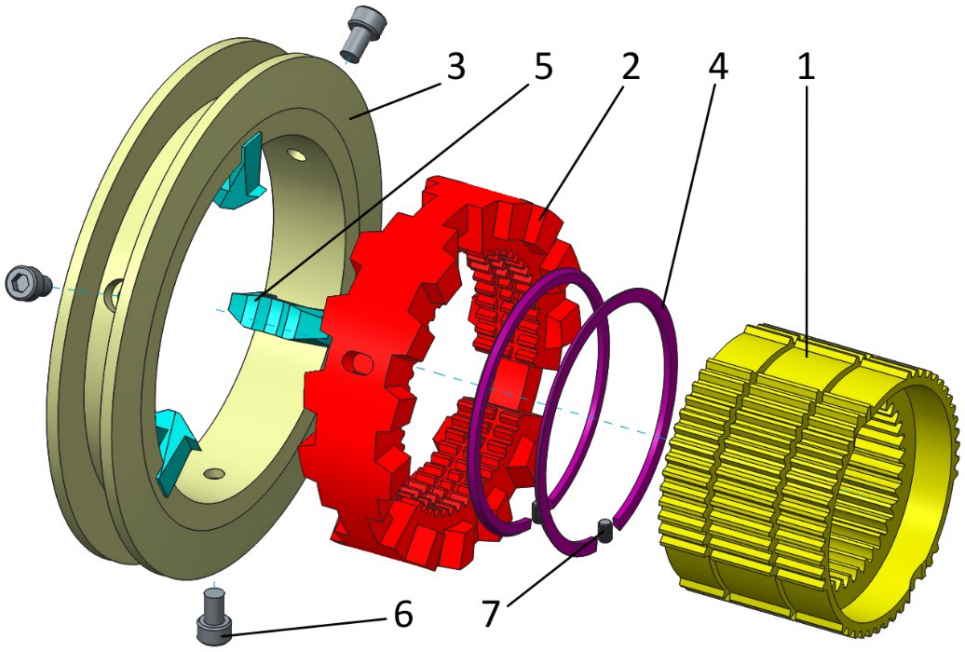

Figure 36: Dog clutch with blocking mechanism – exploded view [43]
1 – hub; 2 – sliding dog; 3 – gearshift sleeve; 4 – blocking rings; 5 – gearshift stones; 6 – gearshift pins; 7 – detent pins

The clutch consists of the hub (1) that is fixed to the gearbox shaft (radially using internal splines and axially sitting between the pair of idler gear wheels (9) – see Figure 36 and Figure 37). The gearshift is provided by the sliding dog (2) which is connected to the hub using internal toothing and can be moved axially. Its dogs mesh with the dogs of crowns (8) in the engaged state. These crowns are attached to the gear wheels (9). Three dogs are missing in the sliding dog and there are three symmetrically placed slots instead of these dogs. The movement of the sliding dog is controlled by the gearshift sleeve (3) through gearshift pins (6). There is an axial backlash between these pins and the sliding dog, which is important for

the mechanism functionality. Gearshift stones (5) are fixed to the gearshift sleeve. Gearshift stones encircle the sliding dog and control the shape of the blocking rings (4). Blocking rings are placed in the hub grooves and cannot rotate freely around the clutch axis of revolution due to detent pins (7). However, the internal diameter of the blocking rings is larger than the external diameter of the grooves. As a result, these C-shaped blocking rings can compress slightly under pressure of the gearshift stones.

In neutral position, the blocking rings are in the non-distorted state (see Figure 37). The width of the sliding dog is the same as the distance between blocking rings inner faces, therefore, the sliding dog cannot move until the blocking rings are compressed. The rings can be compressed due to the gearshift stones inner geometry by axial movement of the gearshift sleeve. However, this requires a force to be applied on the gearshift sleeve by the gearshift fork. As a result, all parts of the clutch are axially secured in neutral position despite the mentioned backlash between the gearshift pins and the sliding dog (visible in the lower half of Figure 37).

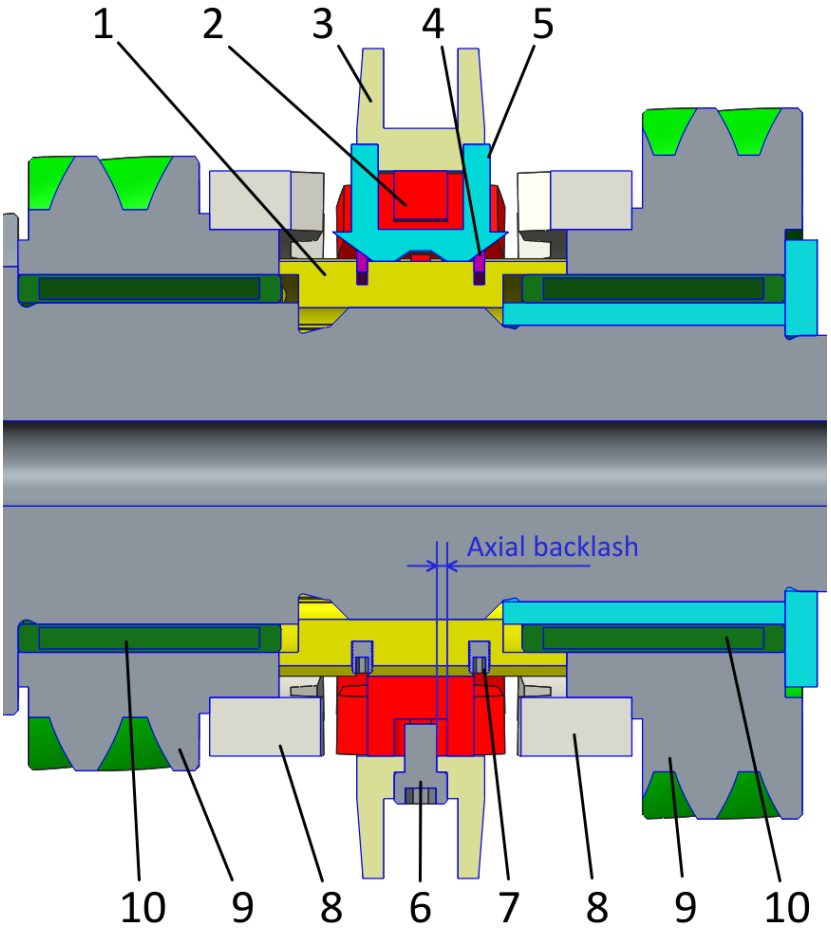

Figure 37: Dog clutch with blocking mechanism mounted into the MQ200 gearbox [43]
1 – hub; 2 – sliding dog; 3 – gearshift sleeve; 4 – blocking rings; 5 – gearshift stones; 6 – gearshift pins; 7 – detent pins; 8 – crowns with face dogs; 9 – idler gears; 10 – roller bearings

The gearshift process starts when the force is applied to the gearshift sleeve. Gearshift stones act on the blocking ring in a selected direction and compress the blocking ring. In this first phase, only the sleeve and stones are move due to the backlash between the sliding dog

and gearshift pins. When this backlash vanishes, phase two takes place. The blocking ring is now compressed and allows the sliding dog to move with the sleeve and engage. As the sliding dog slides into the engaged position, the gearshift stones no longer hold the blocking rings in the compressed state due to the geometry of the stones. The blocking rings are held compressed by the sliding dog inner diameter only. Therefore, they immediately enlarge into their non-distorted shape when the engagement is completed because they fit into the grooves made into the inner diameter of the sliding dog. At this moment the gearshift is finished, all the parts are secured in their position again. The axial force that acts on the dogs cannot disengage the clutch (Figure 41).

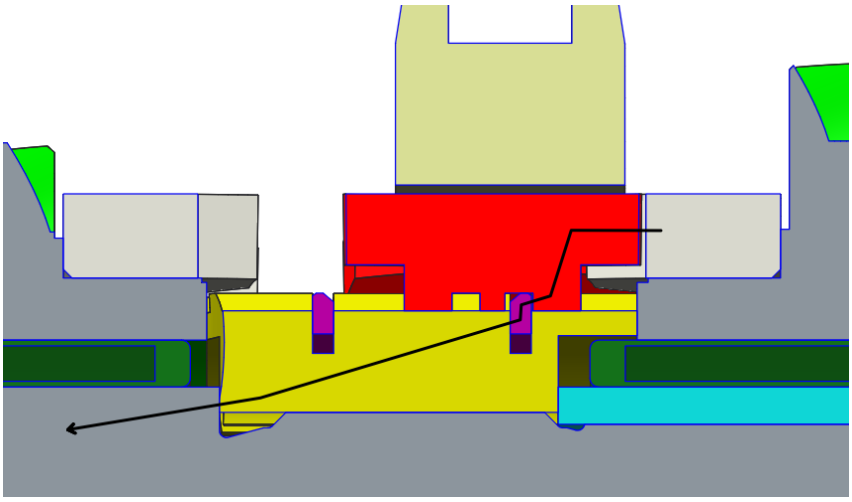

Figure 38: Axial force flow in the engaged state [43]

The disengagement process can also be divided into two phases. In the first one, the movement of the sleeve forces the blocking rings to shrink again through the gearshift stones. The sliding dog remains stationary due to the backlash between the gearshift pins and the sliding dog. In the second phase, when there is no backlash left, the sliding dog is taken to the neutral position by the sleeve. Since the blocking rings tend to expand, they secure the neutral position of all components again.

The dog clutch with blocking mechanism does not require any changes in the gear selector mechanism. It offered axial space saving up to 39% in the test gearbox compared to the original synchronizer.

2.2.6.5 Bous clutch

This clutch was presented in 2019 Ing. Bous' diploma thesis. It was not designed for mass-produced passenger cars as the previous clutches, but rather for racing applications. Its design is based on the Zeroshift idea. It consists of hub (1) which is fixed to the gearbox shaft – radially using internal splines and axially sitting between the pair of idler gear wheels. Gear wheels have face dogs manufactured on their sides. These dogs have negative side angles to prevent unwanted disengagement. Two sliding dogs (4) with gearshift stones (3) are present. However, only one gearshift sleeve (2) is needed. The sliding dogs are connected by coil springs (5).

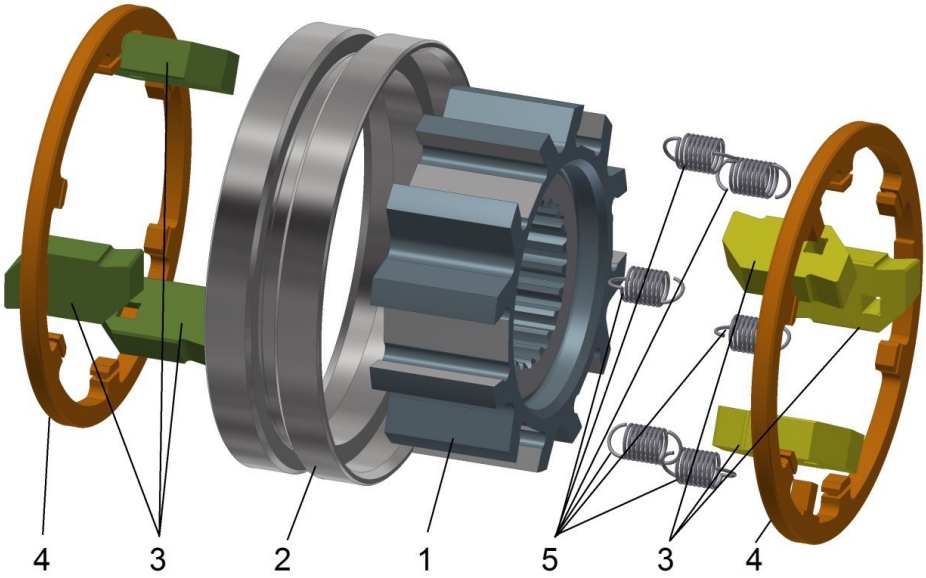

Figure 39: Bous clutch – exploded view [44]
1 – hub; 2 – gearshift sleeve; 3 – gearshift stones; 4 – sliding dogs; 5 – coil springs

The gearshift process is very similar to Zeroshift, especially during upshift. Downshift is more complicated and requires precise engine torque control due to the lack of a second gearshift sleeve. Details are described in the author's thesis [44]. The biggest advantage of the clutch is the ability to upshift without torque interruption – gearshift times are therefore reaching zero. Compared to Zeroshift, the lack of a second sleeve makes this clutch easier to incorporate into standard gearboxes with minimal changes in the gear selector mechanism. Disadvantages include complicated downshifts and shifting of the first gear while the vehicle is stationary.

2.3 Dog Clutches in Passenger Car Gearboxes

Intended usage of the new gearshift mechanism in parallel shaft gearboxes was already discussed in Chapter 1. This chapter lists some recent passenger car mass-produced gearboxes and concepts with dog clutches.

2.3.1 Dedicated Hybrid Transmissions

Dedicated hybrid transmissions (DHT) are purpose-built gearboxes for hybrid vehicles. They integrate an electric motor into their construction to maximize efficiency and reduce the packaging for hybrid vehicles, an external synchronization is therefore present; [11]. The electric motor takes over some of the functions conventionally provided by the gearbox paired with combustion engine (e.g., synchronization during gearshift, torque gap filling). Design of DHTs usually provides more gear combinations for less shifted gear wheel pairs compared to conventional gearboxes; [45].

High gearshift quality of dog clutches combined with torque and speed control in a DHT approves recent study-dissertation thesis of Dr.-Ing. König; [46]. Main target was to implement fast and comfortable gear shifts using parallel-series hybrid powertrain DE-REX (Figure 40) consisting of a 2-speed gearbox with 4 dog clutches, 2 electric motors and an ICE.

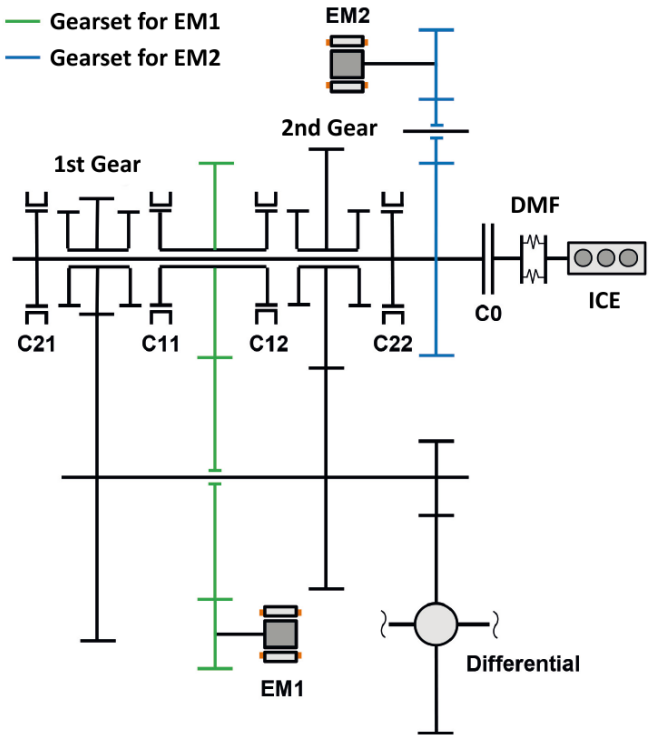

Figure 40: DE-REX transmission diagram [47]

For the investigations of dog clutch engagement, measurements were carried out with dog clutches with tapered faces as well as dog clutches without tapered faces. Nonetheless, the final DE-REX concept is using dogs with tapered faces. Based on the analytical model a control software was designed to coordinate the torque and angular speeds of individual components and later tested in the DE-REX prototype. Figure 41 shows very good power-on upshift quality measured as a lateral acceleration of the vehicle.

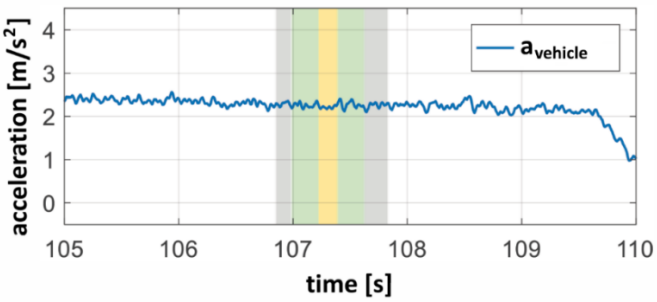

Figure 41: Electric power-on upshift at 50% drive pedal in the DE-REX vehicle [46]

Renault developed in cooperation with AVL its own hybrid DHT transmission offered for the Clio since the model year 2020. It uses three dog clutches for six gear wheel pairs; [48]. In total, 15 drive modes are available. There is one ICE and two electric motors as power sources. The main electric motor (highlighted blue in Figure 42) is capable of torque compensation during gearshifts in the 4-speed gearbox (highlighted red). On the other hand, the smaller electric motor (highlighted green) is responsible for external synchronization. Thanks to reducing the number of gear wheel pairs and replacing the synchronizers with dog clutches, the length of the DHT transmission is similar to conventional mechanical gearbox (for comparison see Figure 43).

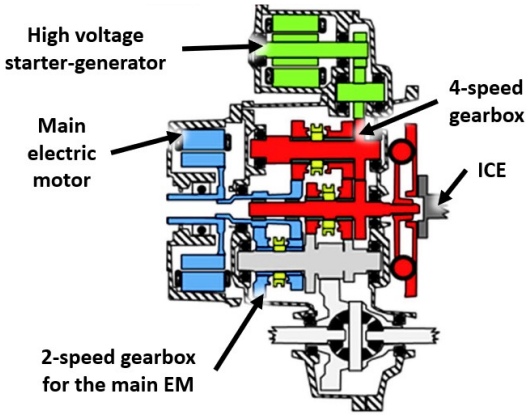

Figure 42: Renault E-tech DHT – schematics of the powertrain [48]

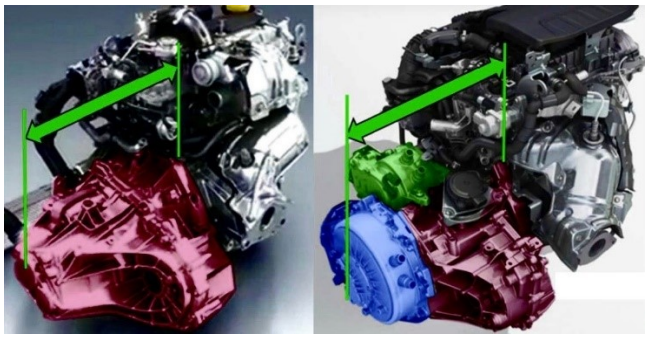

Figure 43: Length comparison of mechanical gearbox (left) and E-tech DHT (right) [48]

Another recent DHT examples include the Future Hybrid concept from AVL (consideration of dog clutches is mentioned in paper [49]) or DHT concept with planetary gearset described in 2018 Ing. Kaněra's diploma thesis [50]. Special dog clutches (described in Chapter 2.2.2) were also designed for Aisin's HAMT concept described in paper [34]. It is based on parallel 2-axis manual gearbox with EM in P2 position (see Figure 44) and aims on efficiency and shift change quality. ICE is used for external synchronization and electric motor to fill the torque gap during gearshifts. Aisin states that their calculations and measurements confirm 1% efficiency increment through whole RPM spectrum just thanks to replacing synchronizers by dog clutches.

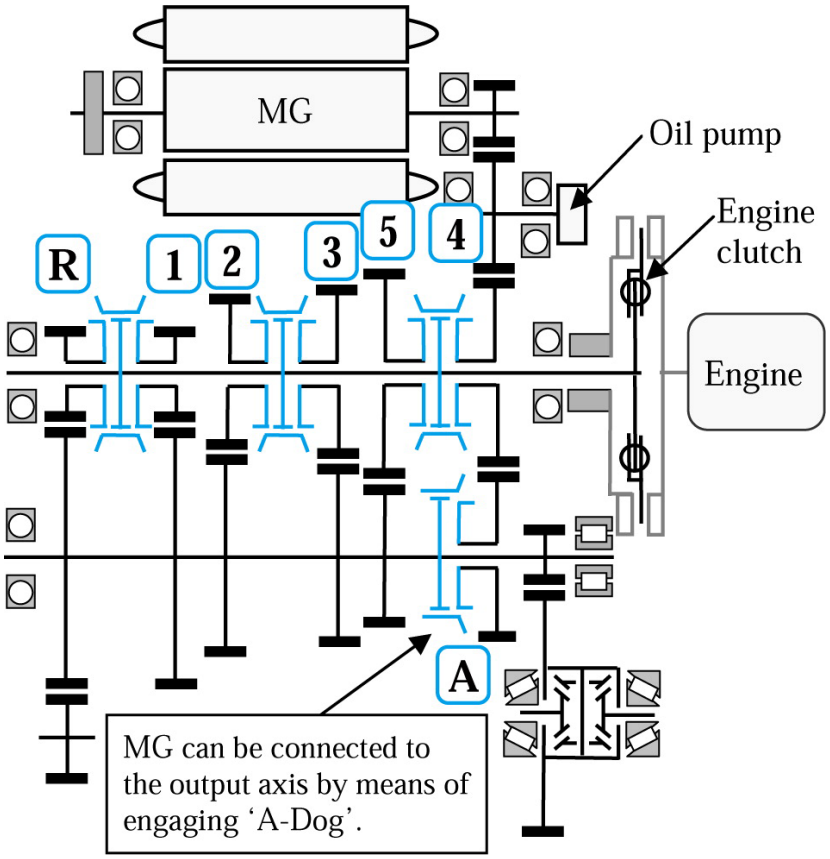

Figure 44: Aisin HAMT – schematics of the powertrain [34]

2.3.2 Transmissions for EVs

A dog clutch is also used in the 2-speed transmission for EVs Porsche Taycan and AUDI e-tron GT at their rear axles; [51]. Here the dog clutch is responsible for shifting 1st gear and parking lock. It connects the sun of the planetary gear set to the stator and only blocks rotation in one direction, the other direction is blocked by freewheel (see Figure 45 for the detailed transmission scheme).

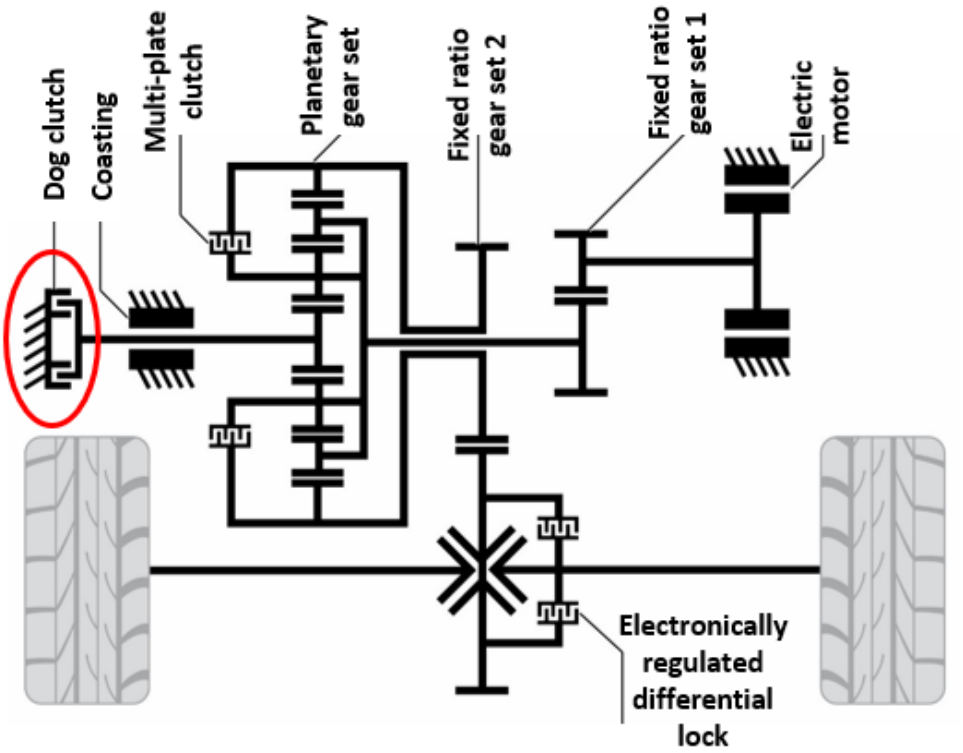

Figure 45: AUDI/Porsche 2-speed EV transmission equipped with a dog clutch [51]

The known issue of this solution is that after engaging the dog clutch under particular conditions, disengaging may not be possible. This happens due to elasticity of the components and pre-tensioning the dog clutch (see Figure 46). Critical situations for this scenario are shifting during rapid acceleration in 1st gear and parking on steep incline. Shifting 2nd gear is then not possible due to the negative angles on the dogs' sides and pre-tensioning with the freewheel. Therefore, electronics and sensors are necessary to monitor the conditions and prevent risky engagement. As a result, the total amount of recuperation is limited as that is not possible without the dog clutch engaged. A dog clutch with positive angles on the dogs' sides would not have to deal with such a problem.

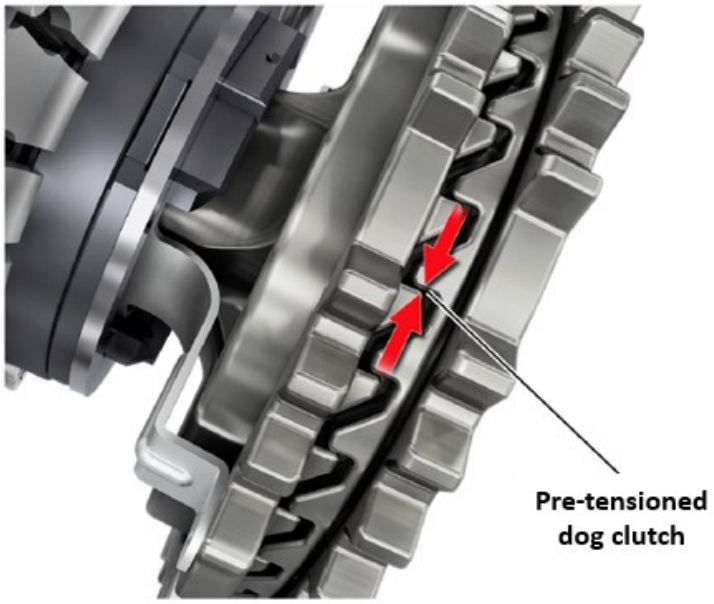

Figure 46: Pre-tensioned dog clutch in the 2-speed AUDI/Porsche EV transmission [51]

2.3.3 Automatic Transmissions

Possibilities of incorporating dog clutches into automatic gearboxes were also investigated; [52].Two dog clutches are used in ZF 9HP48 gearbox (Figure 47) instead of wet multi-plate clutches. Main motivation is reducing friction losses and weight of parts with large diameter and high-pressure oil systems as described in papers by ZF [53] and Toyota [54]. However, without the electric motor and external synchronization, providing comfortable shifts and guaranteeing long service life is complicated; [55]. It requires advanced research in controlling software and shifting strategies such as [56].

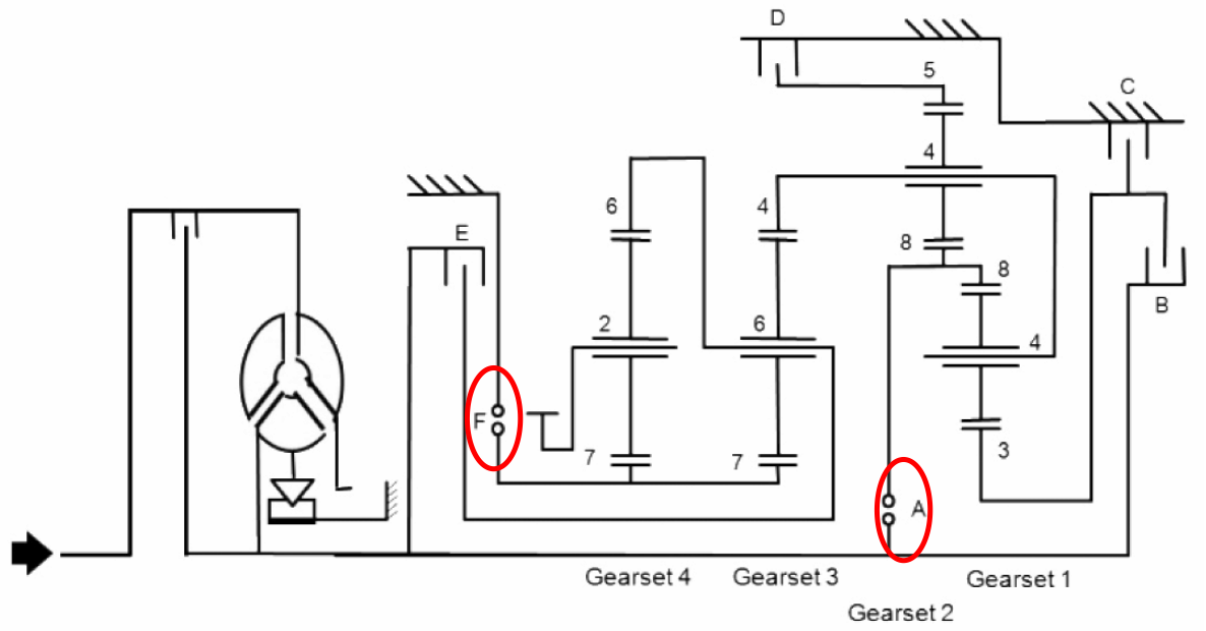

Figure 47: Scheme of ZF 9HP48 equipped with two dog clutches at positions A and F [53]

3 Objectives

Based on the research of existing gearshift mechanisms and their properties, the following objectives of the thesis were defined:

1) **Design a gearshift mechanism based on the dog clutch** capable of fulfilling the following requirements:
   - Angular backlash in the engaged state is minimized.
   - Disengaging is possible even under load.

   The positive angle of the sides of the dogs according to Chapter 2.1.3.1 may be necessary to comply with these requirements. Furthermore, the dog clutch must be competitive with other mass-produced dog clutches and must therefore meet the other standard dog clutch properties listed in Chapter 2.1.3.4.

2) **Verify the gearshift mechanism experimentally** using a physical prototype and a suitable test bench. Testing will focus on the gearshifts and torque transmission and can be divided into the following areas:
   - Functionality.
   - Service life.
   - NVH and comfort.

4 Solution

Based on the research summarized in Chapter 2, the author decided to continue in the development of the *'Dog clutch with blocking mechanism'* described in Chapter 2.2.6.4 since it is the only mechanism capable of fulfilling the requirements described in Chapter 2.1.3.4.

Uniqueness of the design was later confirmed by patent No. 307443 *'Řadicí spojka'* [I.] by the Czech Office of Industrial Property and utility model *'Schaltungskupplung'* [II.] by the German Patent and Trade Mark Office.

4.1 Initial Design of Dog Clutch With Blocking Mechanism

This decision was also supported by early tests of the first clutch prototype manufactured according to the drawings included in the author's diploma thesis [43]. This prototype (shown in Figure 48) was designed as a replacement for the 3rd and 4th gear synchronizer of the 5-speed MQ200 gearbox, similarly to other gearshift mechanisms tested at CTU in Prague. See Chapter 2.2.6 and [37] for further details on the gearbox.

All parts of the prototype were machined and heat treated except for the blocking rings. These were modified CFS-38 constant section snap rings made by company Rotor Clip; [57].The crowns with face dogs were connected to the gear wheels with Loctite 638 glue; [58]. See Chapter 2.2.6.4 and [43] for details on the manufactured prototype, including drawings.

Figure 48: First manufactured prototype of the dog clutch with blocking mechanism

The initial testing of this prototype was carried out mainly at the gearbox test bench in its original configuration described in Chapter 5.1.1 and was mainly focused on functionality of the dog clutch (smooth movement of the shift sleeve, appropriate engagement and disengagement, etc.) and testing possibilities at the test bench. The dog clutch was proven to

be functional. The results were presented in papers [III.], [IV.] and article [IX.]. However, an improvement potential was identified for both the dog clutch and the test bench.

4.1.1 Improvement Potential in Design

Blocking rings are the most important structural part of the clutch and their faultless operation is essential for proper clutch functionality. However, their size, shape and properties must meet contradictory requirements. Height of the rings (see Figure 49) must be large enough to transmit the axial force under load (as shown in Figure 38) and to keep the contact pressures between rings' sides and adjacent parts low. On the other hand, increasing height means increasing force needed for shrinking the ring and therefore increasing contact pressures between the gearshift stones and blocking ring during gearshift. This determines the minimal gearshift force which must be applied by the driver or actuator at each gearshift. Decreasing the gearshift force is therefore necessary to avoid oversized and heavy actuators and gear selector mechanism.

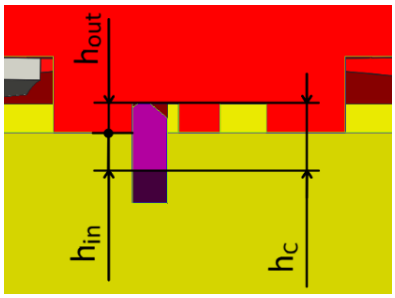

Figure 49: Heights of the blocking ring in the initial design

The height of the blocking ring also significantly influences the mechanical bending stress in the ring during the gearshift. Calculations in author's thesis [43] implied that for the proposed ring height only expensive high strength steel would be able to sustain the stress without plastic deformation. This is even more limiting since the rings are bent and stressed repeatedly during each gearshift of their service life. The original design required two blocking rings for one clutch (one ring for each gear). Under lower bending stress and contact pressures only one ring might be sufficient. Initial tests also revealed that the assembly of the blocking rings into the hub is very inconvenient. The rings must be bended to larger diameter in the opposite direction than for the rest of their service life – which is difficult to perform and may cause plastic deformation. Reducing the height of the rings would be helpful here as well.

Using gearshift pins for sliding connection between the sliding dog and the shift sleeve is inappropriate. The angle between the axes of rotation of the sliding dog and the shift sleeve can go up to degrees and the joint cannot be considered as sliding joint. Assembly of 7 different parts to create the shift sleeve also increases the costs of precise manufacturing.

In the engaged state, one of the rings is not held concentrically with the axis of rotation and must be aligned and centered by the gearshift stones during the clutch disengagement. The tests showed that this enlarges the gearshift force even more because of friction between the ring and the groove in the clutch body and should be redesigned.

Another potential was identified in the production process. The unique shape of the dogs with positive side angles makes the technology of powder pressing suitable. Its principle is densification of the metal powder in a rigid die under high pressure (see Figure 50). This technology is suitable for mass production parts at reasonable costs, its advantages are high productivity and minimal material losses; [59].

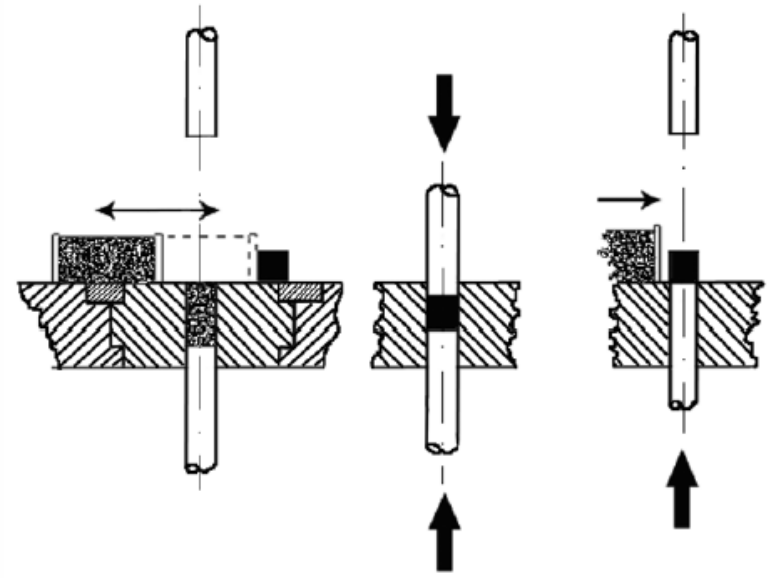

Figure 50: Three stages in a powder compaction cycle during die pressing [60]
1) Filling the die; 2) Densifying the powder; 3) Ejecting the compact

Powder pressed parts in automotive were usually designed to serve a specific purpose and later in their life cycle redesigned to be producible by powder metallurgy; [59]. Design update of the dog clutch with blocking mechanism is a unique opportunity to incorporate the design boundaries and limitations of powder metallurgy into the shape and principles of the final product. Handbooks [60] and literature [61] and [62] were used for design recommendations, properties of materials based on powders etc.

4.1.2 Improvement Potential in Testing

The gearbox test bench lacked precise external synchronization and its connection to the control program. This is a crucial requirement for dog clutch gearshift testing. Also, the quality of various measured quantities was found insufficient. Measurement of NVH during gearshift was impossible due to lacking sensors and infrastructure. Further details can be found in Chapter 5.1.1.

4.2 Final Design of Dog Clutch With Blocking Mechanism

The final design is a result of multiple iterations. Key features described in the patent and utility model were carefully retained in the design and therefore the patent protection still applies (for full text of the patent see Attachment 1). On the other hand, all the areas of potential improvement described in Chapter 4.1.1 were addressed. I would like to express my gratitude to the Department of Gearbox Development at ŠKODA AUTO which was willing to

provide feedback throughout the design process. The final design was presented in [V.] and later [VIII.].

4.2.1 Dog Clutch Design and Improvements

The clutch consists of hub (1) fixed to the gearbox shaft, sliding gear (2) which can move axially to engage selected gear, gearshift sleeve (3) to control the sliding gear movement and blocking ring (4) to secure the sliding gear in desired positions. Sliding gear is divided into two halves connected by screws (5) and pins (6) because of assembly reasons. One blocking ring is enough to secure sliding dog in all three positions (engaged/neutral/engaged) and gearshift sleeve in neutral position as well. No modifications of the standard MT/AMT gear selector mechanism are needed.

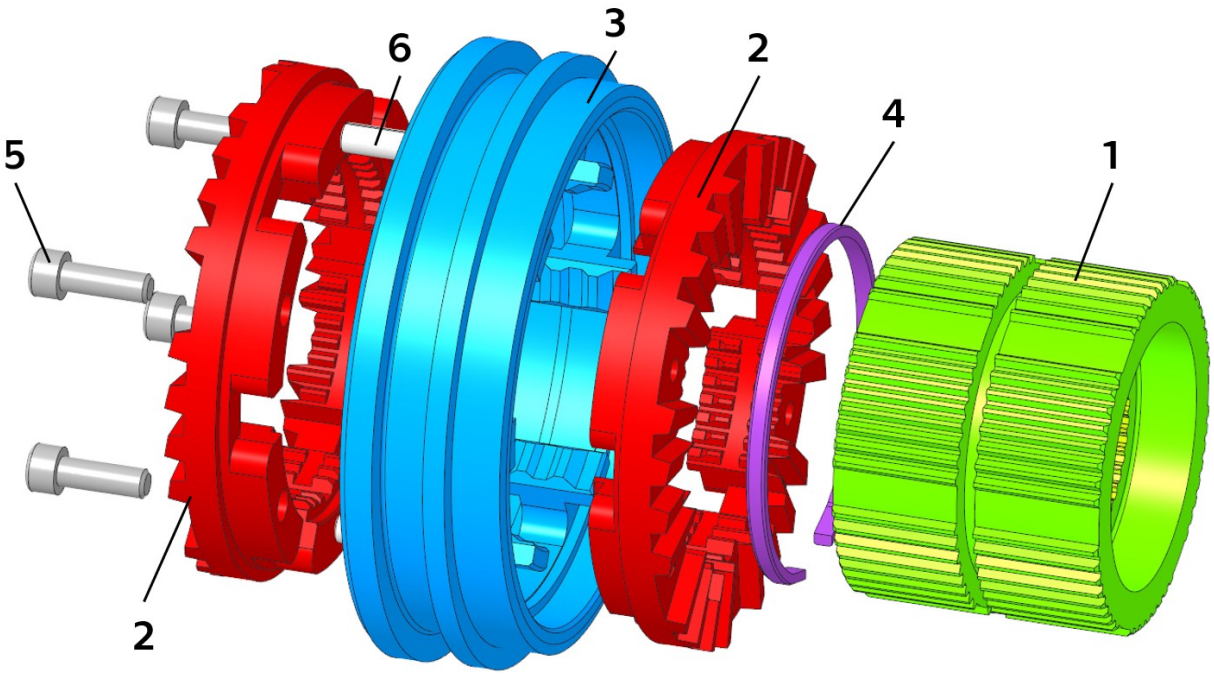

Figure 51: Final dog clutch with blocking mechanism design
1 – hub; 2 – sliding gear; 3 – gearshift sleeve; 4 – blocking ring; 5 – screws; 6 – pins

The width of the blocking ring is now larger than its height. This significantly reduced the maximal bending stress in the ring which grows with the third power of the height. The blocking ring is always held concentric with the hub by the sliding gear or gearshift sleeve, it maintains contact with at least one of them all the time. There are now 6 contact points between the gearshift sleeve and the blocking ring (black arrows in Figure 52) instead of 3. This helps keep the shape of the ring uniform during the compression. Non-uniformly deformed ring would stick out of the groove and would collide with the movement of the sliding gear. This would be accompanied by excessive wear of the ring at the area of greatest bending stress. The ends of the ring are not deformed by the sleeve and are therefore intentionally bent inwards to prevent the wear (purple arrows in Figure 52).

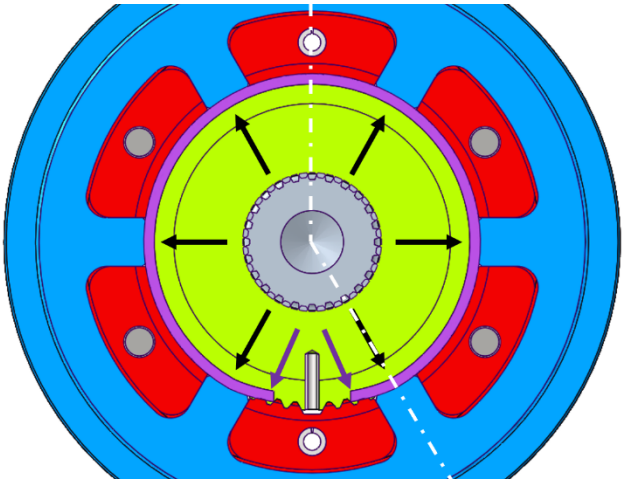

Figure 52: Cross-section of the final dog clutch design in neutral position

The gearshift process is shown below in Figure 53 (the cross section placement is marked by dash dotted line in Figure 52). For animation see Attachment 2). Suppose that the gear on the right should be shifted. The gearshift process will take place as follows:

- **Position 1 – Neutral.** The axial backlash between the sliding gear and gearshift sleeve is marked by the black arrows. The blocking ring holds in neutral position both parts (sliding gear shown in upper half, gearshift sleeve shown in lower half).
- **Position 2 – Engagement preparation.** The sleeve starts moving to the right, controlled by the gearshift fork. It compresses the blocking ring. However, the sliding gear stays in neutral position until the axial backlash disappears.
- **Position 3 – Engagement in process.** The axial backlash disappeared. The sliding gear is pushed to the right by the sleeve. Blocking ring stays compressed.
- **Position 4 – Engagement termination.** The sliding gear reached its furthest position, the gearshift dogs are engaged. The sleeve and the sliding gear stop moving axially. In this position, the blocking ring is not held in compressed state by any of these parts.
- **Position 5 – Engaged.** Therefore, immediately after the previous phase, the blocking ring enlarges into its natural position and fits into the inner groove of the sliding gear. As a result, the axial force acting on the sliding gear in the mesh because of torque transfer cannot disengage the clutch.
- **Position 6 – Disengagement preparation.** To disengage the clutch, the sleeve first must start moving to the left to compress the blocking ring. Again, there is an axial backlash present. Therefore, the sliding gear stays in the engaged position so far.
- **Position 7 – Disengagement in progress.** The blocking ring is fully compressed and axial backlash disappeared. The sleeve pushes the sliding gear into neutral position.
- **Position 8 – Disengagement termination.** The sleeve reaches the neutral position and stops. Because of the axial backlash, the sliding gear is not yet in neutral position. However, it still has kinetic energy in axial direction and the groove on its inside is shaped in the way that the decompressing blocking ring acts on it in the direction towards neutral position.
- **Position 9 – Neutral.** The dog clutch is back in neutral position identical to Position 1.

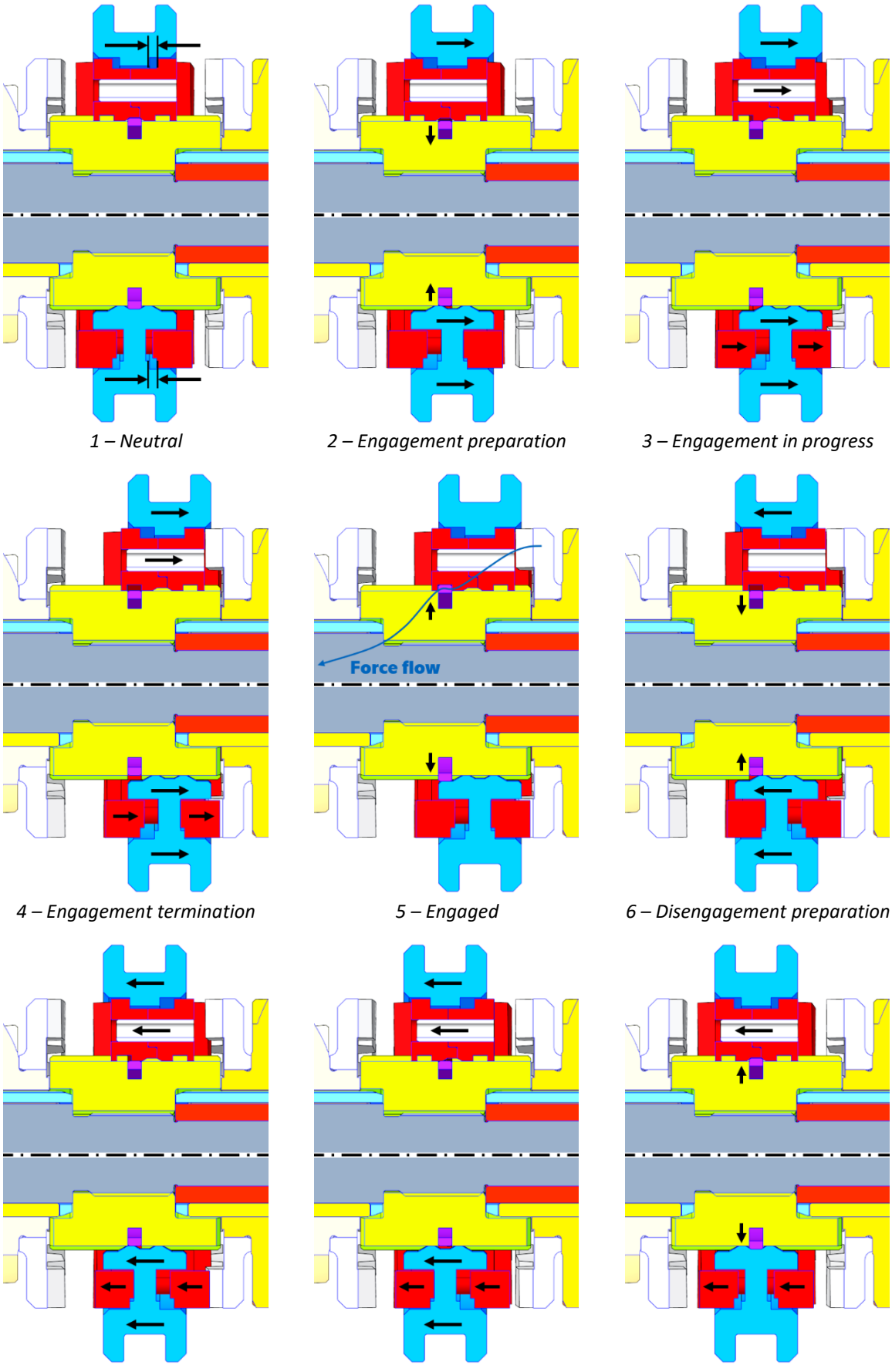

1 – Neutral *2 – Engagement preparation* *3 – Engagement in progress*

4 – Engagement termination *5 – Engaged* *6 – Disengagement preparation*

7 – Disengagement in progress *8 – Disengagement termination* *9 – Neutral*

Figure 53: Gearshift process of the dog clutch with blocking mechanism

Prototypes of the clutch were designed for the MQ200 gearbox similarly to previous designs. In this gearbox, the blocking ring withstands axial forces up to 2 kN. This force arises in the mesh of the dogs when transferring maximum torque of 200 Nm. However, when acting on the gearshift sleeve, the force required for engaging and disengaging the clutch is only approximately 45 N. This is far less than are the permissible values and comparable with the lowest forces needed for manual shifting; [5]. Further details and calculations about the blocking ring are summarized in Chapter 4.2.4.

Sliding gear and gearshift sleeve design were successfully optimized for powder metallurgy. For sliding gear divided into two parts, only the two grooves for blocking rings and threads on one half for screws cannot be produced by pressing and would have to be machined. For gearshift sleeve, this can be said only about the inner groove for neutral position. Even though there is another groove on the outer diameter of the sleeve for the gear selector fork, this remained only due to compatibility of the prototype and test gearbox. This groove can be eliminated as described in e.g., [63].

There are no additional parts between the sliding gear and gearshift sleeve. Figure 54 shows that the axial backlash between these parts was preserved along with the functionality. The contact surfaces between the two parts are located around the entire circumference and guarantee concentric alignment of both parts with the hub.

The blocking ring cannot rotate freely around the shaft axis of rotation because of the pin as shown in the upper part of Figure 54.

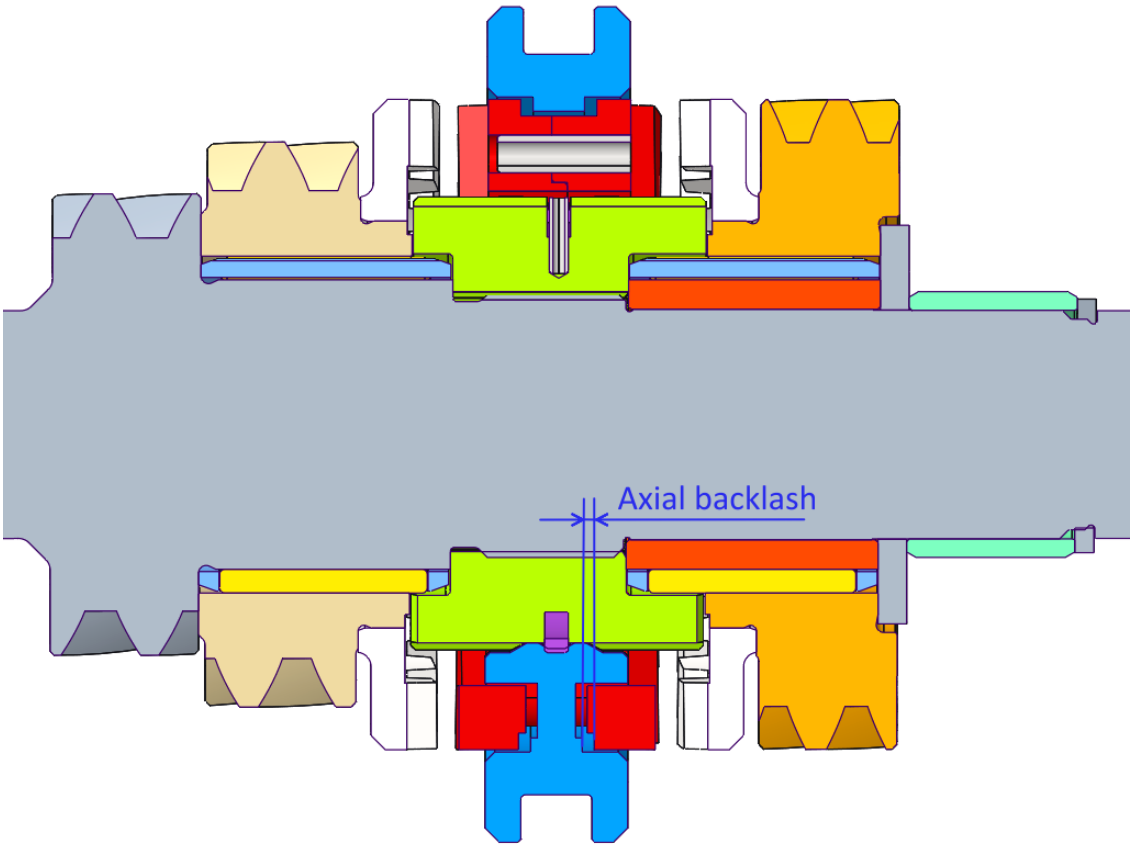

Figure 54: Dog clutch assembled between a pair of shifted gear wheels

4.2.2 Program for Parametric Design

For easy and fast design of the dog clutch with blocking mechanism, a parametric design program was developed in MS Excel. It is particularly suitable when considering the use of the dog clutch in a new type of gearbox or other new application. With a small number of input parameters, the program guides the user through the design of the dog clutch from the shaft through the hub, the sliding gear to the gearshift sleeve. The result is then the basic dimensions of the clutch. Emphasis is placed on clarity and intuitive design flow. The colors of the individual parts of the program correspond to the colors of the individual components of the dog clutch in the pictures and legends. Generally, following input parameters are required for the design:

- Maximal torque in both directions.
- Shaft diameter under the hub.
- Maximal gearshift force allowed at the gearshift sleeve.

Other input parameters are mainly material constants, safety factors etc. These can remain unchanged in default values to quickly find out the approximate dimensions of the clutch or can be tuned for final clutch design.

The program also provides calculations of critical places and parts of the clutch and indicates the results with not only numbers but also red/green color of the result fields. The controlled parameters include, for example:

- Stress in torsion (shaft, hub).
- Contact pressure at splines (shaft, hub, sliding gear).
- Contact pressure at the sides of the ring.
- Gearshift force needed for ring compression.
- Stress in bending (blocking ring).

The design program also interactively shows the size of the contact surface on the side of the dogs based on the given geometry – see Figure 55. This size may be insufficient for low and wide dogs combined with large angles on their faces. Limiting this surface only by maximal contact pressure is not recommended since the dogs are usually hardened and can withstand very high pressures. This would allow very small contact surfaces. However, we must keep in mind that for physical clutch, size of this surface is also determined by manufacturing tolerances. As a result of these and the rounding of the edges of the dogs due to wear, the contact area could be too small. On rounded edges, the angle of the normal, on which the force generated in the dogs lies during torque transmission, would then change. Changing this angle would increase the axial force that the blocking ring has to withstand and therefore the ring would be undesirably overloaded. The user can therefore request not only maximal contact pressure but also minimal length of the contact surface.

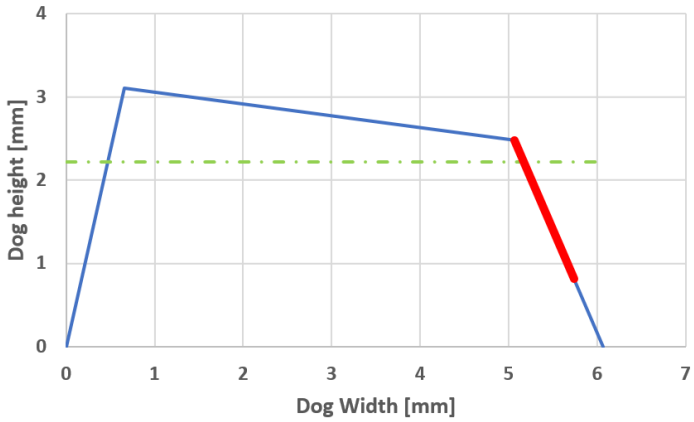

Figure 55: Contact height on the side of the dog as shown by the design program

The majority of the controls and checks provided by the program are simple engineering calculations. Many others were also performed on top of these during the design of the prototype. These will not be elaborated in this text. However, calculations of gearshift dogs and blocking ring will be demonstrated in the following chapters. These were labeled as most critical for successful application of the clutch and performed in deeper detail.

4.2.3 Gearshift Dogs

The basic shape of the dogs without considering the tapered faces is designed according to [24]. The emphasis is on manufacturability and proper function of the dogs during shifting. Parallel edges of the sides of the dogs (marked red in Figure 56) make sure that the sides of the dogs are planar. The geometry for manufacturing is defined at common median line for both engaged sets of dogs to make sure they can successfully engage even with the negative influence of manufacturing precision.

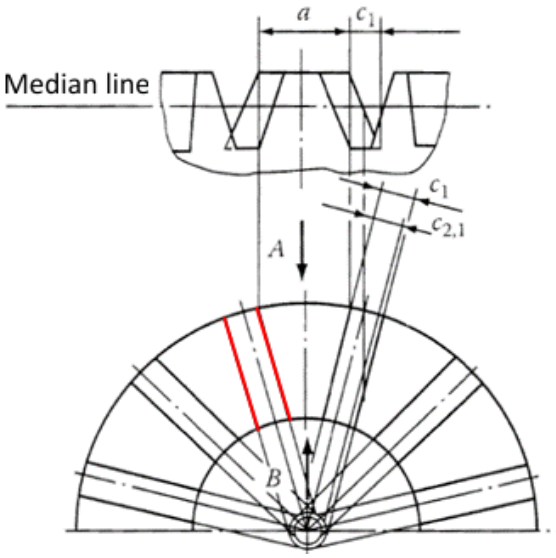

Figure 56: Trapezoidal dogs geometry design diagram [24]

Gearshift dogs at the prototype clutches for MQ200 gearbox have negative angles of both sides (10°) and also tapered faces (10°). These were chosen as a compromise to prevent self-locking, guarantee quick gearshifts, keep sufficient contact surface on the sides and other

criteria based on the research (mainly [19], [24] and [26]), calculations (see following chapters) and experience with previous dog clutch prototypes. The dogs are identical for all the forward gears for easier manufacturing of the prototypes.

Generally, the angle of the sides can be different for each side of the dogs. However, this is useful only in the case of different maximum load of each side (e.g., different maximum torque when powered by an ICE and braked by an ICE). Then the angle of the braked side may be larger to maximize the probability of successful gearshift thanks to larger gap between the dogs. Thanks to the lower load by engine braking, the axial force under load does not exceed the values for the other side when powered by the engine. However, for symmetrical load (e.g., electric motor), this is not applicable.

Compared to the initial design, the dogs in the final design are smaller and there are twice as many of them – see Figure 57. This contributes to faster gearshifts thanks to higher engagement probability and shorter movement of the sliding gear. It also translates into smaller size of the clutch in axial direction. Every fourth dog of the sliding gear is omitted because of the screws and pins. Therefore, there are 18 dogs on each side of the sliding gear for torque transmission in engaged position.

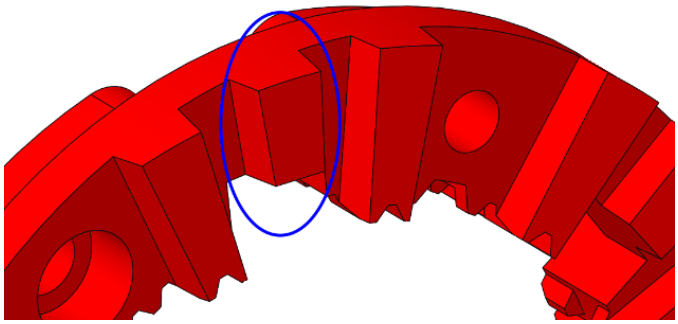

Figure 57: Detail of the dogs at the sliding gear

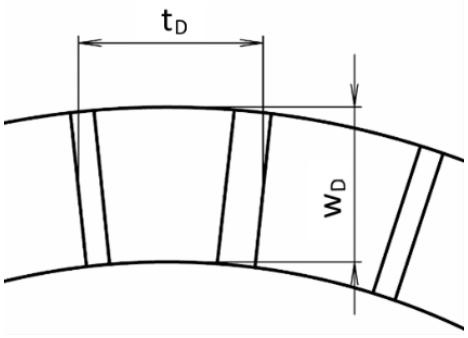

Figure 58: Width and medium thickness of the dog

Table 4 shows numerical values of basic dimensions of the dogs. They will be later used in the calculation of bending and contact stress at the dogs. Figure 58 shows where the width and medium thickness of the dog are measured. Blue circle in Figure 57 marks the basic dog shape used for calculations. The additional parts of the wider dogs near the center of the sliding gear are there for easier manufacturing and are not considered as functional.

Table 4: Dimensions of the dogs

Pitch circle diameter	d_D	61.75 mm
Maximal height	h_D	3.2 mm
Width	w_D	6.7 mm
Medium thickness	t_D	4.66 mm
Contact height (power)	$h_{cD,P}$	3.1 mm
Contact height (braking)	$h_{cD,B}$	1.5 mm
Number of dogs on the sliding gear	n_D	18
Side angle	α	10°

One of the main objectives of this dog design was to minimize the angular backlash in the engaged state. The prototype of the clutch was designed for maximum axial backlash of 0.5 mm in the engaged state due to manufacturing tolerances. For the dimensions specified in Table 4, the circumferential backlash is less than 0.2 mm and angular backlash less than 0.1°. This backlash is approximately an order of magnitude lower compared to conventional synchronizer, even though they might feel gapless at the first glance; [5].

The sliding gear and dog rings at the shifted wheels are made of 14140 steel according to ČSN standards. The steel is then surface hardened. The 14140 steel is also a material commonly used for the manufacture of involute gears. The standard ČSN 01 4686-5 [64] specifies following basic fatigue characteristics (see Figure 59) for a medium quality class 14140 steel:

Table 5: Basic material characteristics of 14140 steel

Tensile strength	σ_m	785 MPa
Yield strength	σ_e	539 MPa
Fatigue strength (bending; R=0)	σ_w	450 MPa
Exponent for S-N curve (bending; R=0)	q	9
Breaking point of S-N curve (bending; R=0)	N_W	$3*10^6$

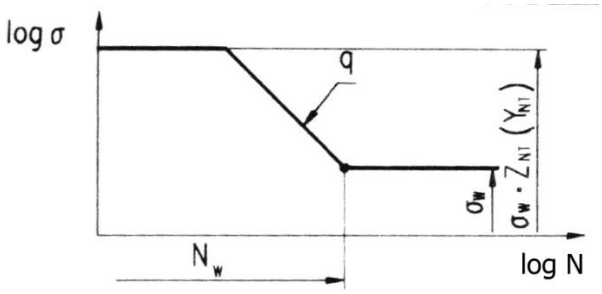

Figure 59: S-N curve (logarithmic scale) showing basic fatigue characteristics [65]

4.2.3.1 Static strength

Calculation of static strength will be demonstrated for the 1st gear. The clutch for 1st and 2nd gear is placed at the output shaft of the gearbox (see Figure 25) and the load is therefore multiplied by their gear ratio. The gear ratio of the 1st gear is the highest. The load is not distributed evenly between the dogs. Coefficient of uneven distribution was used regarding to [66]. This assumes that a lower number of dogs are carrying the load due to limited manufacturing precision and other effects. Input parameters affecting the load of the dogs are summarized in Table 6.

Table 6: Input parameters affecting the load of the dogs

Maximum torque at the input of the gearbox	$T_{max,in}$	200 Nm
Gear ratio of the 1st gear	i_1	3.769
Coefficient of uneven distribution	ψ	0.5

The load (force *F*) acting in half of the dogs' height was considered for all the load states. To calculate the bending stress in the base of the dog, the idea of bending stress of an encastered beam bended by a force according to Figure 60 was used.

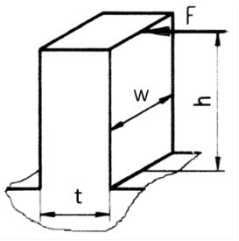

Figure 60: Schematics of bending an encastered beam

$$\sigma_b = \frac{12 \cdot T_{max,in} \cdot h_D \cdot i_1}{d_D \cdot w_D \cdot t_D^2 \cdot n_D \cdot \psi} \tag{1}$$

Shear stress was calculated for the base of the dogs:

$$\tau_s = \frac{2 \cdot T_{max,in} \cdot i_1}{d_D \cdot t_D \cdot w_D \cdot n_D \cdot \psi} \tag{2}$$

The limit for shear stress was calculated based on the von Mises criterion:

$$\tau_e = \frac{\sigma_e}{\sqrt{3}} \tag{3}$$

Contact pressure is different for the two sides of the dogs. In cooperation with combustion engines, generally the maximum load on one side of the dog is larger than on the other side. This is because the braking torque of the engine is lower than the maximum torque output. This is favorable for the shape of the dog with tapered face – the sides with smaller contact surface can be designed to transmit the braking torque only. However, electric motors are capable of identical torque values in both directions. Even though the prototype of the clutch was supposed to be tested in gearbox for combustion engines, the dog clutch with blocking mechanism is designed for both powertrains. Therefore, I decided to calculate the contact pressure at the side of the dog with smaller contact surface for maximal load:

$$p_c = \frac{2 \cdot T_{max,in} \cdot i_1}{d_D \cdot h_{cD,B} \cdot w_D \cdot n_D \cdot \psi} \tag{4}$$

The limit for contact pressure was calculated regarding to [64]:

$$p_e = 4 \cdot \sigma_e \tag{5}$$

Results of the static strength analysis are summarized in Table 7. Calculated maximums for each load state are compared to the limit value. The minimum safety factor is equal to 2.9 for bending stress – the dogs are satisfactory in terms of static strength.

Table 7: Static strength results

Load state	Calculated [MPa]		Limit [MPa]		Safety factor	
Bending	σ_b	184	σ_e	539	k_b	2.9
Shear	τ_s	88	τ_e	311	k_s	3.5
Contact pressure	p_c	270	p_e	2,156	k_p	8

4.2.3.2 Fatigue in bending

First, the fatigue strength in bending and service life of the dogs transmitting the torque. For involute gearing, this area is in literature described in large detail. However, for face dogs, very little to no guidelines can be found. Therefore, literature describing involute gearing (mainly [65], [67] and [68]) was used with modifications reflecting the differences.

The load cycle was based on the drive cycle used by ŠKODA AUTO for service life testing of the engine, gearbox and other components. The data is measured during polygon driving tests as an accelerated life test of the MQ200 gearbox – 120,000 km on the polygon corresponds to roughly 250,000 to 300,000 km by the consumer. The cycle consists of several sub-cycles that respect various driving situations. Each sub-cycle is discretized with a time step of 2 seconds. The measured variables are engine speed, torque at the left and right wheel, and current gear.

Calculation will be demonstrated for the 3rd gear. All gear ratios are known, the gearshift clutch for 3rd gear is located at the input shaft. Considering efficiency of the gears, torque at the gearshift clutch can be calculated:

$$T_{clutch} = \frac{T_L + T_R}{i_{sum} \cdot \eta_{sum}} \tag{6}$$

For 3rd gear only we get the resulting load, one sub-cycle is shown as an example in Figure 61. To determine the damaging effect of the cycle, it must be decomposed into a simpler set of individual stress cycles that will have the same damaging effect.

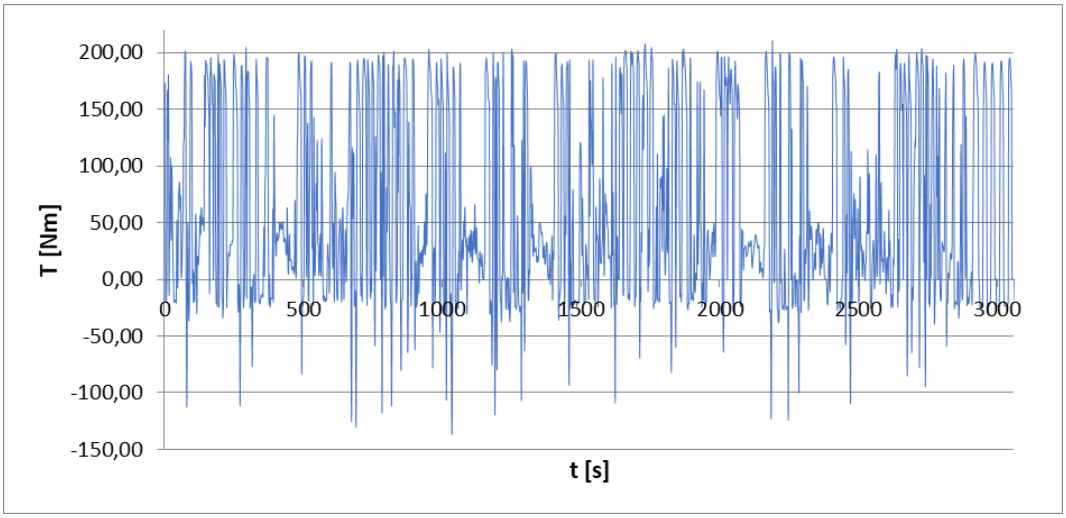

Figure 61: Load at the 3rd gear clutch during the drive cycle

For cycle decomposition, the rainflow-counting algorithm is mostly used. It is based on the physical nature of the behaviour of the actual metallic material in the plastic deformation region; [68]. The MATLAB computational software implicitly includes a rainflow solver within the Signal processing toolbox module according to the standard [69]. The output of this solver is the mean and amplitude values of individual load cycles and their frequencies.

The asymmetry of these decomposed load cycles takes on different general values. Involute gearing is normally stressed by cycles with an asymmetry coefficient equal to zero. In

order to use the meteorology developed for this gearing, it is necessary to convert the decomposed cycles into cycles with identical asymmetry and therefore identical damaging effects. The formula according [70] to was used for the conversion, where it is defined for stress values. The bending and contact stresses in the clutch teeth or dogs are a linear function of the load, so the formula can be rewritten into torque values. Consequently, the upper load torque of the equivalent passing cycle:

$$T_{up,eq} = T_{up} \cdot (1 - R)^n \tag{7}$$

The coefficient of cycle asymmetry *R* is defined as the ratio of the lower and upper values of the load, the coefficient *n* is considered for steels 0.5 as standard, although for some types of steels other values can be chosen to better describe their fatigue behaviour; [71]. Cycles with negative mean values were first converted to cycles with positive mean values using a weighting factor of 1.2 regarding to [65]. This is because these cycles apply bending stress in the opposite direction (in the case of the dog clutch, it is the engine braking mode).

Sorting the equivalent values of the load torques by magnitude, we obtain Figure 62. These values can already be used to calculate the service life of the gearshift dogs.

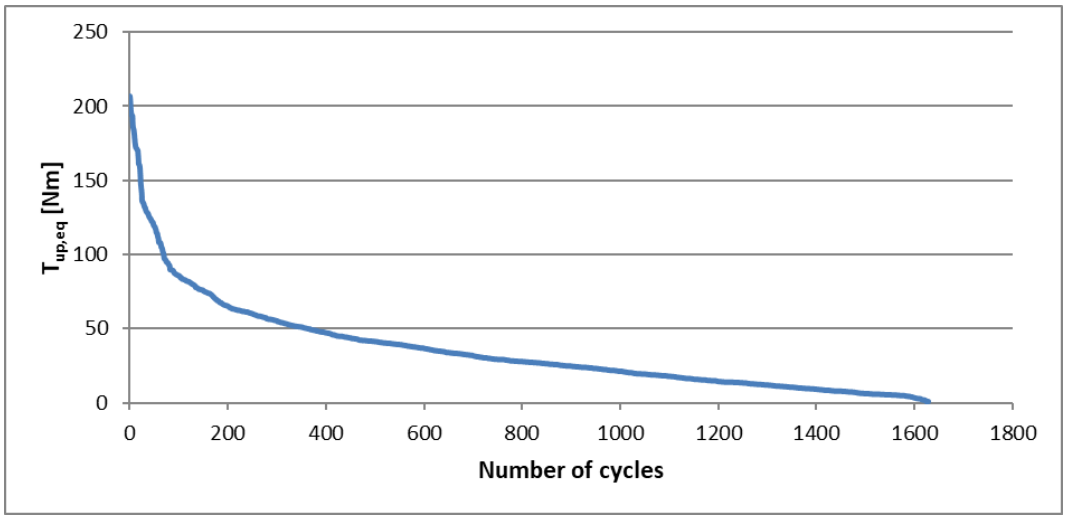

Figure 62: Load spectrum of equivalent torques for 3rd gear

The ČSN standards 01 4686-2 and 01 4686-3 [64] contain many correction coefficients that are used to convert the fatigue limits into permissible bending and contact stresses, some of which may even increase the fatigue limit (e.g., surface roughness and lubricant coefficients). Another way of increasing the fatigue limit in gears is e.g., shot peening – local strengthening of the surface layer of the component; [72]. For the dogs of the clutch, the influence of these coefficients is negligible compared to the factor of uniformity of stress distribution on individual dogs. For involute gearing, a very small number of teeth are simultaneously in mesh (usually ca. one to three teeth), whereas for dog clutches all dogs are in constant mesh. However, due to manufacturing tolerances and other factors, it cannot be assumed that the load is distributed uniformly between the dogs. In the first step of the calculation, the most conservative assumption was made, that only one dog is responsible for transmitting all the load.

To determine the fatigue damage of a component, knowing the load spectrum, we can either perform the calculation using equivalent load or we can use one of the linear fatigue damage accumulation hypotheses. These are based on several simplified assumptions, according to [65], in particular:

- The intensity of damage at a given load level is directly proportional to the number of load cycles at that stress level.
- The total amount of work required to produce a fracture is the same for each stress level.
- The damage at all stress levels is equivalent and the resulting degree of damage to the component is simply the sum of the partial damage at each stress level.
- The S-N curve determined for single stress level loading (constant amplitude) is also valid for variable amplitude.
- The frequency of the applied stress does not affect the result.

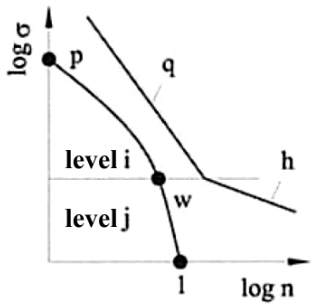

Figure 63: Schematics of Haibach hypothesis (logarithmic scale) [65]

Haibach hypothesis was chosen (for schematics see Figure 63), it is suitable for all types of stress spectra and is becoming the standard for calculating involute gearing, [65]:

$$D_C = \frac{\sum_{i=k}^{p} n_i \cdot \sigma_i^q}{N_W \cdot \sigma_W^q} + \frac{\sum_{j=1}^{w} n_j \cdot \sigma_j^h}{N_W \cdot \sigma_W^h} \tag{8}$$

The resulting fatigue damage of a component D_C consists of partial damage from two groups of stresses visually represented in Figure 63:

1) **Level *i*.** Stresses above the fatigue limit – limited by the curve with exponent q.
2) **Level *j*.** Stresses below the fatigue limit – limited by the curve with exponent h which is regarding to [65] usually calculated as:

$$h \doteq 2 \cdot q - 1 \tag{9}$$

The remaining parameters required for the fatigue damage calculation can be found in Table 5 and the decomposed load cycle. The formula for fatigue bending stress is analogous to the Equation (1) and Figure 60 used in static strength calculation:

$$\sigma_{b,f} = \frac{6 \cdot T_{up,eq} \cdot \frac{h_D}{2}}{d_D \cdot w_D \cdot t_D^2} \tag{10}$$

Although we consider the loading of only one dog, all stress values obtained in this way are less than the fatigue limit of the material. It is therefore clear that the fatigue damage will

be very small. The final value of fatigue damage D_C in bending stress caused by the service life cycle on the dog of 3rd gear is only ca. $2.7*10^{-4}$.

A component failure probability of 50% is represented by fatigue damage of D_C equal to 1. Compared to this value, the calculated fatigue damage is very small. The dogs of the 3rd gear of the prototype clutch are therefore oversized in terms of bending fatigue strength. The same can be said about all the other gears.

4.2.3.3 Fatigue in contact pressure

Similarly to previous calculation of fatigue stress in bending, contact pressure during torque transmission and resulting fatigue strength were calculated. Thanks to very high fatigue strength in pressure of the 14140 steel (1,140 MPa; [64]), fatigue damage in pressure is ca. $1*10^{-10}$ and lower for all the gears and therefore negligible (even when considering only one dog transferring all the load).

4.2.3.4 Static strength and fatigue during gearshifts

All the previous calculations considered load coming from the torque flow between the engine and wheel in the engaged state. However, the dogs are also loaded for a very short time period during the gearshift when their sides first come into contact with the sides of the opposite dogs and the mismatch speed of both shifted parts has to be cancelled out (see Chapter 2.1.3.2 for details of the engagement process). In this case, the dogs are not loaded in the half of their height but rather on the top where the dogs come first into contact. This makes the bending stress even more critical compared to shear stress. For comparison with static bending stress, we need to first calculate at least an approximate value of the load. This can be achieved, for example, by using the following formula:

$$T_{shift,max} = J_{total} \cdot \frac{\Delta\omega}{\Delta t} \tag{11}$$

For simplification of the first estimation, constant angular acceleration and constant load during the time period of the mismatch speed cancellation was considered. mechanical losses were also neglected. Moment of inertia of the output is at least one or two orders of magnitude larger the input; [5]. We can then neglect the change in angular speed of the output and assume that the mismatch speed difference will be equal to the change of angular speed of the input. Components at the input of the MQ200 gearbox and their respective moments of inertia are listed in Table 8.

Table 8: Moments of inertia of the input components

Input shaft including the friction plate	J_{is}	0.00624 kg*m^2
Output gear wheel of 1st gear	J_{w1}	0.00104 kg*m^2
Output gear wheel of 2nd gear	J_{w2}	0.00070 kg*m^2

As mentioned earlier, the clutch for 1st and 2nd gear is placed at the output shaft of the gearbox. As a result, the total moment of inertia will be highest for 1st gear with respect to the gear ratios of the 1st and 2nd gear:

$$J_{total} = J_{w1} + J_{is} \cdot i_1^2 + \frac{J_{w2} \cdot i_1^2}{i_2^2} \quad (12)$$

Optimal mismatch speed for successful engagement may be somewhere between 100 and 200 min^{-1} based on [19], [26] – the upper bound of this interval will be used. Length of the mismatch speed cancellations phase based on previous test of dog clutches in the MQ200 gearbox may be estimated to ca. 0.01 seconds; [39], [41]. Both values were also verified during the tests of the initial design of the dog clutch with blocking mechanism.

Using these inputs, Equation (11) yields the load of ca. 96 Nm. Modifying the Equation (1) for the load acting on top of the dog, the resulting bending stress equals ca. 47 MPa (coefficient of uneven distribution remained unchanged – 0.5). In other words, the bending stress during gearshift equals ca. 26% of the stress caused by the torque transfer and has a safety factor of 11.3 – gearshift dogs can be considered capable of withstanding the bending stress during shifting.

Regarding the contact pressure during shifting – its magnitude is random and depends on the relative position the dogs have when the shifting is initiated, theoretically grows to infinity for edge-edge contact. In actual operation, sharp edges round themselves after a few gearshifts as described in e.g., paper [39]. Figure 64 shows such edge of a Maybach dog after ca. 500 gearshifts, while some of these gearshifts exceeded mismatch speed of 1,000 min^{-1}. This behavior was also confirmed during consultations with ŠKODA AUTO engineers who had experience with dog clutches for race cars where the gearshifts occur for large mismatch speeds and moments of inertia (usually without disconnecting the engine from the gearbox).

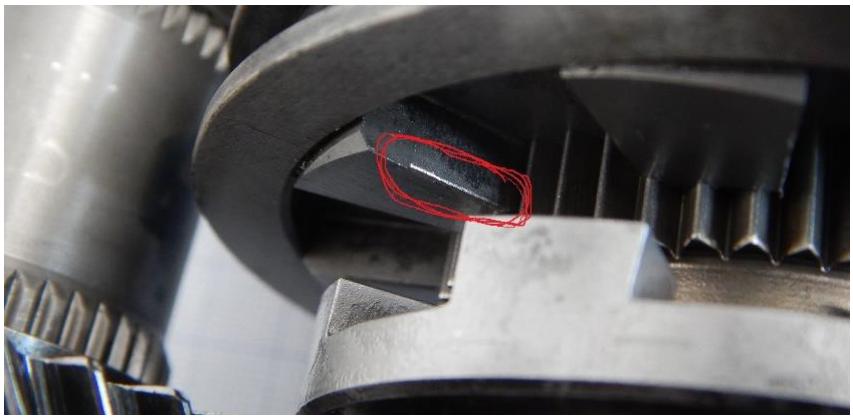

Figure 64: Rounded edge of the Maybach dog after ca. 500 gearshifts [39]

For more precise calculation of the behavior during gearshift, much more precise input data would be necessary, especially the torsional stiffness of the whole input. However, based on the research and testing, as the parameters which increase the stress during shifting rise (e.g., mismatch speed, torsional stiffness, moment of inertia and others), so does the noise caused by the impact and its energy. The dog clutch with blocking mechanism is designed for use mainly in passenger cars where NVH is very important and precise calculation of limit states during shifting was therefore decided as unnecessary since they would be accompanied with unacceptable level of noise anyway.

4.2.4 Blocking Ring

Trouble-free operation of the blocking ring is essential for proper functionality of the clutch. Its design must fulfill contradictory criteria. The blocking ring must be as thin as possible to minimize the gearshift force and bending stress during gearshift. On the other hand, its contact surface on the sides must be as large as possible to minimize the axial pressure caused by the axial force during torque transfer in engaged state.

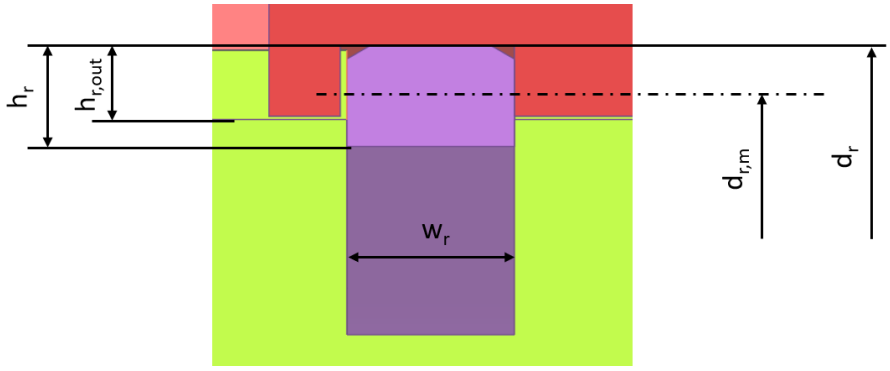

Figure 65: Cross-section of blocking ring in engaged position

Table 9 lists numerical values of basic blocking ring dimensions with respect to the notation in Figure 65.

Table 9: Blocking ring dimensions

Outer diameter	d_r	48.1 mm
Medium diameter	$d_{r,m}$	46.6 mm
Cross-section height	h_r	1.5 mm
Cross-section width	w_r	2.5 mm
Outer cross-section height	$h_{r,out}$	1 mm

The blocking ring is made of low-alloy manganese spring steel belonging to group 13 according to ČSN standards. High fatigue resistance and yield strength were the main criteria during the selection process. Table 10 lists the basic material characteristics provided by the steel supplier and the friction coefficient used for calculations. Higher friction coefficient than for the dogs was used due to small contact areas and limited lubrication possibilities – especially in the area between the blocking ring and the groove in the hub since there is just a manufacturing tolerance gap of 0.05 to 0.15 mm. Also using higher friction coefficient generally directs calculations of the blocking ring towards higher coefficients of safety.

Table 10: Basic material characteristics of blocking ring spring steel

Tensile strength	σ_m	approx. 800 MPa
Yield strength	σ_e	approx. 520 MPa
Young's modulus	E	205 GPa
Friction coefficient (steel-steel)	f	0.2

The shape of the blocking ring is relatively complicated compared to its size and thin cross-section. The manufacturing process of the prototype started with machining the basic

rotational shape. Then the gap was cut, and the ends bent. Spare rings were made in case of damage during assembly, disassembly, or testing.

4.2.4.1 Bending stress

The blocking ring is subjected to cyclic bending stress. During each engagement and disengagement, the shape changes rapidly from the free position to full compression and back again. Analytically, the stress can be calculated based on deformation of a curved beam of constant cross section. The load is then kinematic since the outer diameter of the ring must be reduced to allow axial movement of the sliding gear.

The objective is therefore to calculate the maximum bending stress in the blocking ring as a function of the radius change. A derivation of this relation can be found in papers [73] and [74]. It is based on the calculation of a quarter of a circular beam of radius *r*, encastred at one end and loaded with force F_R at the other end as shown in Figure 66.

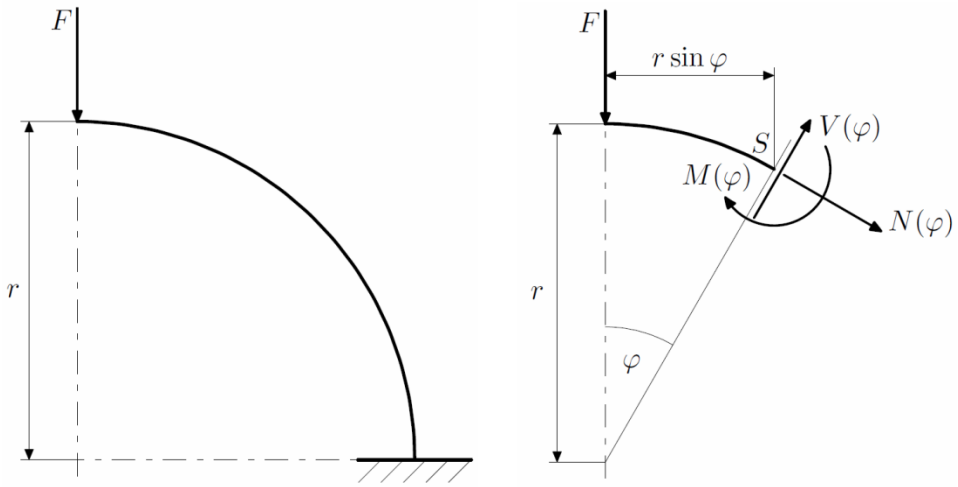

Figure 66: Diagram for calculating the bending stress in a quarter of a circular beam [73]

Using Castigliano's theorem and Maxwell-Mohr method, we can derive the force necessary for the required deformation. Assume that the displacement in the direction of the radial force F_R approximately corresponds to the change in the radius of the beam (ring) around its circumference. Then the required displacement under the radial force will equal the outer height of the ring $h_{r,out}$. The radial force required for the quarter of the circular beam with area moment of inertia *I* will be:

$$F_R = 4\frac{E \cdot I \cdot h_{r,out}}{\pi \cdot r^3} \tag{13}$$

Highest value of bending stress will be located in the encaster at the inner and outer diameter of the ring (in half of the cross-section height h_r):

$$\sigma_b = \frac{\frac{F_R \cdot r}{2 \cdot I}}{h_r} = \frac{4 \cdot E \cdot I \cdot h_{r,out} \cdot r \cdot h_r}{2 \cdot \pi \cdot r^3} = 2 \cdot \frac{E \cdot h_{out} \cdot h_r}{\pi \cdot r^2} \tag{14}$$

This equation yields a maximum bending stress of approximately 370 MPa. However, its derivation involved some simplifications and differences between the configuration used

for the derivation and the real situation (e.g., the ring is compressed and loaded at six places by the sleeve, there is also no encaster or rigid connection to any frame, assumption about elation between the deformation and radius change was made).

Analogy with piston rings can be used for alternative stress calculation. Piston rings are preloaded between piston and cylinder to ensure proper sealing function. Their diameter is therefore smaller compared to free unloaded shape, similarly to the blocking ring. Source [75] lists an equation for direct calculation of the piston ring bending stress based on the piston ring gap *z* in the unloaded state (illustrated in Figure 67).

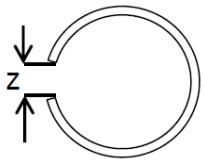

Figure 67: Piston ring gap [75]

The equation assumes that the gap in the loaded state is zero. This is not true for the blocking ring – the design ensures that there is always a gap larger than the diameter of the blocking pin. However, the difference in perimeter of the unloaded and loaded blocking ring is equal to twice the outer height $h_{r,out}$. Assume that this difference is equal to the piston ring gap *z*. The equation for bending stress can then be expressed as follows:

$$\sigma_b = 0.848 \cdot \pi \cdot E \cdot \frac{h_r \cdot h_{r,out}}{(d_r - h_r)^2} \tag{15}$$

This equation yields a maximum bending stress of approximately 386 MPa. Even though the results of both analytical calculations are comparable, the approximations and simplifications in them, together with great importance of the blocking ring, led to the decision of validating the calculations by a simulation.

The simulation was performed in Abaqus. Static, general method was used (no inertia forces). Geometric nonlinearity was considered. The simulation begins in the engaged state where the blocking ring is in unloaded state. Then the clutch disengages and engaged again. All parts were meshed using standard linear hex elements – C3D8R. The finest mesh size was used for the ring – approximately 0.2 mm edges. All contacts are surface to surface type and have normal and tangential behavior. Normal behavior is represented by 'hard contact'. Tangential behavior is represented by a friction coefficient. Young's modulus and friction coefficient were used with respect to Table 10. There are four main interactions defined:

1) **Hub-ring.** The groove in the hub (master) is in contact with the ring (slave).
2) **Sleeve-ring.** The pads of the sleeve (master) are in contact with the outer surface of the ring (slave). This forces the ring to deform in the initial phase of disengaging.
3) **Sliding gear-ring.** The inner surface of the sliding gear (master) is in contact with the outer surface of the ring (slave). This keeps the ring deformed and gradually releases it at the end of the disengaging process.

4) **Sleeve-sliding gear.** The sleeve (master) is in contact with the sliding gear (slave) through circumferential frontal faces. This results in movement of the sliding gear in respect to the sleeve. This could also be realized by a boundary condition.

The boundary conditions restrict motion in predefined directions and enforce motion during the gearshift process. No forces or toques are applied. The blocking ring is placed freely in the assembly and its movement and deformation are caused by interactions with other parts These parts are restricted by the following boundary conditions:

- **Hub.** The hub is encastred (all 6 DOF removed) to the gearbox shaft.
- **Sliding gear.** The sliding gear has one DOF left (axial movement). This DOF is then controlled by the contact with the sleeve as described above.
- **Sleeve.** The outer surface of the sleeve is constrained in all directions except axial movement that has prescribed displacement.

The maximal Mises stress at the blocking ring during the gearshift is 316 MPa, located at the outer diameter. The simulated task is symmetrical and so is the resulting stress, there are therefore two locations of the maximum, only one of them is shown in Figure 68. As expected, this value occurs at maximal compression of the ring caused by the shape of the sleeve pads and then the sliding gear. This stress remains more or less constant during this gearshift disengaging.

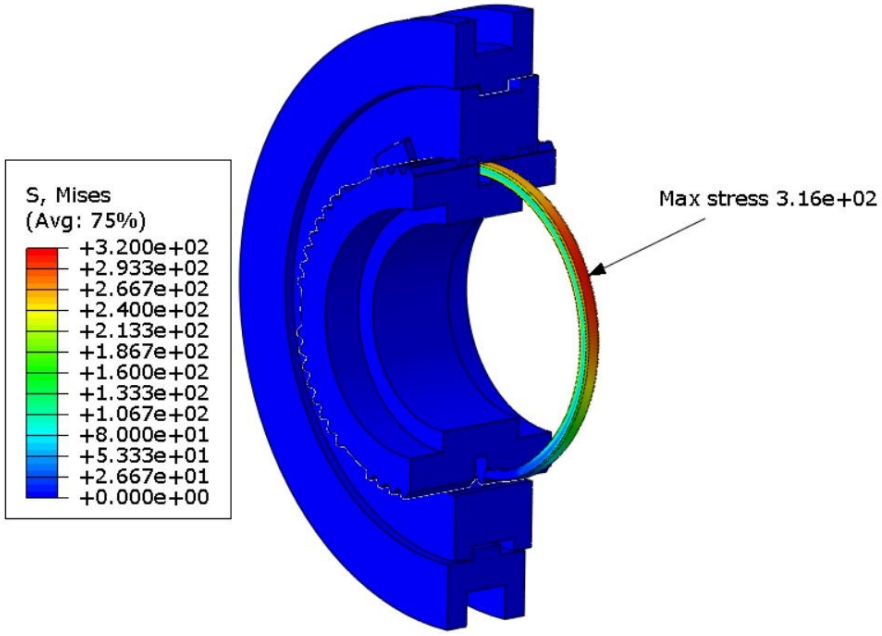

Figure 68: Maximum stress at the blocking ring during simulated gearshift

Figure 69 shows the blocking ring stress in respect to simulation progress. It starts at 0 (engaged), goes through 0.5 (disengaged) and ends at 1 (engaged) The black dotted line plots the average of 5 elements with the highest stress. The gray line plots the average of the area of 54 elements around the element with the highest stress. The residual stress in the neutral position is intended. It keeps the radial forces acting between the ring and sliding gear. This prevents axial movement of the sliding gear.

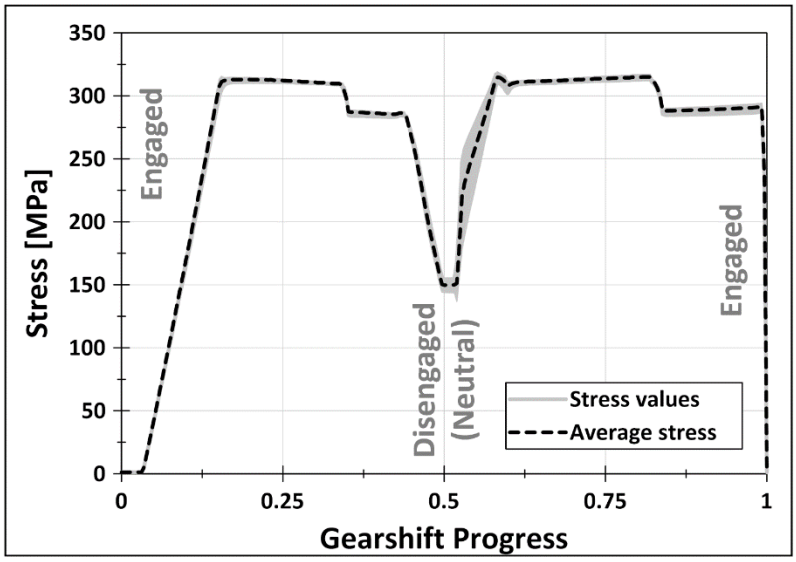

Figure 69: Stress at the blocking ring during the simulated gearshift

Videos of the simulated gearshift showing the blocking ring deformation and movement are listed in Attachment 3). Table 11 presents a comparison of the resulting bending stress obtained by analytical calculations and simulation.

Table 11: Bending stress in the blocking ring according to different methodologies

Methodology	Bending stress
Analytics – curved beam deformation	370 MPa
Analytics – piston ring analogy	386 MPa
Simulation in Abaqus	316 MPa

In terms of static strength analysis, all the values in Table 11 are lower than the yield strength of the material. In terms of fatigue strength analysis, further details about the load must be obtained.

Each gear of the gearbox has a different expected number of gearshifts over its service life. The highest number of gearshifts for a single gear according to ŠKODA AUTO service life tests is 180,000. One blocking ring serves two adjacent gears and is compressed twice for each of these standard gearshifts (once when engaged and once when disengaged). This sums up into 720,000 cycles in total for one blocking ring. This number of cycles falls into the breaking point area of steel S-N curves. Consequently, it is justified to require that the bending stress in the ring during compression must be lower than the fatigue strength of the material. However, the fatigue strength for the material of the blocking ring was not provided by the supplier. Therefore, an approximate formula will be used based on sources [68], [76] and [77] (bending, coefficient of asymmetry equal to zero):

$$\sigma_w \cong 0{,}6 \cdot \sigma_m \tag{16}$$

With respect to this formula, the fatigue strength of the blocking ring is equal to 460 MPa. Compared to the highest bending stress according to Table 11 (piston ring analogy), the safety coefficient is only 1.19. A more accurate determination of the fatigue strength of

the material or the use of a material with a higher tensile strength may probably be necessary for the mass production of the clutch.

4.2.4.2 Axial contact pressure

The load in this state is given by the axial force arising at the sides of the dogs during the transmission of maximal torque. This force than flows from the dogs at the sliding gear through the blocking ring to the hub and then to the shaft (see Figure 70).

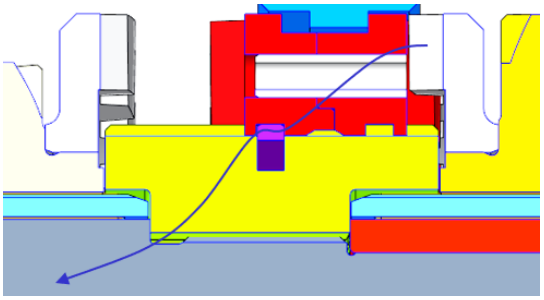

Figure 70: Axial force flow in the engaged state

Force responsible for the torque F_T can be calculated based on the dimensions of the dogs listed in Table 4 and maximal torque listed in Table 6. Largest force will be present again at the dogs of the 1st gear:

$$F_T = \frac{2 \cdot T_{max,in} \cdot i_1}{d_D} \tag{17}$$

Corresponding axial force can be calculated according to the force decomposition diagram on the side of the dog shown in Figure 71. The force F_T is acting on the side of dog and can be decomposed into a normal component F_n and a tangential component F_t. The tangential component acts outward in the disengagement direction, and the frictional force F_f acts against it. The magnitude of the friction force is equal to the product of the magnitude of the normal force F_n and the friction coefficient f. The vector sum of the forces F_t and F_f gives the force $F_{A'}$. If we project this force in the direction of the axis of rotation of the clutch, we obtain the axial force F_A.

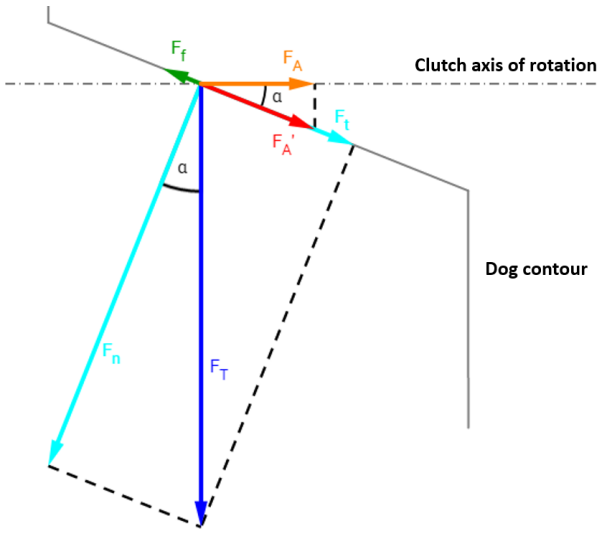

Figure 71: Force decomposition on the side of the dog during torque transmission

This can be written down into following formula:

$$F_A = F_T \cdot \cos\alpha \cdot (\sin\alpha - f \cdot \cos\alpha) \tag{18}$$

The final value to obtain is the contact surface between the sliding gear and the blocking ring A_{gr}. This contact surface is smaller than between the ring and hub, it is therefore more critical. Its shape is quite complicated due to the inner splines at the sliding gear and chamfer at the outer blocking ring diameter. However, it can be easily measured using the CAD model. Then we can calculate the contact pressure:

$$p_r = \frac{F_A}{A_{gr}} \tag{19}$$

The resulting contact pressure between the sliding gear and blocking ring for 1st gear equals ca. 53 MPa. For static contact of steel materials, this contact pressure can be considered as compliant; [66].

4.2.4.3 Gearshift force

The dog clutch with blocking mechanism requires a certain minimal gearshift force to be applied during each engagement and disengagement. The magnitude of this force is determined mainly by the stiffness of the blocking ring and for lower than minimal force the gearshift would not be successful. This minimal force is significantly greater than the force to overcome the blocking mechanism of a synchronizer, where, in addition, the magnitude of the force correlates with the gearshift length.

To compress the blocking ring, the gearshift sleeve must exert a force on the ring proportional to the bending stiffness of the ring. However, the sleeve moves in the axial direction and blocking ring moves in radial direction when compressed, so the radial force must be converted to an axial force by means of a force decomposition analogous to the diagram shown in Figure 71. In addition, we must consider the additional frictional resistance created by the ring being pressed against the side of the groove in the hub. The crucial variable in the transfer between radial and axial force is the angle β at the inner sleeve surface. For the clutch prototype, angle β equals 30° measured from the axis of rotation of the clutch as shown in Figure 72.

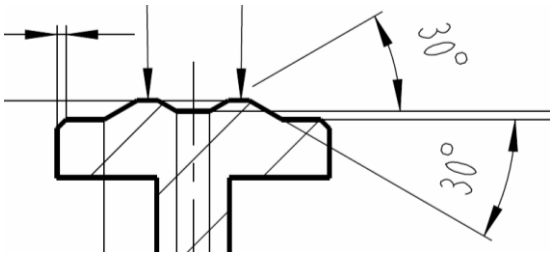

Figure 72: Angle β at the inner sleeve surface

Using radial force calculated in Equation (13), we can write formula for minimal gearshift force:

$$F_G = F_R \frac{\tan\beta}{1 - f \cdot \tan\beta} \tag{20}$$

This gearshift force is in case of the prototypes identical for all gears and equal to ca. 32 N. According to [5], for manual gearbox, the gear ratio between the gearshift fork acting on the gearshift sleeve and the shifter may be roughly 10:1 with efficiency often less than 70%. For these values, the effort required from the driver would be approximately 5 N. Regarding consultations with ŠKODA AUTO, the average effort with the synchronizer is ca. 10 to 20 N. This is a very promising result for the dog clutch with blocking mechanism. Even though it is mainly designed to be shifted by actuators, smaller gearshift force means lighter actuator system. Comparison of calculated and measured values can be found in Chapter 5.2.3.

4.2.5 Prototypes of the Clutch

Following the design optimization and calculations, prototypes of the dog clutches with blocking mechanism were made. Production drawings can be found in Attachment 4). Two clutches for MQ200 gearbox were made to shift 1st, 2nd, 3rd and 4th gear. These can be seen in the lower part of Figure 73. The clutch on the left is for 1st and 2nd gear and the gearing on the outer sleeve diameter is designed for the reverse gear. In the upper part of Figure 73 there are shifted gear wheels with crowns with gearshift dogs laser-welded to them. The production of the prototypes was financed and supported by ŠKODA AUTO.

Figure 73: Prototypes of the clutch for the 1st, 2nd, 3rd and 4th gear

For the prototype testing, the gear wheels had to stay in their positions in gearbox. To minimize production costs, standard gear wheels were used, the synchronizer cones and teeth were removed, and rings with gearshift dogs were welded to the gear wheels instead. However, for mass production, the gear wheels could be redesigned, and the gearshift dogs could be manufactured directly on their sides. This would mean that the gear wheels could move closer to each other and the whole gearbox could be made shorter. Figure 74 shows

possible axial length saving for 1st gear dog clutch compared to synchronizer (marked with green arrows) of 13,7 mm which translates into ca. 30% of the synchronizer axial length.

This saving is only possible when the maximum diameter of the gearshift dogs is smaller than the root diameter of the adjacent gear wheel. For the MQ200, this condition is not fulfilled only at the clutch for 3rd and 4th gear. Only a small saving would be possible in this case by redesign focused on minimizing the gap between the crowns and gear wheels visible in Figure 37. The total possible axial saving for the MQ200 gearbox thanks to the dog clutches with blocking mechanism equals approximately 30 mm.

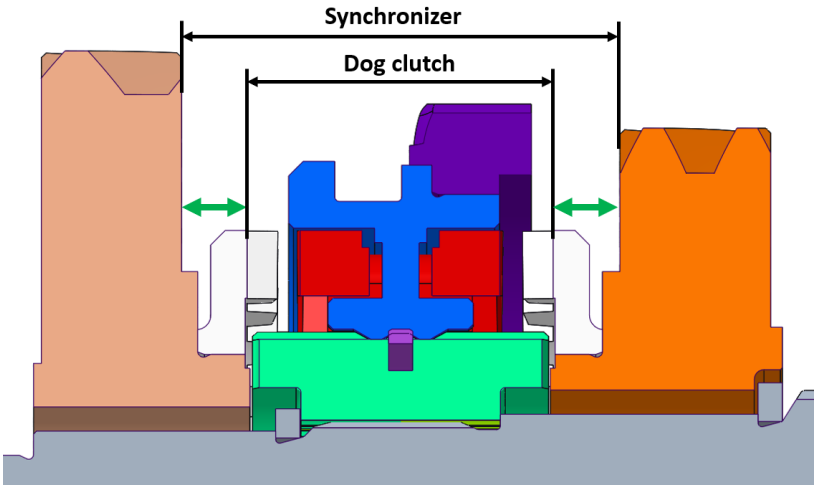

Figure 74: Possible axial length saving for 1st gear dog clutch compared to synchronizer

4.2.6 Gearshift Simulation Model

The geometry of the dogs is independent from the blocking mechanism and both can be tuned separately. However, as an experimental optimization this process would include manufacturing many dog clutch variants, assembling and testing. This would be extremely ineffective in terms of time and costs. A multi-body simulation model which would represent the real engagement process was created in cooperation with University of West Bohemia, Faculty of Applied Sciences and presented in [VI.] and [VIII.].

Multi-body systems in general are formed by rigid or flexible bodies which are connected by kinematic joints and affected by forces and torques. There are two main phases in determination of the kinematic and dynamic characteristics of the multi-body system. The first one is obtaining system parameters and creating mathematical model of the multi-body system, i.e., deriving equations of motion. The second one is using suitable methods to perform numerical simulation and analysis of the system motion.

Many approaches to create the mathematical model can be employed; [78]. MSC Adams was used to create the multi-body system. This software uses the Lagrange formulation for the equations of motion. For dog clutch with blocking mechanism, the multi-body model was created using five rigid bodies and five kinematical joints. The scheme of the system is shown in Figure 75, where bodies are depicted using rectangles and joints are denoted using circles. There are also several nonlinear forces. Contact interaction between gears is maintained using nonlinear contact forces. Typical formulation of the normal contact force

represented by constant stiffness coefficient multiplied by the penetration to the power of certain exponent and regularized damping term is used; [79]. The shifting force acting on sleeve is defined as piecewise linear function of time with customizable maximal value. The effect of blocking ring is also defined using nonlinear force acting on proper bodies. The friction forces are represented by regularized Coulomb friction model with Stribeck effect. Further reading about transmission and gearshift simulations in ADAMS can be found in sources [80] and [81].

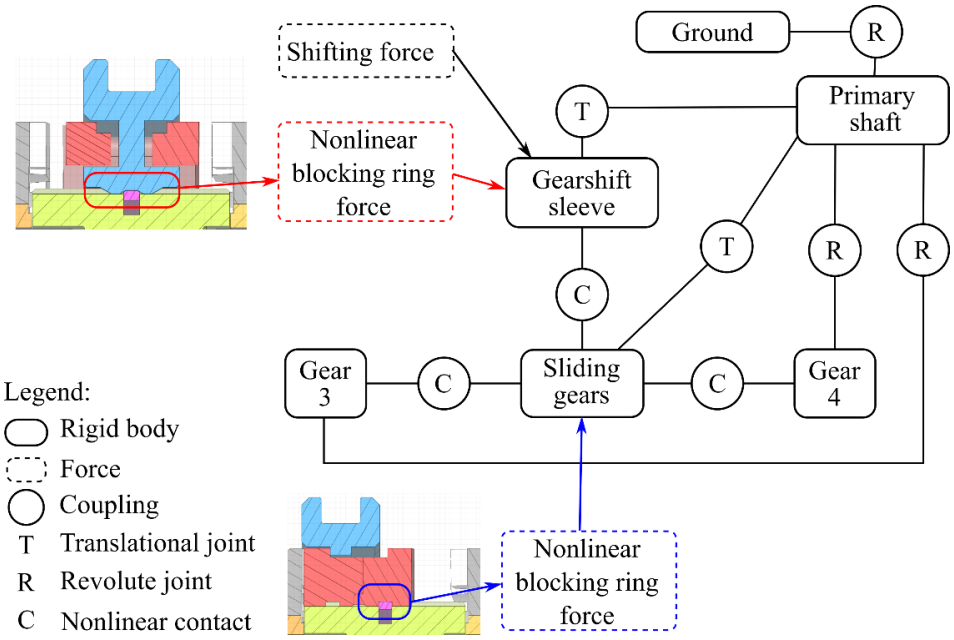

Figure 75: Kinematical scheme of the created multi-body model

The model was validated and tuned based on experimental data. This data was measured at the inertia test bench during gearshifts of the dog clutch with identical geometry. A matrix of gearshifts with various gearshift force and initial mismatch speed was performed. Gearshift displacement and gearshift time were compared with the simulation results. Since the initial position of the dogs and slots is generally random, an average result of 10 measurements was always used for comparison.

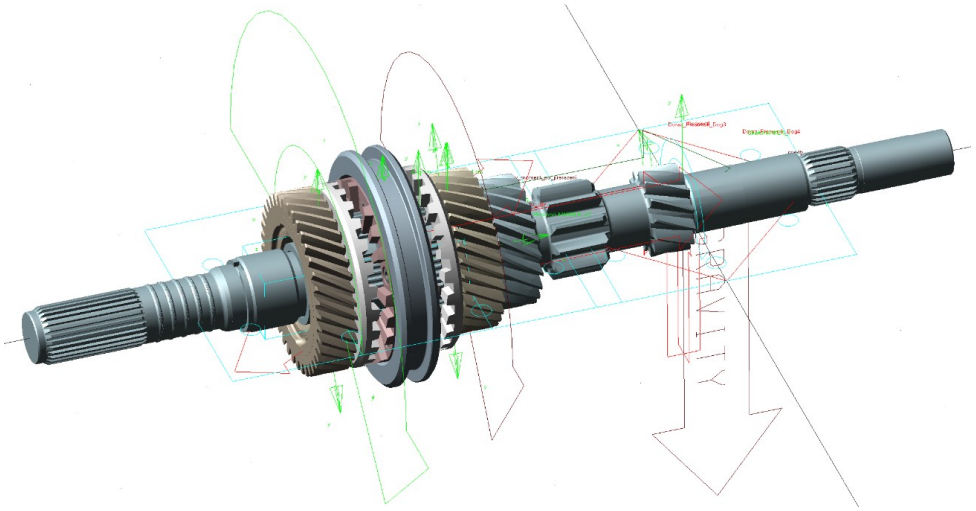

Figure 76: ADAMS multi-body model of the Input shaft with the dog clutch

Typical results obtained from numerical simulations are illustrated in Figure 77. There is the time history of shifting force starting from 0 N with maximum value of 50 N. Then two curves representing defined angular velocity of the third gear and calculated angular velocity of the primary shaft are plotted. The last subplot represents the time history of sleeve and sliding gear displacements. It is apparent that the gearshift sleeve gradually overcomes the blocking effect of blocking ring force up to time approx. 0.1 s, when the sleeve and sliding gears are finally unblocked and they can move towards the dog ring. From 0.11 s to 0.18 s the sliding gear is in contact with the faces of the dogs and the primary shaft starts to rotate due to friction and inclined dog faces. The sudden decrease in the angular velocity is caused by the sliding of the tapered dog sides. Then, the final dog clutch engagement is reached, and the sliding gear is blocked by the blocking ring.

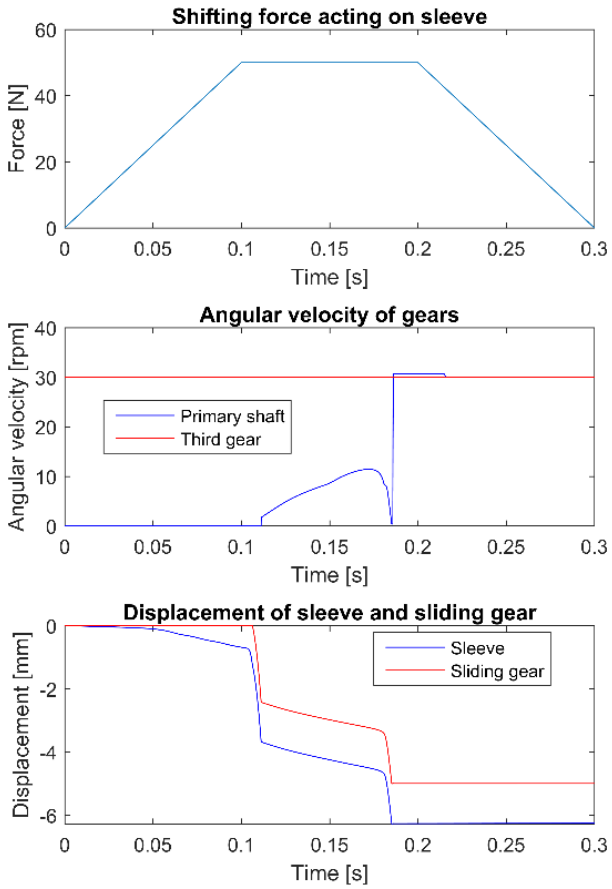

Figure 77: Example of simulated gearshift results
Gearshift force 50 N; mismatch speed 30 min^{-1}

This multi-body simulation model was used for validating the adaptation of the dog clutch with blocking mechanism to sequential shifting as described in Chapter 4.3.2. Unfortunately, optimization of the shape of the dogs for faster gearshifts was not carried out. Cooperation could not be continued by the University of West Bohemia due to insufficient time available for the project.

4.3 Adaptation for Sequential Shifting

The dog clutch with blocking mechanism was initially designed for cooperation only with shifting mechanism based on the standard MT or AMT system. This means that the driver or gearshift actuator acts on the shifting mechanism until it senses that further movement is not possible and the engaged position has been reached, the gear is fully engaged. Only then the gearshift force is removed. This system ensures that the sliding dog is pushed to its furthest position and the blocking ring stretches into the desired shape. However, this scenario does not apply for a gear selector mechanism with kinematic endpoints – typically sequential shifting with a rotating gear selector drum (examples in Figure 78 and Figure 80). In this case, the furthest point of the sliding dog travel is given by the dimensional precision of many components, including the dog clutch, shaft, gearbox case, and gear selector mechanism.

To make sure that the dog clutch with blocking mechanism is as widely usable as possible, modifications were proposed to make it compatible with sequential shifting. Results were presented in paper [X.].

Figure 78: Gear selector drum of Subaru Impreza R4 [44]

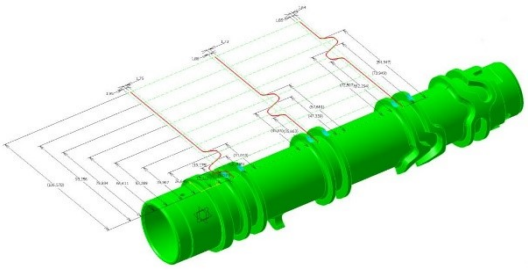

Figure 79: Gear selector drum with gearshift trajectories for individual gears [80]

4.3.1 Additional Flexible Elements

The idea of adapting the dog clutch for sequential shifting is based on adding a flexible spring-like element somewhere between the sliding dog and the selector fork. As a result, the travel of the selector fork would always be longer than the travel of the sliding dog. The difference between them would be compensated by deformation of the flexible element to provide secure blocking under every circumstance.

The spring used for this purpose must meet specific requirements. Its size should be as small as possible to keep the current packaging of the clutch. It must allow large enough deformation to cover the required operating range (see Figure 80). The lowest deformation in the operating range must be greater than zero, otherwise the spring would provide very little force in this area. Overlap on the other side of the range is also required for safety reasons. Stiffness and force under deformation of the spring must correspond to the stiffness of the blocking ring. When the stiffness of the spring is lower than the resistance of the sliding dog against axial movement (caused mainly by the stiffness of the blocking ring at the beginning of the engagement), the spring reaches the maximal possible deformation during each shifting. This may negatively affect its service life. On the other hand, excessive stiffness would

require a stronger and therefore heavier and more expensive gear selector mechanism and actuator.

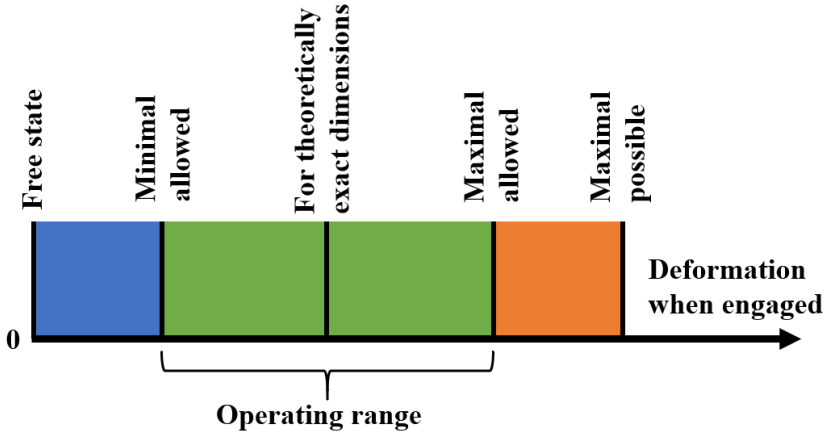

Figure 80: Operating range of the additional spring

Investigations into the spring placement resulted in only one possible location – between the sliding dog and the gearshift sleeve. It meets the requirement of the dog clutch with the blocking mechanism being a system not requiring changes in the gear selector mechanism. For the prototype of the dog clutch, the following parameters were selected:

- Operating range width = 1.5 mm
- Maximal possible deformation = 2.5 mm

Wave springs and disc springs were considered. Wave springs offer high stiffness for small dimensions. On the other hand, the maximum bending stress can be very high for the required maximal deformation and after FEM analysis of various possible dimensions and configurations, the wave spring was discarded due to the bending stress.

Disc springs offer high stiffness for small dimensions as well. Furthermore, their stiffness can be adjusted by using multiple disc springs in series stacking as in Figure 81. This multiplies the maximal compression of one spring by the number of springs used. However, the force necessary for this compression stays the same as for one spring – see Figure 82.

This stacking is possible for the wave spring as well. However, for series stacking, the waves must be permanently connected at their contact points, otherwise they would rearrange themselves into parallel stacking because of instability. This makes disc springs a more cost-effective and versatile solution for different dog clutch designs and requirements. It also brings us to another advantage of the disc springs – better material under stress usage. Disc springs have complete contact curves around their circumference. Their deformation is symmetric, and the stress, therefore, does not concentrate at local maximums but spreads equally instead. Four-wave spring on each side was selected as a suitable solution. Their diameters are 70.7 mm (outer) and 65.3 mm (inner) with 0.5 mm thickness. The free height of one spring 1.125 mm gives us the required maximal deformation of 2.5 mm.

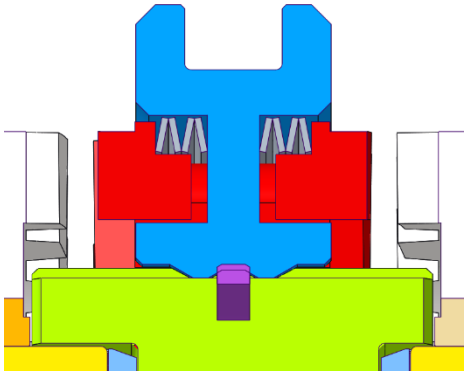

Figure 81: Dog clutch with additional disc springs – cut section

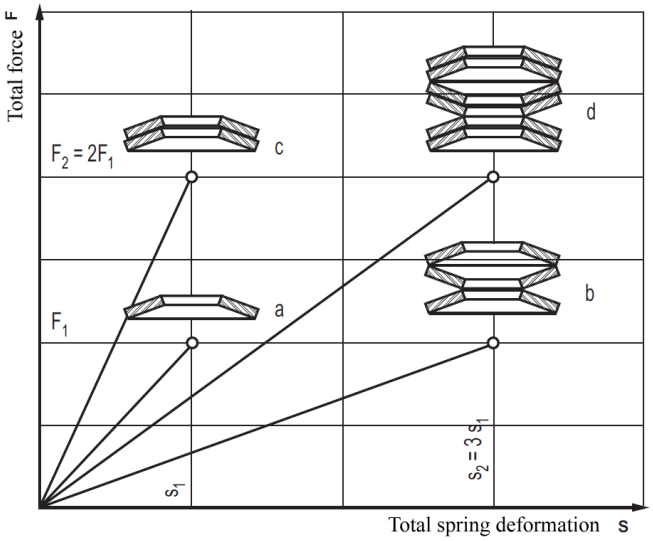

Figure 82: Comparison of disc springs stacking

Reaction forces and stress under deformation of disc springs were calculated regarding DIN 2092 – Calculation of Disc Springs. Figure 83 shows that the reaction force of the spring disc stack is not linear. However, this type of curve is favourable for our application for two reasons:

1) The force in the engaged state throughout the operating range varies less.
2) Lower spring deformation is required to reach the force necessary for blocking ring compression.

On the other hand, higher stiffness around the free state may result in a bigger conflict when setting the neutral position of the sliding dog.

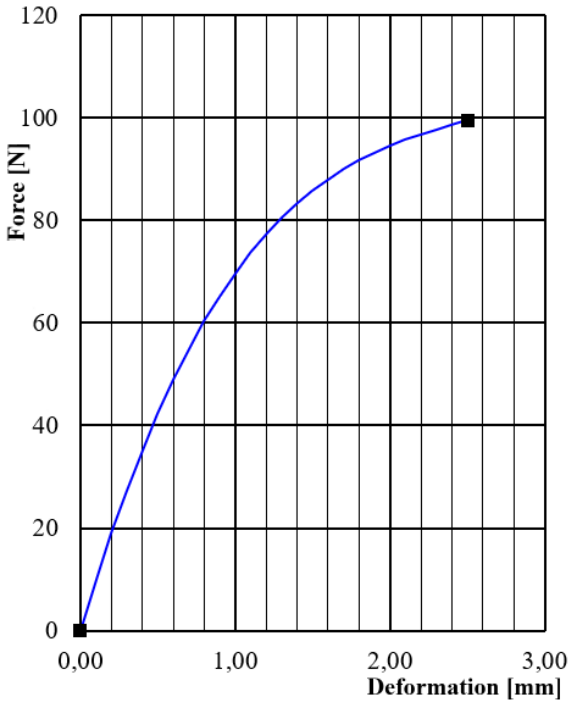

Figure 83: Reaction force of the disc spring stack during deformation.

The neutral position of the sliding dog is affected by both the blocking ring and additional springs since both of these act on it. The initial assumption was that the position of the engaged gearshift sleeve could vary. This means that the neutral position of the sleeve can vary as well, and the neutral position of the sliding dog will be a compromise. This effect was not thoroughly examined, but generally, it can be said that it may be necessary to enlarge the gap between the sliding dog and shifted wheels to accommodate this neutral position uncertainty.

Stress values for 2 mm deformation find themselves between 600 and 650 MPa located on the inner and outer diameters. These values can be optimized by tuning the stack properties. One disadvantage of the disc springs is bigger packaging. It may be necessary to enlarge the diameter of the dog clutch to accommodate all disc springs and still fulfil the strength requirements, especially of the sliding dog.

4.3.2 Gearshift Simulation

Simulation model described in Chapter 4.2.6 with the addition of disc springs was used to validate the gearshift based on the prescribed gearshift sleeve motion. The following input parameters were varied:

- Additional spring stiffness 10/20/40/60 [N/mm].
- Maximal displacement of the gearshift sleeve 7/6.25/5.5 [mm].

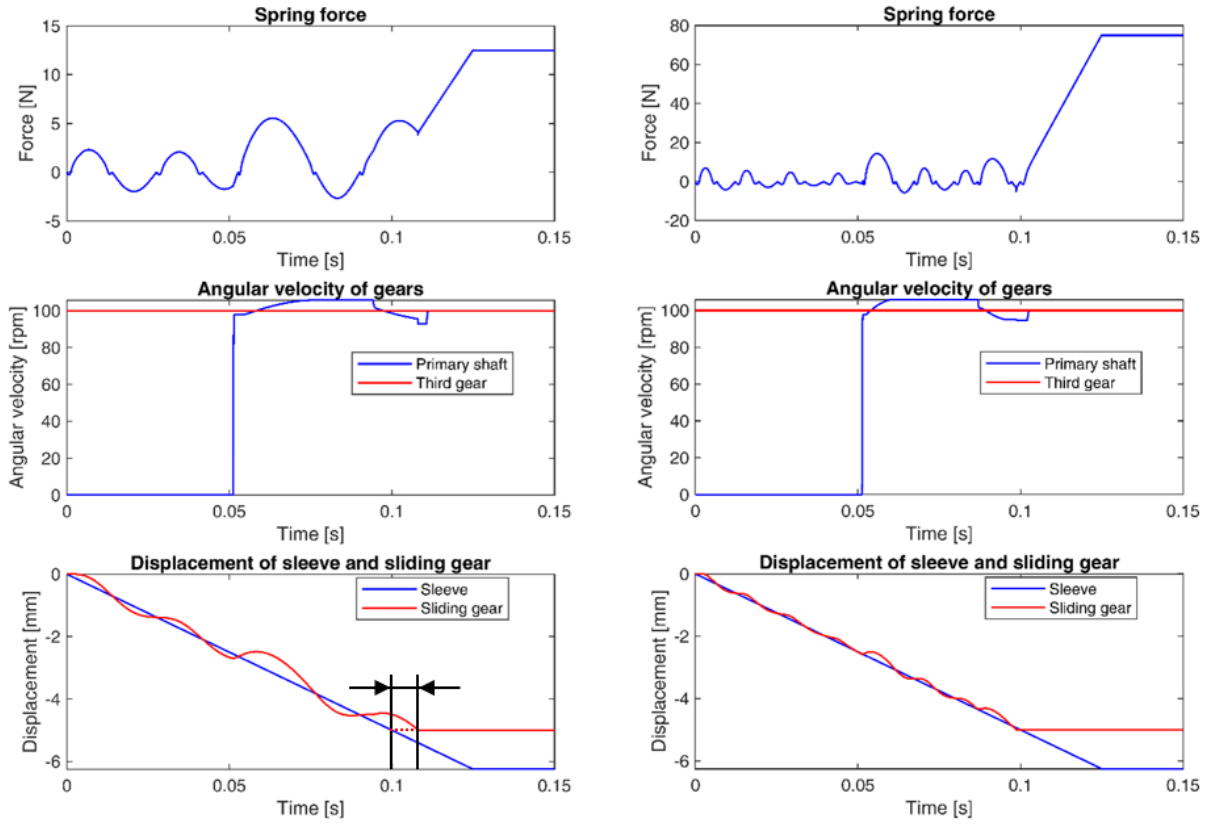

Figure 84: Comparison of engagement with nominal gearshift sleeve displ. (6.25 mm)
Left: Spring stiffness 10 N/mm. *Right: Spring stiffness 60 N/mm.*

The main target of the simulation was to confirm that the sliding dog always reaches the desired engaged position, and the blocking ring stretches to secure the engaged gear. According to the simulation, this happened successfully for all input parameters.

The secondary target was to investigate the effect of the input parameters on the engagement duration. The expected scenario of the sliding dog reaching the engaged position later because of additional spring compression is present. However, the highest observed delays in engagement are only roughly 0.01 s for the softest spring (shown in the left side of Figure 84, marked by arrows in the Displacement graph). The oscillating movement of the sliding dog is tighter for the harder spring (shown in the right side of Figure 84). These values are very low and lower than expected. The negative effect of the additional spring on the engagement duration, therefore, seems to be negligible.

Note that the Force graphs in Figure 84 show only the additional force caused by the spring compression, not the total gearshift force.

5 Verification

Fulfillment of the requirements put on the dog clutch with blocking mechanism had to be verified with respect to the dog clutch design and thesis objectives. This chapter describes the test benches and the performed testing.

5.1 Inertia Test Bench

The majority of the testing was carried out at the inertia test bench situated in Juliska laboratories. It is an open test bench designed for testing of gearshift mechanisms inside of a tested gearbox.

5.1.1 Initial State of the Test Bench

The test bench was designed and built by Dr. Pakosta as part of his dissertation thesis [42]. However, it was prepared only for gearshifts without external synchronization and with disconnected friction clutch between the gearbox and the engine/motor at the input. It was mostly used for service life tests of synchronizers which could be operated in fully automated mode being controlled by LabVIEW program measuring and recording important parameters of the gearshifts.

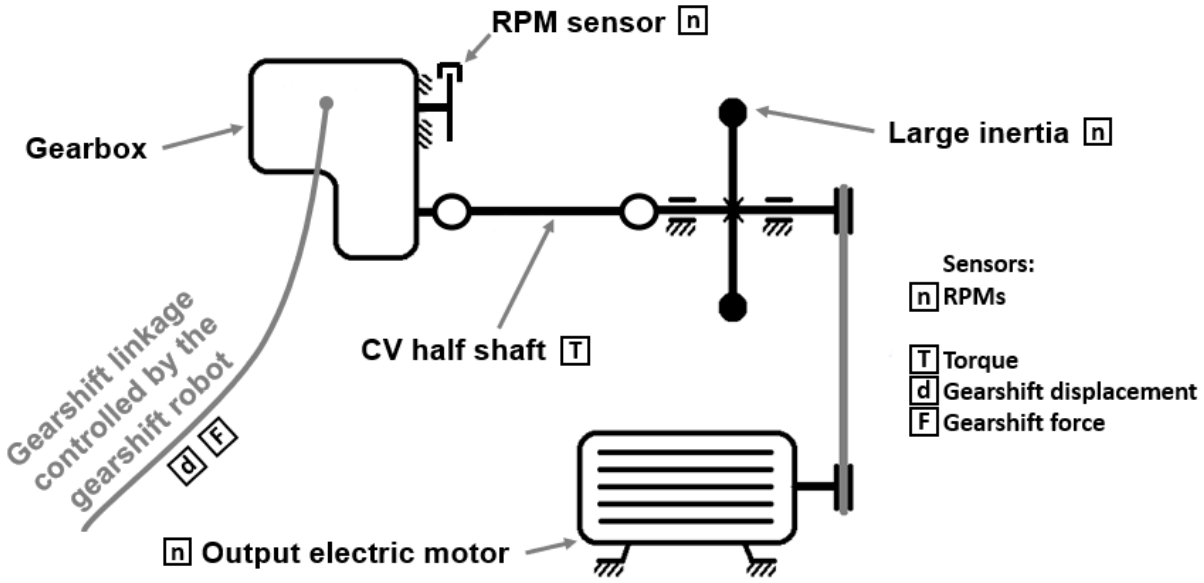

Figure 85: Initial state of the test bench with major measurement locations

The initial layout of the test bench can be seen in Figure 85. There is only an RPM sensor connected to the clutch friction plate at the input shaft of the tested gearbox. Power comes from an output asynchronous motor which keeps the RPM of large inertia disc constant during the test. The energy of the rotating disc represents the energy of a moving vehicle, its moment of inertia equals approx. 14 kg*m^2. The inertia is connected to only one of the differential output flanges using a tensometric shaft (measuring torque and RPM) and standard CV half shaft, the differential therefore must be mechanically blocked.

Gearshifts are carried out by pneumatic shift robot connected to the gear selector mechanism of the tested gearbox using standard gear linkage. The gearshift force and displacement are measured at the shift robot. Sensors are placed on the connection between pneumatic cylinder and cable for gearshift actuation. Further details of the bench can be found in the thesis [42] and paper [82].

MQ200 gearbox from ŠKODA is mainly used as the gearbox for tested gearshift mechanisms. Thanks to its design it offers the possibility of connecting an external synchronization motor with the input shaft instead of the 5th speed gear wheel. However, this motor for external synchronization could not be controlled by the control system and could be used only with this specific gearbox. Furthermore, mounting this motor increased significantly the input shaft's moment of inertia and it could not be disconnected during the gearshift. It also limited the gearbox to a maximum of 4 gears. Without proper external synchronization, testing shifting for various mismatch speed was extremely limited.

Additionally, the quality of the input shaft RPM data was not sufficient. The RPM sensor was not placed directly on the input shaft but rather connected to the friction plate of the clutch. Torsional springs between the hub and the friction plate of the clutch were responsible for oscillations lasting much longer than the gearshift itself.

5.1.2 Adding External Synchronization

With the addition of external synchronization, other disadvantages mentioned above were addressed as well. The updated layout of the test bench can be seen in Figure 86. Addition of external synchronization and friction clutch were presented in [VII.] and [XI.].

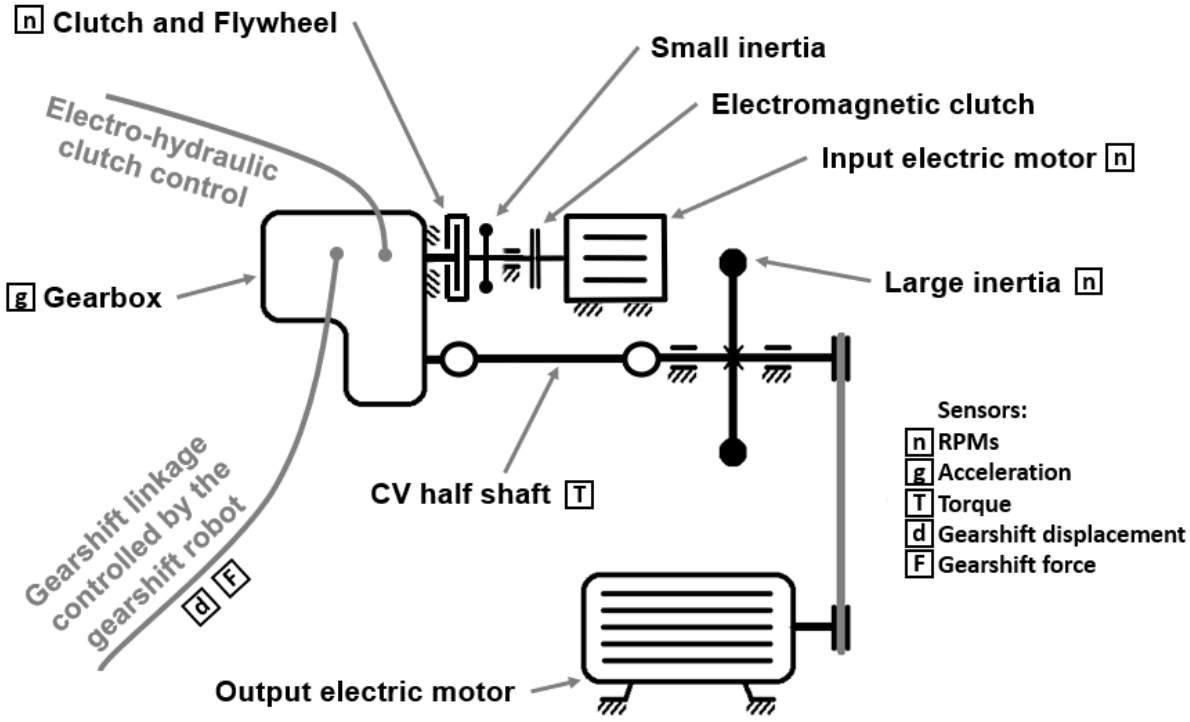

Figure 86: Updated test bench with major measurement locations

The output of the gearbox remains unchanged. At the input, there is a standard dry single plate friction clutch with flywheel. The clutch engagement is controlled electro-hydraulically. An electric pump generates pressure in the brake fluid, which is then carried through a standard hydraulic linkage to the piston placed on the gearbox. This piston operates the clutch through a standard actuation system. This whole system of friction clutch control will be referred to as 'eClutch'. Inductive sensor measures the flywheel RPM using standard teeth for the starter.

Detail of the input assembly can be seen in Figure 87. The friction clutch can connect the input shaft to an additional shaft with a small inertia disc to reflect the inertia moment of all the components connected to the flywheel (mainly the engine/motor with its accessories). The disc is easily interchangeable and can be tailored to a specific powertrain. Most importantly, a synchronous electric motor which provides external synchronization can be quickly coupled with the additional shaft using electromagnetic clutch. The motor is capable of maximum 6,000 min^{-1} to match the standard ICE RPM range and has very low moment of inertia of the rotor (roughly one order of magnitude smaller than the input shaft of the gearbox with friction plate) for quick external synchronization. Rated torque output equals 3.3 Nm.

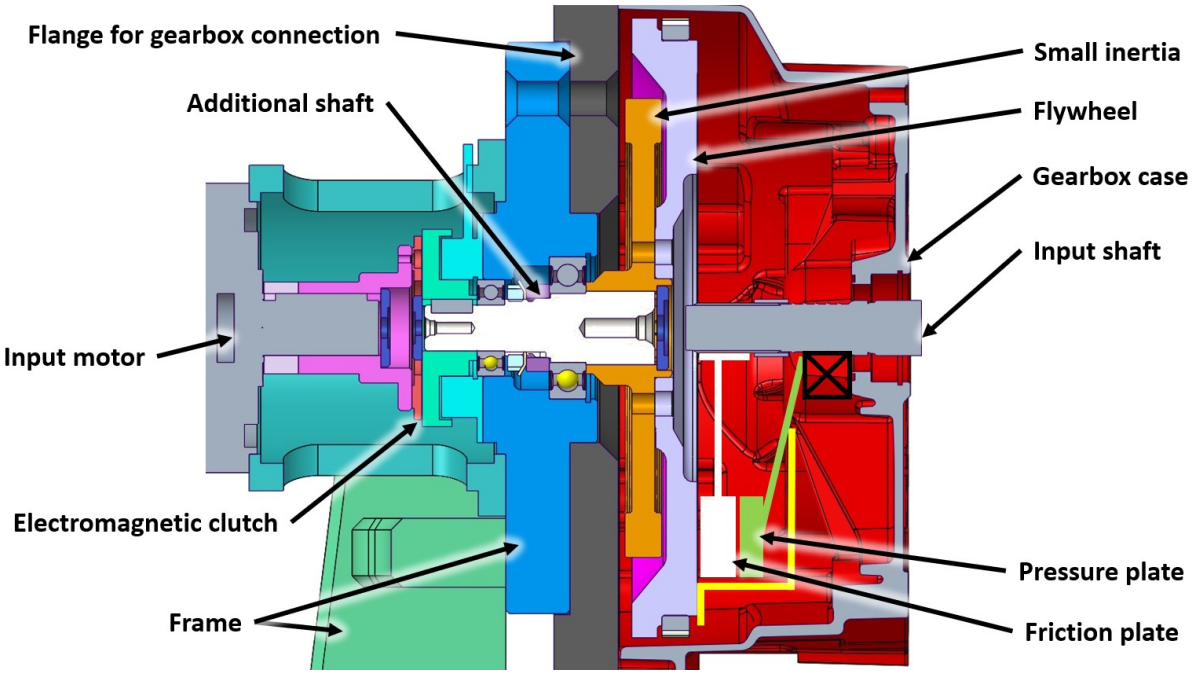

Figure 87: Input assembly – section cut

The update required designing and manufacturing of new parts for mounting the gearbox to the test bench and mounting all the other components for external synchronization. Detail of the external synchronization assembly can be seen in Figure 88.

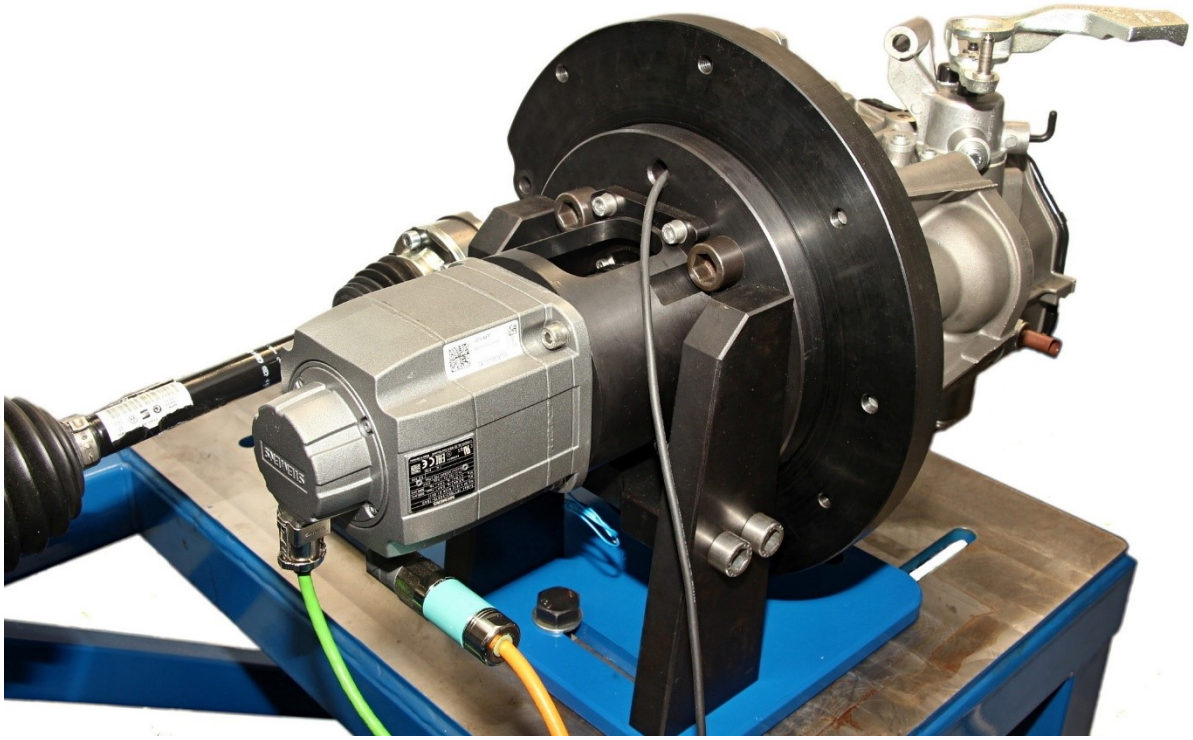

Figure 88: External synchronization assembly at the test bench

5.1.3 New Control System

The original plan was to update and expand the original LabVIEW control system to include the new input electric motor, eClutch, electromagnetic clutch and sensors. However, the original system did not comply with modern LabVIEW programming standards based on state machines and its modification turned out to be very difficult with uncertain results. It was also inconsistent in triggering the start of data acquisition – occasionally one or more sets of the measured data was shifted up to 200 ms behind the rest of the data. A new control system and user interface were therefore built from scratch using only specific parts of the original program (e.g., basics of the control loops for the output motor and gearshift robot in the form of SubVIs). This control system includes loops and state machines for following tasks:

- Program initialization and termination, event watching.
- Limits setup and monitoring.
- Output ABB motor control.
- Input Siemens motor control.
- Gearshift robot control.
- eClutch control.
- Counter measurement (variable sampling rate).
- Temperature measurement (constant sampling rate – 1 Hz).
- Acceleration and noise measurement (constant sampling rate – 51.2 kHz).
- Other measurements (constant sampling rate – 100 Hz).
- Data logging.
- State machine for the gearshift procedure.

- State machine for sequence measurement – automated gearshift procedure control.
- State machine for continuous service life testing.

During the initialization of the program, user must choose between three following modes of operation regarding the gearshift robot:

- **Manual.** Individual pressure valves at the gearshift robot can be operated. This mode is useful for the setup of the gearshift robot, particularly the position sensors at the pneumatic pistons. These give the control system necessary feedback whether the selected gear was successfully engaged or not. Each gearshift mechanism for each gear may have a different length of the gearshift sleeve movement which must be taken into account by different position of the corresponding sensor.
- **Automatic.** Only Individual gears can be shifted. The control system operates individual valves automatically. This mode is useful for setup and functionality verification of the whole test bench, debugging, heating up the gearbox oil etc.
- **Sequential.** Gears are shifted automatically by the program. All the gearshift buttons are grayed out and inactive. This mode is suitable for all the testing controlled by the state machines mentioned above.

User interface is shown in Figure 89. The left part shows the measured data in real time in charts. In the middle column there are the controls for gearshift in automatic mode, controls and indicators of data logging, emergency stop button 'AZ-5' and some other real-time values indicators. The upper right part controls the eClutch, electromagnetic clutch, ABB and Siemens motors, pressure valves in manual mode, and there are buttons for limits setup and standard termination of the program. The box in the lower right corner is the main input center for the user. The state machines for testing can be started here and there are also controls for all the required input parameters (e.g., input and output RPM, shifted gear, gearshift pressure, eClutch position, mismatch speed etc.).

In the example in Figure 89, the system is in sequential mode – all the buttons in 'Automat' and 'Manual' boxes are grayed out. The state machine for sequence gearshift measurement is controlling the test bench and collecting a data set – current gearshift is number 906 in the series. The 4^{th} gear is being shifted and data acquisition is on (indicated by the LED in lower right corner). Full resolution images of the LabVIEW control program interface and VIs block diagrams are listed in Attachment 5).

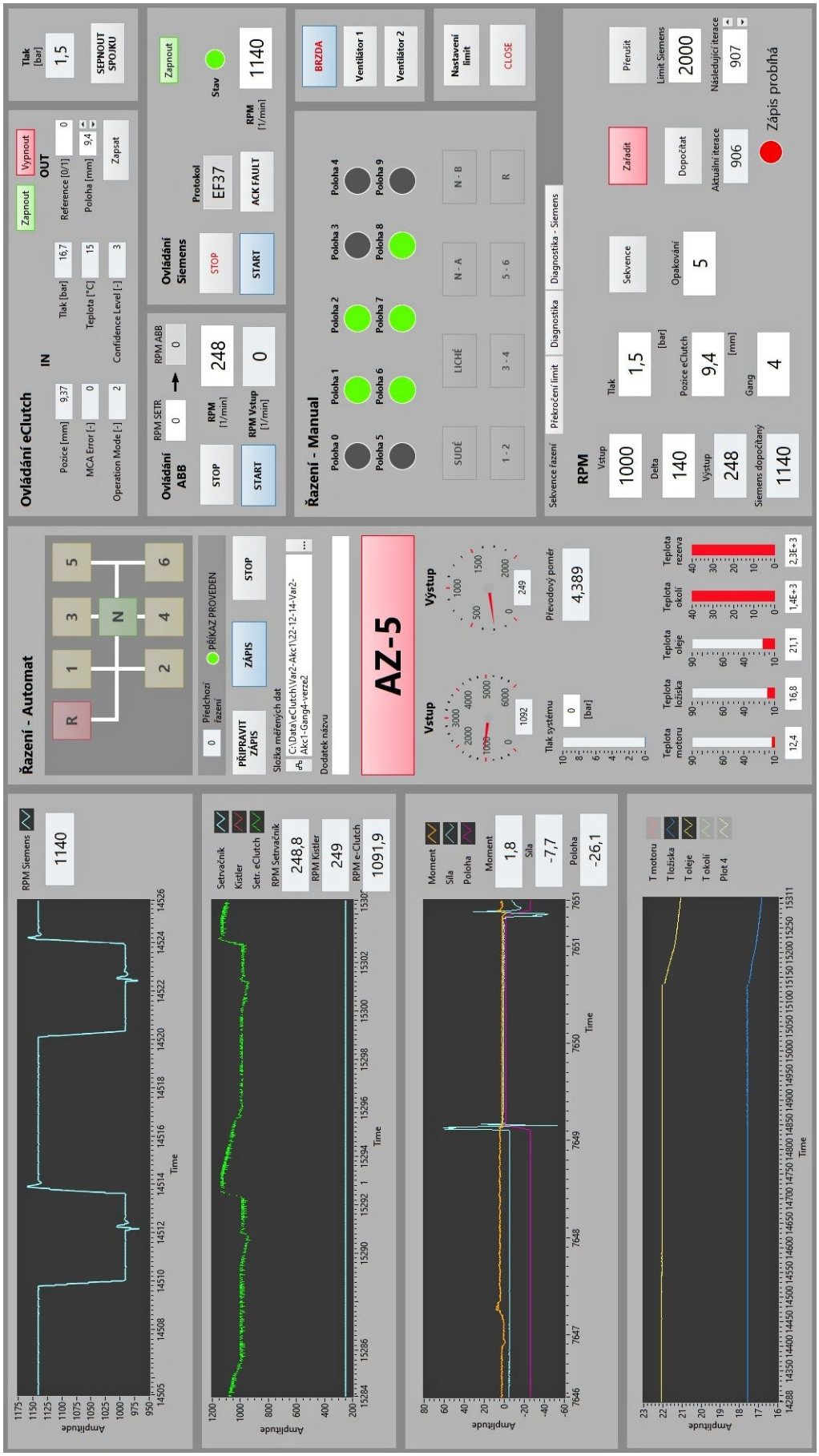

Figure 89: Front panel of new control system

5.2 Functionality

This chapter describes all measurements and experiments that were performed on the dog clutch prototypes described in Chapter 4.2.5.

5.2.1 Assembly

The first step was to assemble the clutches. This can be done without any special tools or assembly jigs. However, for quick assembly at the assembly line, two simple tools would be useful during the following steps. The process is also shown in Figure 90, tools marked grey:

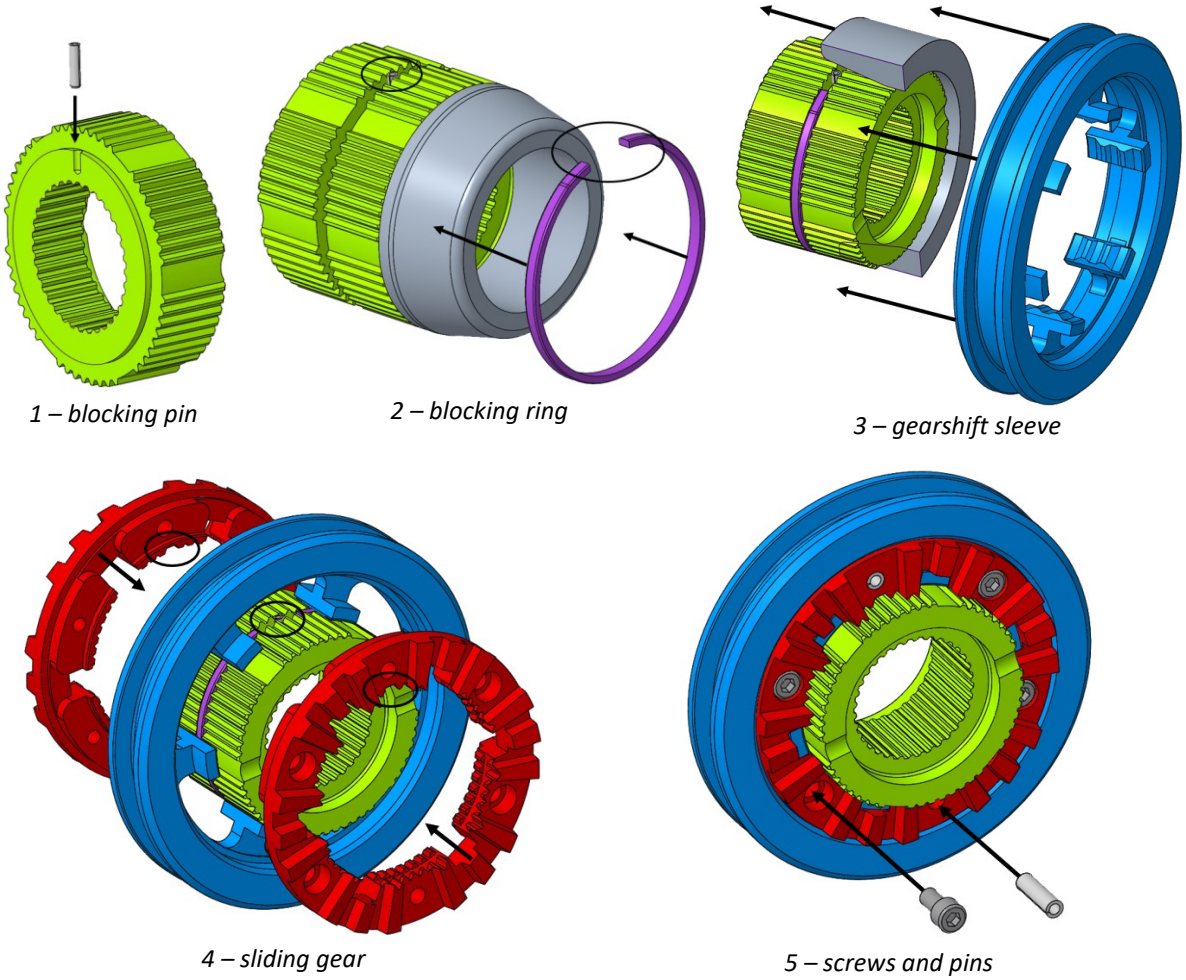

Figure 90: Assembly of the dog clutch with blocking mechanism

1) Sliding the **blocking pin** into the groove of the hub.
2) Sliding the **blocking ring** into the groove of the hub. The blocking ring must be stretched and then slid over the outer splines of the hub. A simple tool with conical outer surface would make stretching the ring and sliding it onto the splines easier. The gap in the blocking ring must be lined up with the blocking pin.
3) Sliding the **gearshift sleeve** over the blocking ring into neutral position. The groove in the hub must have a smaller diameter than the blocking ring inner diameter to allow its compression. Therefore, the current position of the blocking ring can vary slightly.

A simple tool with conical inner surface which would make the ring concentric with the hub before sliding the sleeve over the ring would be therefore suitable.

4) Sliding the two halves of the **sliding gear** to the neutral position, one from each side of the hub. It is important to keep track of which side of the assembly belongs to which shifted gear and respect it when adding the parts as the dog clutch is generally not symmetrical. Also, there is only one correct angular position of the sliding gear because of the groove for the blocking pin.
5) Connecting the sliding gear using **screws and pins**.

5.2.2 Gearshift Force

The clutches were then assembled into the gearbox and a few thousands of gearshifts verifying correct functionality were made with them. This also smoothened the movement of the clutches and lubricated them properly. Then the clutches were removed from the gearbox for visual inspection. Furthermore, two experiments were carried out with one of the clutches at analog laboratory scales. The clutch was placed onto the scales in engaged position, axis of rotation perpendicular to the ground. The clutch and the scales dial were simultaneously recorded on camera.

In the first experiment, a steel pipe and a plastic box were placed on top of the clutch touching only the gearshift sleeve. Then the box was gradually filled by steel pellets, increasing the load at the sleeve and simulating the gearshift force acting on it. Figure 91 shows the exact moment when the gearshift force compressed the blocking ring via the sleeve and the gear is being disengaged – the sleeve is blurry on the video snapshot. At the scales dial we can read the current ca. 3.6 kg. However, this readout is not accurate since the load has already started moving. In quasistatic equilibrium before it started moving, the load equals ca. 4 kg. Adding the weight of the steel pipe and plastic box (ca. 0.5 kg), the resulting gearshift force needed for blocking ring compression equals ca. 45 N.

This is a higher value compared to the calculations in Chapter 4.2.4.3 (ca. 32 N). However, the derivation of Equation (13) for the compression force might be slightly inaccurate and affecting this difference. The measured force of 45 N was therefore selected as more trustworthy for future consideration.

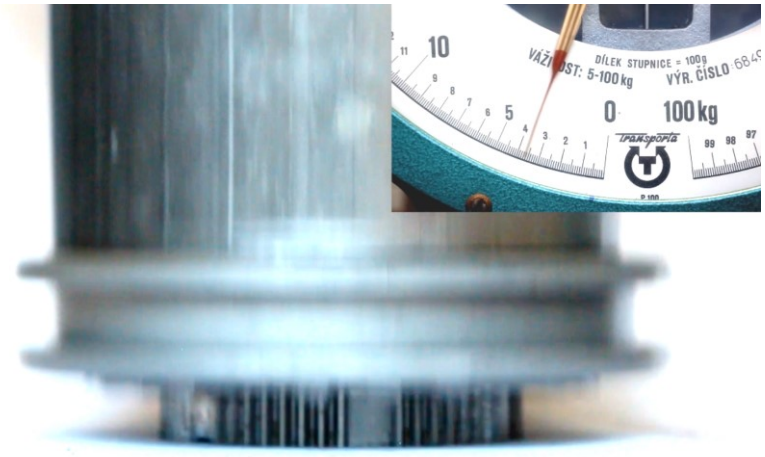

Figure 91: Gearshift force verification on the scales

In the second experiment, a steel pipe was placed on top of the clutch touching only the sliding gear. The top of the pipe was then loaded until the scales limit was reached (approximately 110 kg corresponding to ca. 1,080 N gearshift force). Even though this is a smaller force compared to the maximal load at the dogs of the 1st gear clutch (ca. 1,800 N) and cannot be therefore considered a strength test, it demonstrates that the blocking ring is successfully serving its purpose and prevents unwanted disengagement of the clutch. Videos of both experiments are listed in Attachment 6).

5.2.3 Shifting Gears

The first phase of testing of the clutch prototypes in the gearbox was carried out at the inertia test bench, the output shaft connected to the large inertia disc. The testing was focused on smooth movement of the shift sleeve and appropriate engagement and disengagement of the dogs. During the initial observation the gearbox was running very slowly – the input shaft was stationary, and the output shaft was set to 10 min^{-1} at maximum. This resulted in mismatch speed of roughly 20 to 50 min^{-1} for 3rd and 4th gear when shifted from neutral. The gears were shifted manually using the gear selector arm on top of the gearbox. Behavior of the clutch was monitored directly in the gearbox using an Everest XLG3™ VideoProbe as shown in Figure 92.

Samples of recorded gearshifts are listed in Attachment 7). One of these samples shows two consecutive unsuccessful gearshifts. This was purposeful to demonstrate the sensitivity of dogs with tapered faces to the initial mismatch speed sign as discussed in Chapter 2.1.3.3. No unexpected behavior was detected.

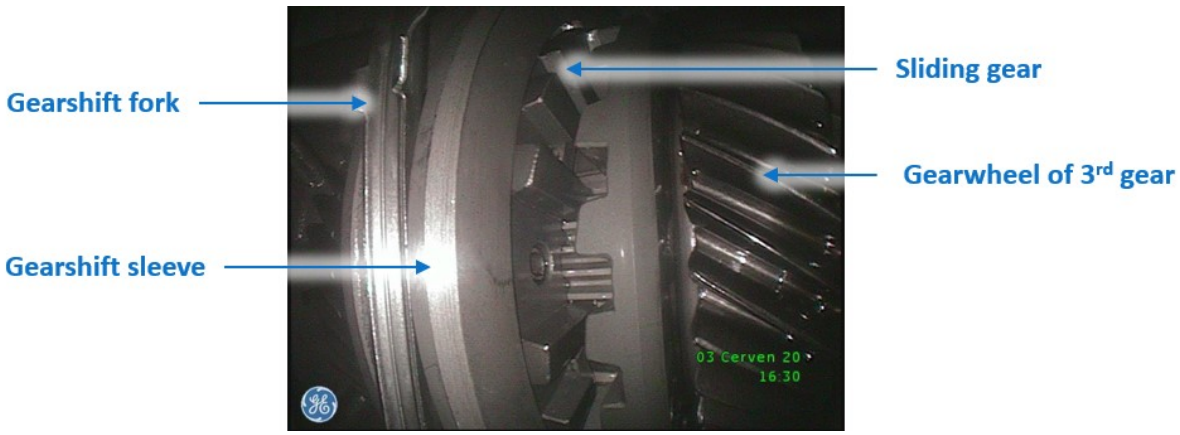

Figure 92: Gearshift verification using video inspection probe

Then the gearbox was connected to the gearshift robot (see Figure 93) and a variety of gearshifts for different input parameters was made. Unfortunately, at that time the inertia test bench was still in its initial setup as described in Chapter 5.1.1. This means that the external synchronization of the input shaft was not available. This significantly limited the testing possibilities and sped up the need for update of the test bench. Mismatch speed could only be set as a difference between stationary input shaft and rotating shifted wheel or difference given by the gear ratios of two gears when shifted directly between them.

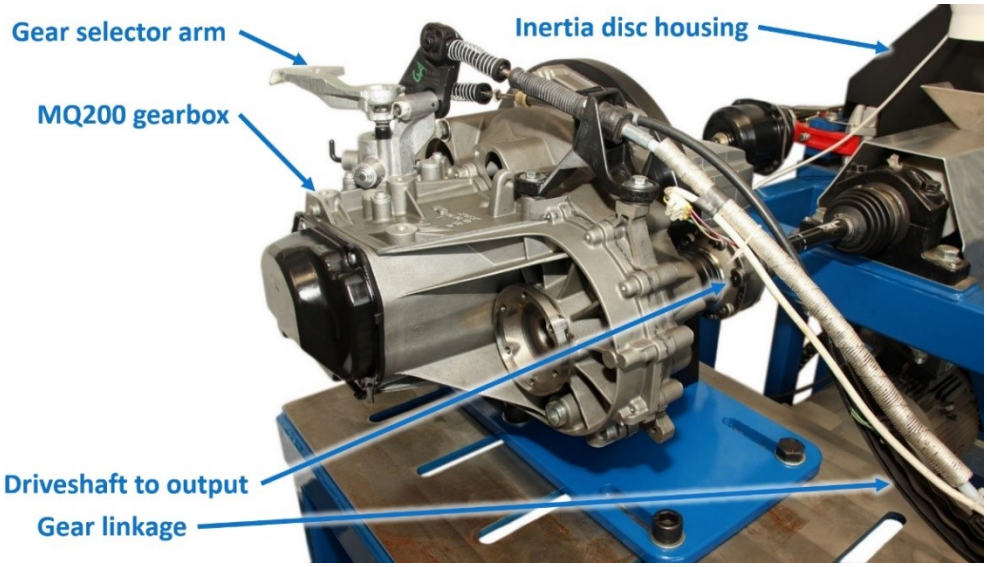

Figure 93: Gearbox with clutch prototypes at the inertia test bench

Figure 94 shows typical measured data of a successful gearshift – 3rd gear was shifted with mismatch speed 30 min^{-1}. The gearshift process starts at time 0.96 s – the curves of displacement and force start to rise. As described in Chapter 5.1.1, these two quantities are measured at the gearshift robot and their curves are therefore smoother than if they could be measured directly at the gearshift sleeve. Nevertheless, a sharp drop in gearshift force at 1.02 s is clearly visible. This means that the blocking ring is compressed, and the sliding gear and all the other components of the gear selector can continue moving. Shortly after this drop, the gearshift force starts rising again together with input RPM and output torque as the gearshift dogs come into contact. At the time 1.08 s the engagement process is finished, further increase in the displacement is caused only by the gearshift pressure which is still building up and compressing the components between the sensor and clutch. Shortly after, the control program evaluates the gearshift as successful, from 1.17 s the gearshift force drops again, the tension in the gear selector mechanism is released, the displacement decreases slightly. Gearshift duration was roughly 60 ms.

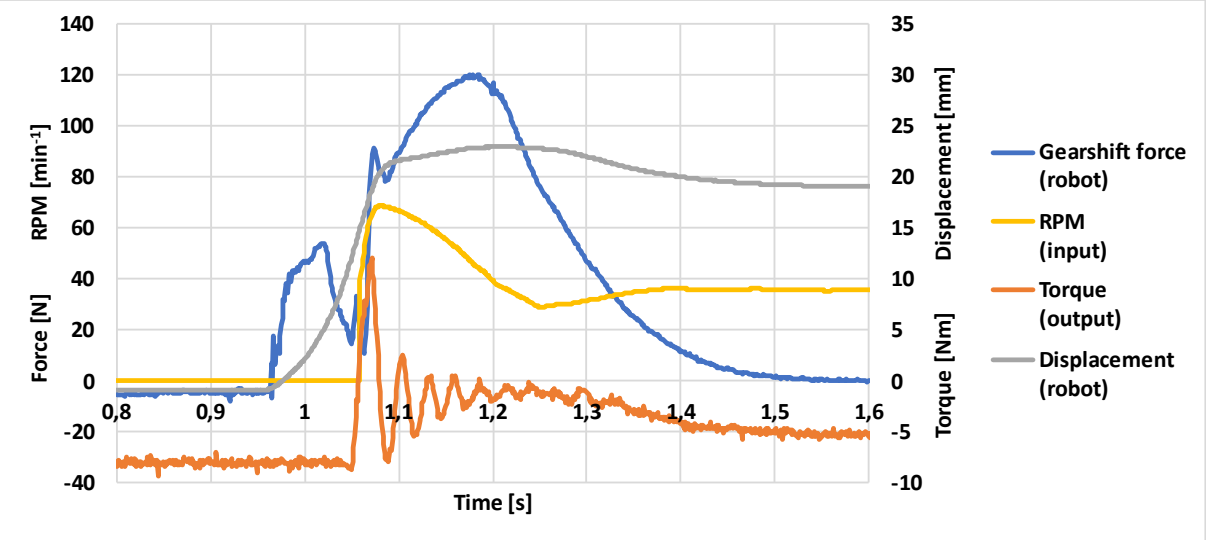

Figure 94: Shifting 3rd gear; mismatch speed 30 min^{-1}

5.2.4 Torque Load

Functionality of the blocking mechanism in the engaged state could not be verified at the inertia test bench, where only the output shaft could be loaded with torque, the input shaft rotated freely. The gearbox was therefore mounted at another test bench – an open test bench located in the same test hall. Here, each side of the gearbox (input and output) could be easily connected to a dynamometer to provide adjustable torque load of the gearbox (see Figure 95 for schematic).

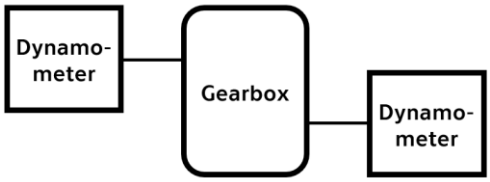

Figure 95: Schematic of an open gearbox test bench

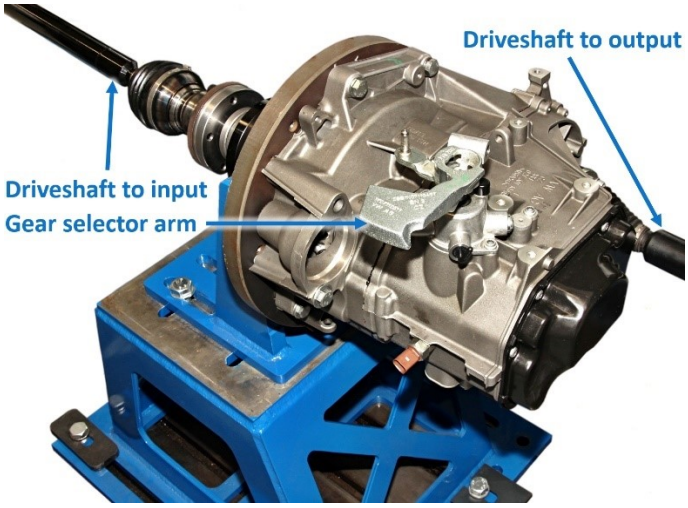

Figure 96: Gearbox with clutch prototypes at the dynamometer test bench

Figure 96 shows the input and output of the gearbox connected to dynamometers using standard driveshafts. Gears were shifted manually using the gear selector arm on top of the gearbox. Then one of the dynamometers was set to keep constant RPM and the second gradually increased the torque load. For 3rd and 4th gear, the blocking ring successfully blocked the gear. When reaching the equivalent of ca. 250 Nm input load, the friction clutch at the input was overloaded and began to slip.

The torque characteristics of the dynamometers limit the maximum available torque load for low RPM. The total gear ratios of the gearbox for the 1st and 2nd gear are too high and kept the output shaft in the low RPM range. Therefore, loading these gears at maximum torque was not possible on the test bench.

Despite that, incorrect blocking functionality was detected for the 1st gear. When increasing the load, the clutch always disengaged after reaching 20 to 30 Nm at the input. This was caused by incorrect chain of manufacturing tolerances in the axial direction of the clutch. The sliding gear therefore could not reach the engaged position to line up its inner groove with the outer groove of the hub, the blocking ring never fully stretched to secure the sliding gear in the engaged position. The clutch was disassembled, and a few tenths of millimeter were removed at the face surface of the shifted gear wheel where it is in contact with the hub. Then the test was repeated with successful results – the maximal load available at the test bench was reached.

5.3 Service Life

Service life tests were carried out at the inertia test bench for the 3rd and 4th gear clutch. Each gear was shifted 180,000 times. The gearbox output was set to 89 min^{-1}. This would mean unrealistically low vehicle speed for the 3rd and 4th gear in real operation. However, the service life test was designed mainly for the blocking ring as the most critical component, not the gearshift dogs or other components.

The reason for the 89 min^{-1} output speed is that for this RPM value, there is ca. 140 min^{-1} mismatch speed when shifting directly from 3rd to 4th and back from 4th to 3rd. The gearshift dogs for these gears were designed to have their faces tapered in the opposite directions. Therefore, the sign of the mismatch speed is always favorable for successful gearshift. This made using external synchronization unnecessary, which was beneficial for two main reasons – time saving and energy (respectively costs) saving. The state machine controlling the test was optimized for the shortest time possible. One gearshift took slightly longer than 2 seconds (see video in Attachment 8) which translates into 220 hours of continuous testing for one gearshift clutch and one blocking ring respectively. The mismatch speed 140 min^{-1} was chosen to maximize the number of successful gearshifts.

During the test, gearshift force and output torque were monitored and maximum for each gearshift was calculated. These were than compared to limit values set independently for both gears. In case of exceeding one of these values, the test would have been stopped to prevent damage of the test bench or the clutch due to an unexpected failure, e.g., blocking ring breakage. Based on the displacement maximums during gearshift, successful and unsuccessful gearshifts were also monitored.

Initially, the program stopped the test after each unsuccessful gearshift. However, it turned out that for 4th gear, the gearshift was unsuccessful roughly once for every 15,000 gearshifts. This was causing undesirable delays in testing. Examination of the data showed no malfunction or unexpected behavior except for unwanted face-to-face contact of the dogs. The code was then changed to stop the test only after two consecutive unsuccessful gearshifts of the same gear. The test was then finished without further complications.

Interestingly, throughout the 180,000 gearshifts, no unsuccessful gearshift due to face-to-face contact occurred for the 3rd gear. Analysis of the data and situation at the clutch suggests the following explanation – even though the probability of this happening is very low, for such a large number of gearshifts, the first contact of the dogs is edge-edge with the resultant contact force in such direction, that the mismatch speed is reduced to almost zero and after a short bounce-back, face-to-face phase occurs. Due to the opposite angle of the face taper of the dogs, the force and torque equilibrium in this face is also different. The angular speed of the shifted wheel is kept approximately constant by the large inertia disc and the large output motor. The dogs of the sliding gear are pressed against the dogs of this shifted wheel. Due to the tapered face, tangential force and corresponding torque arises at the face contact of the dogs. No additional active torque load is acting on the sliding gear. However, it is directly connected to the input shaft, which is subjected to friction losses in bearings, oil losses etc. For the 3rd gear, this torque caused by losses is acting in the same direction as the

torque in the face-to-face contact. Therefore, the situation is resolved, the dogs slide on each other, and the gear is engaged. However, for the 4th gear, these torques act in opposite direction and the clutch stays stuck in the face-to-face phase, gearshift is unsuccessful.

The friction losses and friction torque depend on the various parameters, e.g., angular speed of the gearbox, oil temperature etc. The angular speed was lower than during usual operation of the gearbox, given by the desired mismatch speed between 3rd and 4th gear. The oil temperature was comparable to the air temperature in the laboratory due to no load and low angular speed. Furthermore, the assumption of constant angular speed of the output is also not always valid in actual operation. As a result, general advice to prevent this phenomenon would be choosing such a face taper angle of the dog that both torque loads act in the same direction, similarly to the 3rd gear of the prototype.

The gearbox was completely disassembled in the half of the test and then after the test for visual check. No failures were found, the operation of the clutch is even smoother than when it was new. Most concerns about the service life capabilities related to the blocking ring. After 720,000 cycles, there is no plastic deformation of the ring caused by the bending stress. The outer diameter still complies with the dimension 48.1±0.2 mm required in production drawing. The most visible wear is located at the outer diameter, at the edges where the blocking ring is compressed by the gearshift sleeve, near the ends of the C-shape – see Figure 97 and Figure 98.

Figure 97: Ring after service life test

Figure 98: Ring after service life test – detail

Figure 99 and Figure 100 show the wear of the dogs at the sliding gear which is barely visible at the faces of the dogs. The edges of the dogs remained sharp and intact. However, the test was designed mainly for the blocking ring validation and the load at the dogs was lower than it would be during normal operation. Even though the mismatch speed during the test corresponded to the mismatch speed expected during normal operation, the kinetic energy difference was smaller due to the lower angular speed of the input shaft. However, the dogs are not expected to cause any problems for reasonable mismatch speeds, as described in Chapter 4.2.3.

Figure 99: Sliding gear after service life test

Figure 100: Sliding g. after service life test – detail

The only other visible wear of the clutch is shown in Figure 101 and Figure 102. It is the contact surface between the hub and gearshift sleeve.

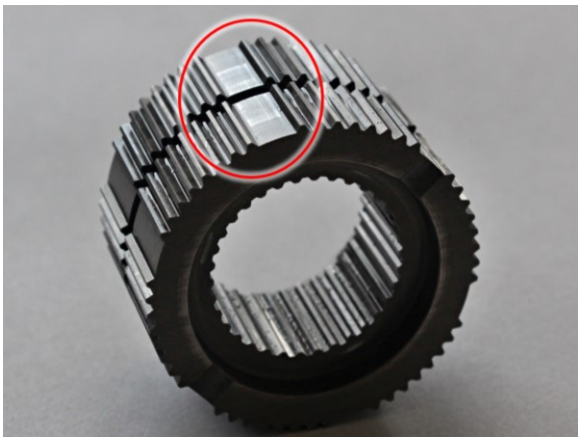

Figure 101: Hub after service life test

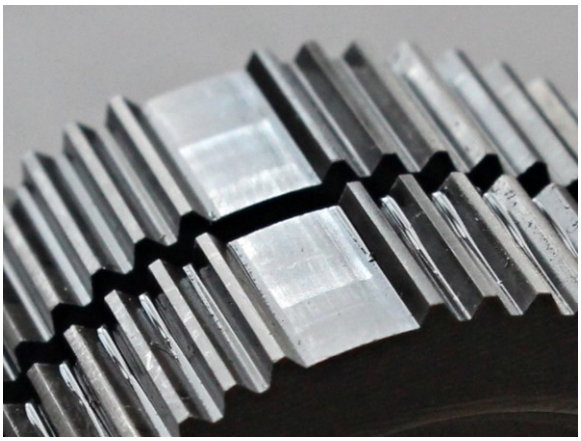

Figure 102: Hub after service life test – detail

In summary, the service life test results can be assessed as very positive. All the components of the dog clutch with blocking mechanism succeeded with little to no visible wear.

5.4 NVH and Comfort

Automotive gearboxes have been thoroughly studied regarding the NVH due to torque transmission and high-speed rotational movement. Many sources and papers addressing gear noise and its minimization can be found. However, very little research is available for NVH of the gearshift mechanisms, especially methodology and measured values for reference. For this reason, methodology based on vibration and noise measurement and comparison of various gearshift mechanisms in identical gearbox at the test bench was designed.

5.4.1 Test Bench Setup

All the measurements were carried out at the inertia test bench after the updates described in Chapters 5.1.2 and 5.1.3. In this setup, the total input moment of inertia was 0.16 kg*m^2 (represented mainly by the flywheel and small inertia disc – see Figure 86) – this

corresponds to a standard 4-cylinder combustion engine. Three variants of the MQ200 gearbox differing only in the gearshift mechanism were prepared for the measurement:

1) **Variant 1.** Standard synchronizers, no modifications. Synchronizers were taken as a benchmark for NVH and comfort during gearshift. However, no reference data was available for the synchronizers. And even if it was, the vibrational characteristics of each car and each test bench are different. Therefore, measurement of this variant was carried out in the first place to gather benchmark data.
2) **Variant 2.** Standard synchronizers, locking toothing removed at synchronizer rings for all gears (see Figure 103). Function of the locking toothing in synchronizers was described in Chapter 2.1.2.1. Without this toothing, the synchronizers lose their blocking function – they behave similarly to dog clutches. Even though the friction cones are technically still able to synchronize, the gearshift force acting on the sleeve pushes the sleeve toothing into mesh with the synchronizer hub toothing regardless of the initial mismatch speed. This variant was suggested as the cheapest way to test the functionality of the test bench and gather data for less favorable dog clutch gearshift scenarios (e.g., high mismatch speed or high input moment of inertia) without risking damage of the much more valuable prototypes of the dog clutch with blocking mechanism.
3) **Variant 3.** Dog clutches with blocking mechanism. Finally, the prototypes were tested to compare them with the previous two variants.

Figure 103: Synchronizer ring after the removal of locking toothing

There are many input parameters which affect the gearshift process and the resulting NVH values. Some of them were marked as insignificant or hard to simulate (e.g., oil temperature in the gearbox). In the end, five parameters adjustable at the test bench were taken into consideration as variable input parameters:

1) **Shifted gear.** Only the 1st, 2nd, 3^{rd,} and 4th gear were shifted. A prototype for the 5th and 6th gear was not manufactured, these gears were therefore not tested.
2) **Input shaft angular speed [min^{-1}].** With respect to the limitations of the gearbox and test bench, the range of 1,500 to 4,500 min^{-1} was considered. Even when testing the clutches for 1st and 2nd gear placed at the output shaft, the indicated angular speed is recalculated to the input shaft angular speed for easier comparability.

3) **Mismatch speed [min^{-1}].** The mismatch speed is indicated directly at the shifted gear wheel. Positive sign means that the input shaft is rotating faster than necessary and must be slowed down during the gearshift and vice versa.
4) **Gearshift pressure [bar].** Due to the pneumatic gearshift system of the robot, the maximum value of gearshift force cannot be directly set – the gearshift force is dependent on the pressure of the air which flows to the shift pistons. For previous service life and functionality tests of the MQ200 gearbox, the range of 1 to 2 bar was calibrated as correlating to the gearshift forces required for these tests by the manufacturer. The same range was therefore used for the NVH tests.
5) **Position of eClutch [mm].** The position of the eClutch control system determines the behavior of the friction clutch (see Figure 104). The friction clutch is located between the input shaft of the gearbox and the flywheel and small inertia disc simulating the rotational mass of the engine as described in Chapter 5.1.2. The original idea behind this input parameter is the effort to minimize NVH during gearshifts – the friction plate of the clutch is equipped with torsional springs. Keeping the friction clutch somewhere between the kiss point and residual friction phases may utilize these torsional springs to reduce the NVH caused by the impact during the gearshift – especially combined with minor slip of the clutch friction plate. The resolution of the eClutch system is 0.1 mm and speed approximately 7 mm per 0.1 s. The range of 0 to 12 mm was used for the measurements since for any higher values the clutch remains fully open.

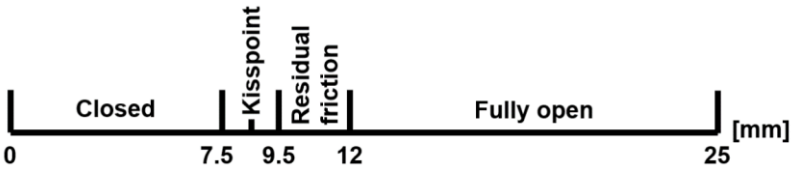

Figure 104: Engagement phases of the friction clutch regarding the position of eClutch

The gearshift process and data acquisition were automized and performed by the corresponding state machine of the control program as described in Chapter 5.1.3. Each measured gearshift automatically followed these steps:

1) The gearbox is in neutral. The friction and electromagnetic clutch are both closed. User defines the input variables and starts the gearshift process.
2) Required input variables are set (angular speed of the input and output shafts, gearshift pressure).
3) Data acquisition and logging of all measured data is initiated by a common trigger.
4) Required friction clutch position is set and the electromagnetic clutch disengages (the input motor cannot affect the gearshift).
5) Selected gear is shifted, and the control program waits about a second after the gearshift is approved as successful (to record possible oscillations after the gearshift).
6) Data acquisition and logging is terminated.
7) The friction clutch gradually engages back to position 0 mm (closed).
8) Neutral is shifted.

9) The input EM matches the angular speed of the input shaft, and the electromagnetic clutch engages.

Now the test bench is back in the initial state and ready for another gearshift. Each gearshift cycle takes about 10 seconds. The user can then change the input variables and start another gearshift. For practical use and acquisition of large data sets, the state machine for automated gearshift procedure control is prepared. The user defines the variable input parameter, its range and step (e.g., the eClutch position). The control program then performs a series of measurements automatically. Furthermore, the required number of gearshifts for each unique combination of input parameters can be set – 5 recurrent gearshifts were performed for all the measurements to minimize the statistical error.

Despite the effort to shorten the delay between phases 4 and 5, the gearshift does not occur immediately after the input motor is disconnected. Therefore, the real mismatch speed at the time of the gearshift is lower than set by the motor due to friction losses of the input. This difference in mismatch speed was examined experimentally using the RPM sensor at the clutch and flywheel and correction coefficient of 40 min^{-1} was used to set the mismatch speed at the input motor. However, the theoretically correct value of this coefficient varies due to temperature (and friction) changes and also the eClutch position. As a result, the error of the mismatch speed may be up to ca. ±20 min^{-1}.

Two output files are created for each gearshift. The first of them contains the NVH data measured by an accelerometer and a microphone. This data is acquired using the 4-channel NI 9234 Sound and Vibration Input Module and will be thoroughly described in the following two chapters. The second file contains all the other parameters measured by the test bench as described in Chapter 5.1.3. Two of these parameters can then be automatically evaluated by a DIAdem script for the whole data set:

- **Gearshift time.** Based on the gearshift displacement data and positions of neutral and engaged gears, the gearshift time can be calculated. Short gearshift time is one of the main qualities of the gearshift clutch. Furthermore, plotting the gearshift time for the whole data set is extremely helpful in tracking the gearshifts with abnormal behavior. The color spectrum is used for marking these gearshifts which deviate from the average values of their surroundings. Such gearshifts can then be manually inspected and discarded from the data set if there is any kind of error found.
- **Maximum torque.** The maximum value of torque during the gearshift is found based on the output torque measurement. It is considered an indicator of the comfort level during the gearshift.

5.4.2 Vibration Measurement

Vibrations were measured with the Brüel & Kjær cubic triaxial CCLD accelerometer type 4524 designed for automotive body and powertrain applications; [83]. The frequency range is 0.25 to 3,000 Hz and adhesive mounting clips were used (see Figure 106) – accelerometer can be easily relocated to different position or gearbox. Three positions on the

gearbox case (see Figure 105) were chosen for measurement according to advice from ŠKODA AUTO engineers and recommendations from [84]:

1) **Position 1.** Top side of the gearbox. Near the input shaft bearing and gearshift clutch for 3rd and 4th gear.
2) **Position 2.** Bottom side of the gearbox. On the cover of the internal gearshift rod.
3) **Position 3.** Bottom side of the gearbox. Near the output shaft bearing and gearshift clutch for 1st and 2nd gear.

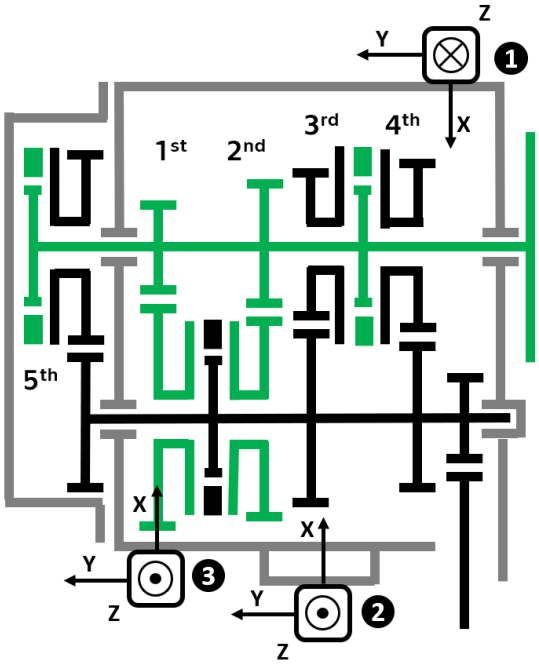

Figure 105: Available accelerometer positions 1 to 3 and orientations on the gearbox case

Figure 106: B&K accelerometer in position 2

The accelerometer measures acceleration in [m*s^{-2}] in three different directions (X, Y, Z) – geometrical resultant of these signals was calculated for further processing. The total number of samples varied slightly for each gearshift due to the triggering method used in LabVIEW for data acquisition. The data was therefore reduced to a constant number of samples. Measured data of gearshift displacement were used to determine the gearshift start and consequently the first preserved sample was chosen ca. 0.1 s before this event. In total, constant number of samples equal 1.5 s was preserved to make the signal length identical for all the gearshifts (even the longest gearshifts had to fit in this time window).

The sampling rate was common for vibration and noise measurement. The highest value available for the NI 9234 module was used – 51.2 kHz. This was suitable for aliasing prevention, highest observable frequency without aliasing (Nyquist frequency) equals 25.6 kHz; [85]. However, the accelerometer has a recommended frequency range of up to 3 kHz, which corresponds to a resonance frequency of around 9 kHz. With the 51.2 kHz sampling rate, even frequencies in the resonance area of the accelerometer were recorded. This distorts the measured signal due to the increased sensitivity of the accelerometer in this area; [86]. Therefore, a low-pass filter set to 3 kHz was used which gradually suppresses higher than limit frequencies.

There are many ways to quantify the signal in time domain (e.g., peak value, peak-to-peak, RMS, average absolute value, crest factor) or frequency domain; [84]. Time domain was chosen since the gearshifts were mainly carried out for lower input angular speeds to minimize the gearbox vibrations non-related to gearshift and there is no specific range of dominant gearshift vibration frequencies. Furthermore, the calculation in time domain is much faster. After initial calculation and comparison of various metrics, root mean square (RMS) of the resultant was chosen as the main metric; [87]:

$$RMS = \sqrt{\frac{\sum_{n=1}^{N}[A(n)]^2}{N}} \tag{21}$$

This metric represents the square root of the arithmetic mean of the squares of the measured resultant vibration values. Even though the output is a single number, this metric takes into account all measured samples of the signal. The physical analogy for RMS is the 'mechanical power' of the measured signal. Maximum value was also analyzed as a supplementary metric.

5.4.3 Noise Measurement

Noise was measured with the ½" Brüel & Kjær prepolarized free-field microphone type 4189 and Brüel & Kjær microphone preamplifier type 2671. The output is one channel – the amplitude of air pressure fluctuation in [Pa]. Similarly to vibration measurement, each gearshift data set was shortened to a time window of 1.5 s fixed length and filtered with a 20 kHz low-pass filter.

The main metric used to quantify the measured signal in the time domain was again the RMS according to Equation (21). As a supplementary metric, the maximum sound pressure level (SPL) based on the audible threshold of $2*10^{-5}$ Pa was evaluated; [85]:

$$dB_{SPL} = 20 \cdot log\left(\frac{p_{MAX}}{2 \cdot 10^{-5}}\right) \tag{22}$$

Analysis in frequency domain using fast Fourier transform was also carried out. However, no characteristic frequencies were found for the noise of the gearshift and the results are therefore not presented.

Noise measurement was supplementary to vibration measurement. The reason for that is that measuring exclusively gearshift noise is not truly possible at the test bench – there are many other sources of noise. The most disturbing of them is the pneumatic gearshift robot. Specifically, impacts in connection between the piston rods and gearshift cables. To minimize this noise, the microphone was placed on the opposite side of the gearbox as far from the robot as possible and close to the gearbox (only about 10 cm). Furthermore, the fan of the electric motor is a significant background noise.

5.4.4 Determining Input Parameters Range

The general boundaries for the input parameters are listed in Chapter 5.4.1. However, for each gearshift mechanism, it was necessary to specify the range of input parameters based

on the behavior during gearshift – this applies especially for the mismatch speed. The following figures show an example of the gearshift process for each gearshift mechanism variant. It is necessary to point out that these are gearshifts for extreme input parameters that would not be appropriate for practical operation. However, they most clearly demonstrate phenomena that are typical for each variant and can be simulated on the test bench. Furthermore, these phenomena were identified based on the measured data analysis and used to determine the range of input parameters.

5.4.4.1 Variant 1 – Synchronizer

Regarding NVH, the mismatch speed and eClutch position have only a small influence on the synchronizer with blocking functionality. However, they have a strong effect on gearshift time – the torque capacity of the friction clutch (set by eClutch position) must be smaller than torque capacity of the synchronizer. Otherwise, the synchronizer is overloaded for non-zero mismatch speed and the gearshift times are unacceptable. This is expected behavior for a synchronizer with blocking functionality.

Generally, the range of input parameters did not have to be limited, and reference data could be measured for any required combination of input parameters.

Figure 107 shows a 3rd gear synchronizer (variant 1) gearshift with closed eClutch and mismatch speed of 500 min^{-1}. The effect of the large input moment of inertia is clearly visible – the synchronization phase lasts approximately 0.5 s starting at timestamp 1.6 s. During the synchronization phase, the gearshift force, displacement and torque are roughly constant – no vibrations are present. Two vibration peaks are visible – one when the gearshift sleeve comes into contact with blocking ring, and the second one when the sleeve reaches the engaged position. These gearshifts were used to obtain a more precise dependency between the eClutch position (input adjustable parameter) on the one hand and the friction clutch phases and the actual torque capacity on the other.

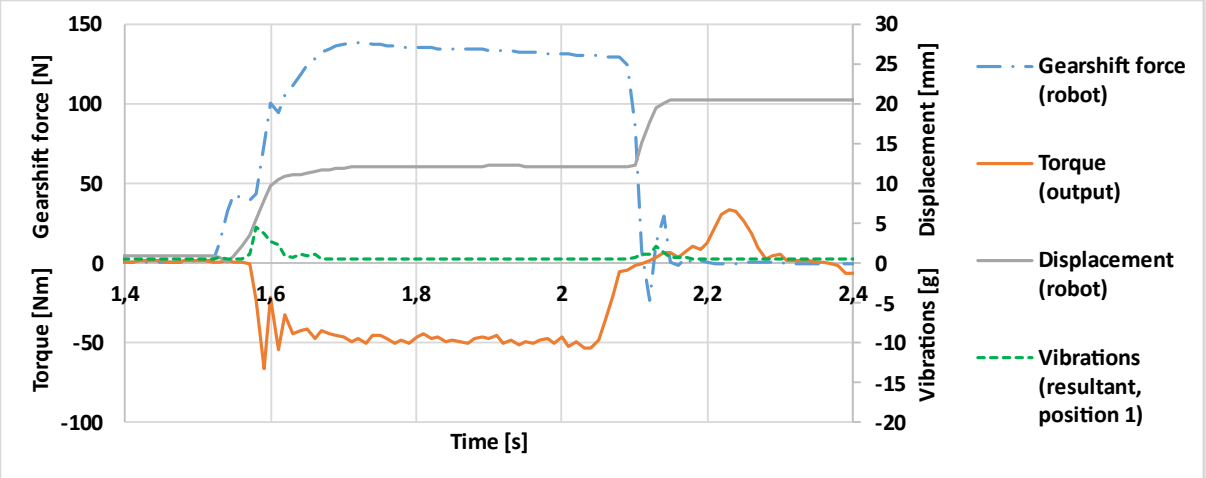

Figure 107: Gearshift of variant 1 – synchronizers
Mismatch speed 500 min^{-1}; eClutch 0 mm (closed); gearshift pressure 1 bar; 3rd gear

5.4.4.2 Variant 2 – Blocking rings removed

For variant 2 without blocking rings, the effect of the mismatch speed and eClutch position on NVH is significant. For higher mismatch speeds than 100 min^{-1}, the eClutch range had to be reduced to the kiss point or open area to prevent unwanted damage from torque shocks. Otherwise, the output torque would reach values of ca. 200 Nm and the gearshift noise was audible and very loud. Using higher gearshift pressure and gearshift force reduced the probability of bounce-back and therefore reduced the NVH on average.

Figure 108 shows a 4th gear gearshift with blocking rings removed (variant 2), eClutch in the kiss point area and mismatch speed -125 min^{-1}. This particular gearshift was detected by gearshift time analysis as abnormal. It was caused by a bounce-back, as described in Chapter 2.1.3.3. For the symmetric toothing of the synchronizer with side angles of ca. 45°, this occasionally happened under various combinations of input parameters. Bounce-back makes the gearshift much longer and increases the NVH. In the case shown in Figure 108, the gearshift lasted approx. 0.2 s longer than the average gearshift without bounce-back for identical input parameters. The vibrations curve has only one visible peak, most of the mismatch speed was reduced during the first impact. For some gearshifts, this peak is lower, and a second peak corresponding to the second impact after bounce-back is present.

Testing of this variant was mainly focused on the analysis of test bench behavior during non-synchronized gearshift with the effect of input moment of inertia and eClutch position. This variant is not suitable for real operation in particular due to the gearshift toothing shape and bounce-back occurrence frequency.

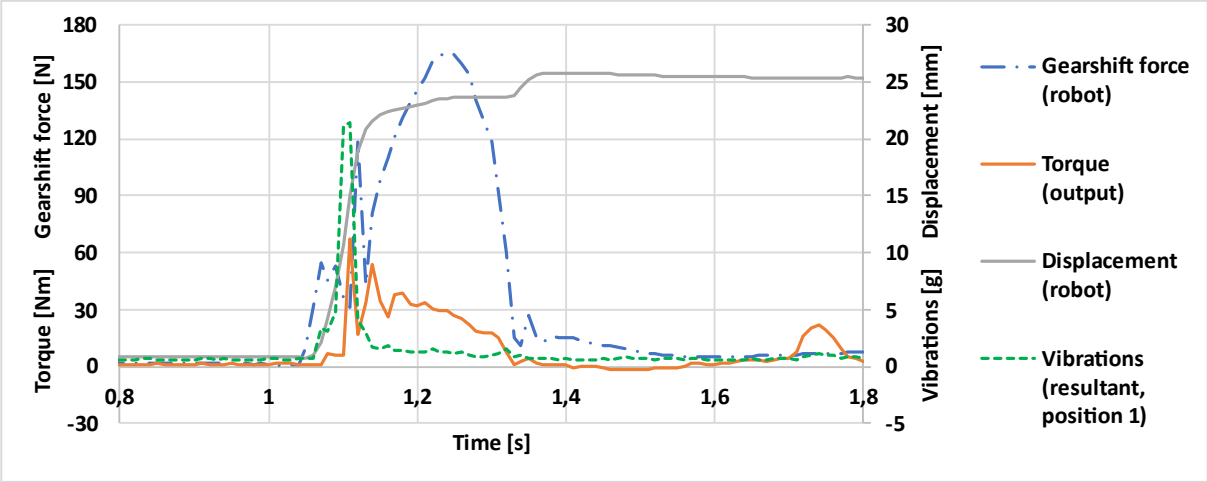

Figure 108: Gearshift of variant 2 – blocking rings removed
Mismatch speed -125 min^{-1}; eClutch 8 mm (kiss point); gearshift pressure 1.5 bar; 4th gear

5.4.4.3 Variant 3 – Dog clutch with blocking mechanism

Generally, the upper mismatch speed boundary due to NVH was similar to the previous variant 2. However, in the open clutch area, no bounce-back occurred for the correct mismatch speed direction. Therefore, the dog clutch with blocking mechanism was tested at higher maximum mismatch speeds (ca. 450 min^{-1} compared to ca. 250 min^{-1} for variant 2). On

the other hand, gearshifts for the mismatch speed close to zero were too long and were proven to be not suitable for real operation.

Figure 109 shows a 3rd gear dog clutch with blocking mechanism (variant 3) gearshift, eClutch in the kiss point area and mismatch speed 0 min^{-1}. Due to the zero mismatch speed, face-to-face contact occurred. The gear was eventually successfully engaged – accompanied by a large drop in gearshift force as the sleeve clutch started moving again. Very little vibration peaks are visible, almost no change in kinetic energy occurred, and torque oscillations are minimal. However, the gearshift time is very long – a minimal value of the mismatch speed for the dog clutch with blocking mechanism was identified as ca. 50-100 min^{-1} (depending on the gear, respectively, face angle direction).

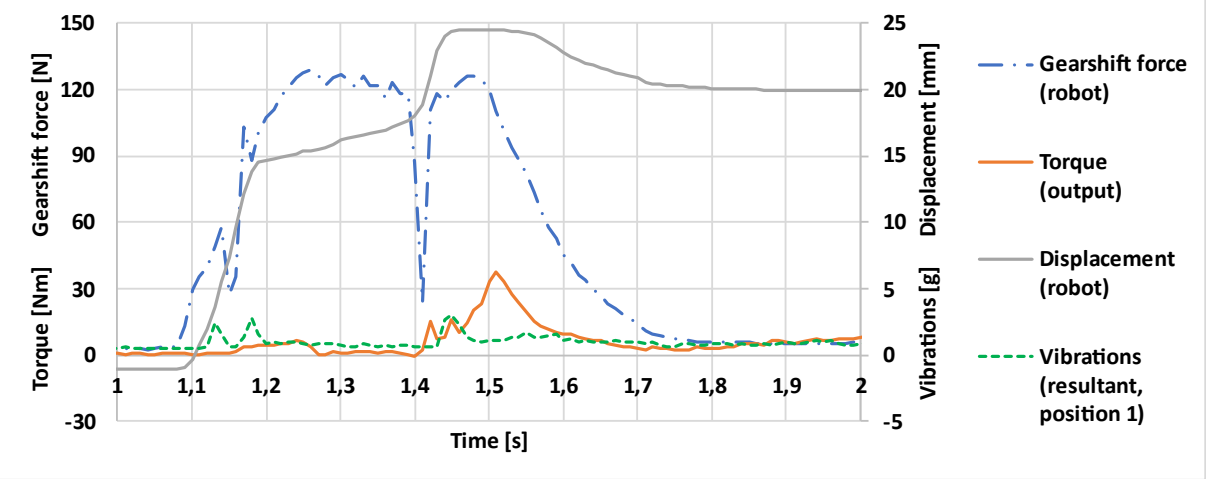

Figure 109: Gearshift of variant 3 – dog clutch with blocking mechanism
Mismatch speed 0 min^{-1}; eClutch 8 mm (kiss point); gearshift pressure 1 bar; 3rd gear

5.4.4.4 Summary

Thousands of gearshifts were analyzed to understand the behavior of all three variants – the examples above only demonstrate specific cases. To reduce the amount of data combinations for further measurement and analysis, the following boundaries were set based mainly on the behavior of the dog clutch with blocking mechanism.

The input shaft angular speed was set exclusively to 1,500 min^{-1}. Higher speeds added more background noise to the NVH data with no significant changes in behavior during gearshifts. The 3rd and 4th gear together with the accelerometer in position 1 were mostly used. The gearshift pressure was usually set to 1.5 bar as the mean value of the available range.

The position of eClutch and mismatch speed were identified as the two most important variables with respect to the influence on NVH and gearshift quality. Figure 110 shows their approximate range used for tests of the dog clutch prototype.

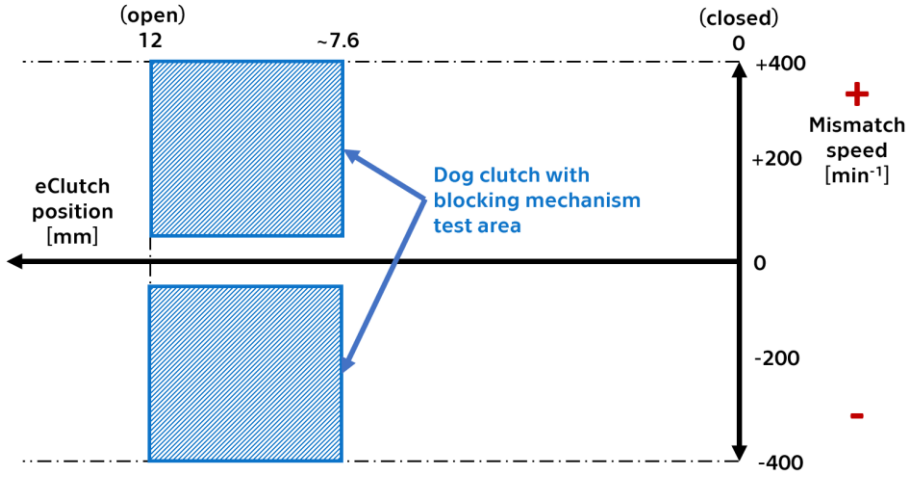

Figure 110: Input range of eClutch and mismatch speed for the dog clutch testing

5.4.5 Results

This chapter summarizes the NVH results of the dog clutch with blocking mechanism. All values in the plots represent an average of 5 measurements for the same initial gearshift conditions.

The first point to address is the hypothesis mentioned in Chapter 5.4.1. The idea was to improve gearshift quality by keeping eClutch (and the friction clutch, respectively) somewhere between the kiss point and residual friction phases during the gearshift – thanks to the torsional springs of the friction plate and minor slip of the clutch friction plate.

Unfortunately, the results suggest that there are no gearshift conditions that would show a significant improvement thanks to this method. Figure 111 shows a typical plot of vibrations (RMS) during gearshift depending on the eClutch position (kiss point area) and the mismatch speed. For constant mismatch speed, the RMS stays approximately constant or even slightly decreases as the eClutch closes. However, there is no significant drop for a particular eClutch position.

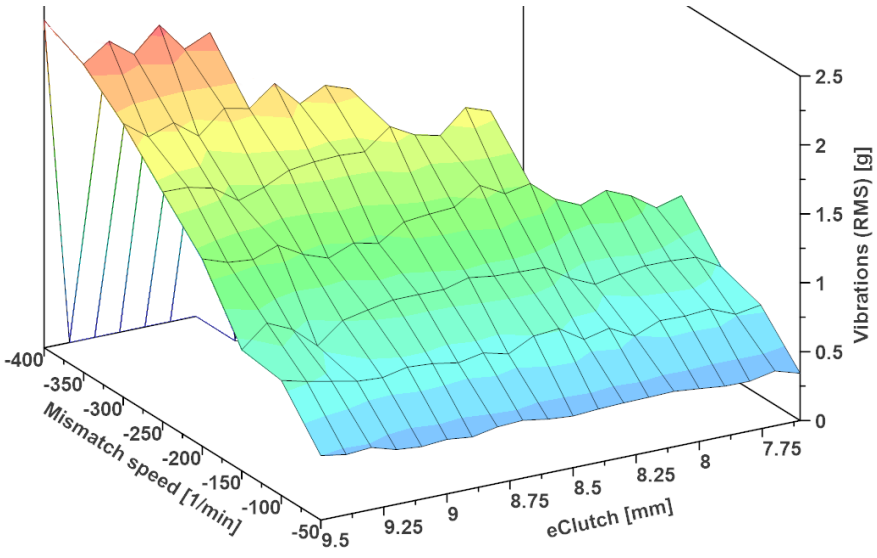

Figure 111: Vibrations (RMS) during gearshift of the dog clutch with blocking mechanism
Gearshift pressure 1 bar; 3rd gear; accelerometer position 1

Furthermore, the maximum torque caused by the impact increases significantly as the eClutch closes – see Figure 112. This is also the reason for limiting the maximum mismatch speed for lower eClutch position values (represented by the missing rear corner of the 3D plots). Therefore, conventional gearshifts with open eClutch would be further analyzed in comparison of vibrations and noise with the synchronizer.

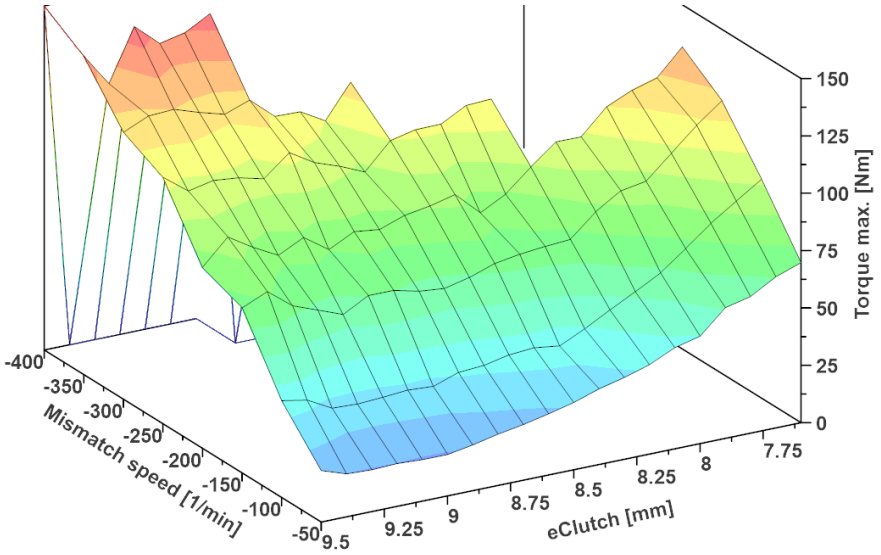

Figure 112: Torque max. during gearshift of the dog clutch with blocking mechanism
Gearshift pressure 1 bar; 3rd gear

The typical gearshift time plot is shown in Figure 113. The shortest time for the mismatch speed -100 min^{-1} is clearly visible – regardless of the eClutch position. This result is completely in line with expectations according to the design of the dogs. For lower mismatch speed, it sometimes takes a long time for the dogs to align against corresponding slots and engage. For higher mismatch speed, the engagement process is prolonged due to oscillations caused by the impact.

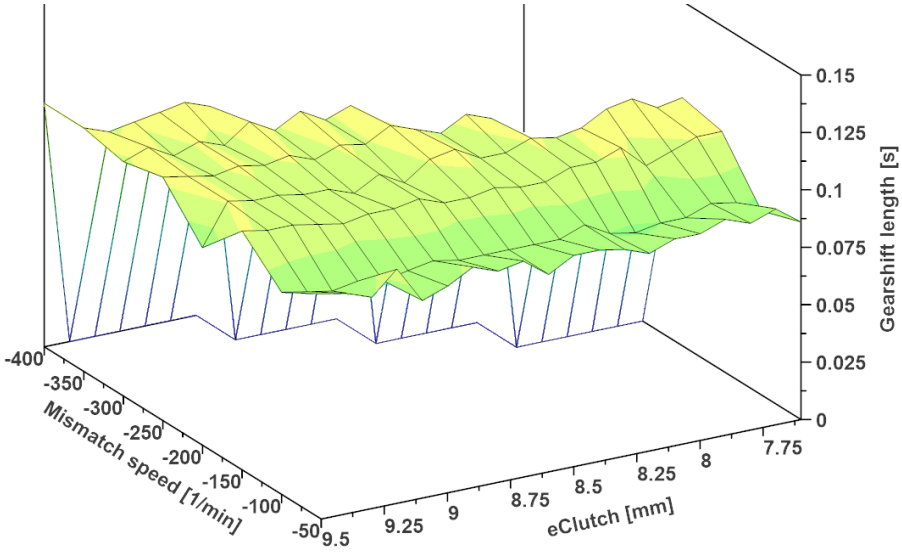

Figure 113: Gearshift time of the dog clutch with blocking mechanism
Gearshift pressure 1 bar; 3rd gear

The gearshifts of the synchronizer and the dog clutch with blocking mechanism are not directly comparable in terms of the gearshift comfort – the dog clutch is expected to perform worse due to the lack of synchronizing function. However, the synchronizer can serve as a benchmark to show the difference between the two mechanisms, especially in relation to the mismatch speed. As mentioned above, this comparison considers only conventional gearshifts with the friction clutch open, and the additional input moment of inertia disconnected.

An example of the dog clutch and synchronizer comparison is shown in Figure 114 and Figure 115. Vibrations (RMS) and maximum torque for 3rd and 4th gear are plotted.

The 4th gear was not tested at the mismatch speed 50 min^{-1}. The reason is that for such a low mismatch speed, the face-to-face contact was often too long and misrepresented the results. This does not apply for the 3rd gear. As explained in Chapter 5.3, negative mismatch speed is more suitable for the case where the output shaft RPM stay more constant than the input RPM, which drop faster due to friction losses when rotating freely. This is due to the torque equilibrium on the faces of the dogs. Therefore, the face angle used at the 3rd gear dogs is more suitable for general automotive gearbox application than the 4th gear dogs angle.

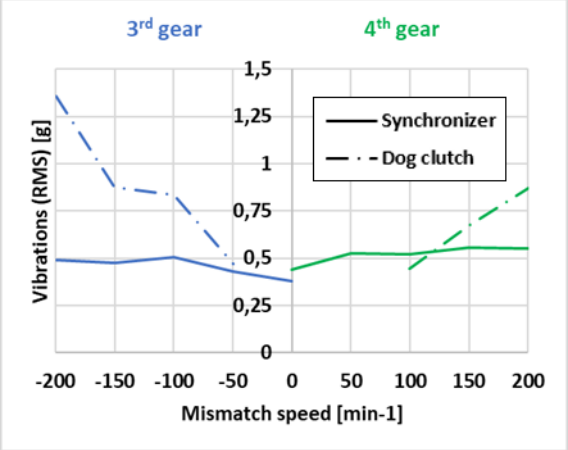

Figure 114: Comparison – vibrations (RMS)
Gearshift pressure 1,5 bar; accelerometer position 1

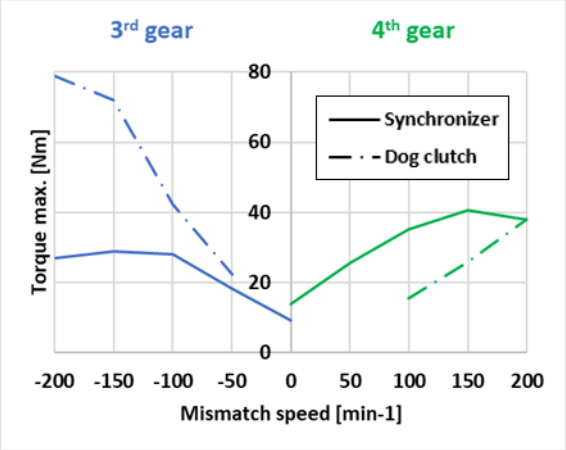

Figure 115: Comparison – maximum torque
Gearshift pressure 1,5 bar

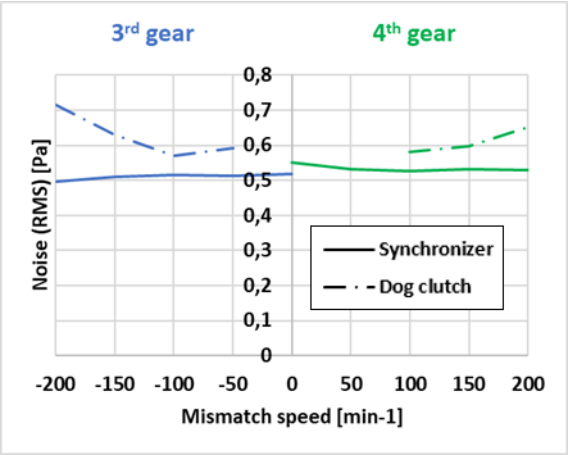

Figure 116: Comparison – noise (RMS)
Gearshift pressure 1,5 bar

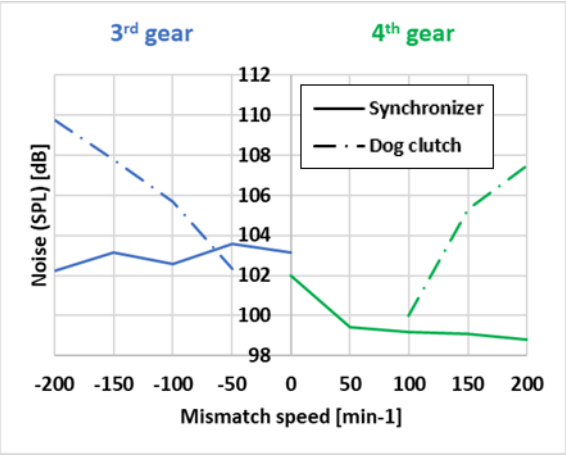

Figure 117: Comparison – noise (SPL)
Gearshift pressure 1,5 bar

At first sight, the curves for the dog clutch may seem more unsymmetric around the zero mismatch speed than might be expected. Their tendency is clearly different. However,

when elongated, they approximately meet at the vertical axis of zero mismatch speed (bearing in mind the limited precision of mismatch speed determination as described in Chapter 5.4.1). Overall, the increase in vibrations and torque is visible but still manageable, especially in the area of intended use around the mismatch speed ±100 min^{-1}.

Figure 116 and Figure 117 show a comparison of noise (RMS) and noise (SPL) for the same measurement of the 3rd and 4th gear. The tendencies of the noise correlate to the vibrations and torque. For the mismatch speed ±100 min^{-1}, there is very little increase compared to the synchronizer. This is a very promising result since low noise is the main quality parameter perceived by the driver and also one of the main target properties of the dog clutch with blocking mechanism.

Table 12 summarizes the comparison of the dog clutch with blocking mechanism and synchronizer – input gearshift parameters are listed in the table description. Most importantly, gears 1st to 4th were shifted and analyzed, which significantly affects the span of the results. Therefore, each cell contains a range of values representing the minimum and maximum recorded increase over the synchronizer for each evaluated metric. For some conditions, the dog clutch even managed to perform better than the synchronizer (marked green). The average performance of the dog clutch with blocking mechanism is expected to fall somewhere in this range.

Table 12: Increase based on the mismatch speed (dog clutch compared to synchronizer)
1st to 4th gear; gearshift pressure 1 to 2 bar; eClutch open; input shaft 1,500 min^{-1}

Mismatch speed	±100		±150		±200		min^{-1}
Vibrations (RMS)	**-20**	+50	0	+100	+50	+150	%
Maximum torque	**-50**	+50	**-25**	+100	0	+200	%
Noise (RMS)	+5	+20	+10	+30	+15	+50	%
Noise (SPL)	0	2	+2	+4	+6	+8	dB

Overall, these results indicate that the NVH and comfort of the dog clutch with blocking mechanism during gearshift should be manageable in real operation, especially for the intended mismatch speed of 100 min^{-1}, where its performance is comparable or slightly worse than the synchronizer. However, as mentioned previously, the measurement did not follow any standardized methodology, and the results should serve only as an approximate comparison.

Nevertheless, it would require a carefully designed shape of the gearshift dogs and precise external synchronization to match the performance of the synchronizer in a wider range of mismatch speed.

6 Consequences for Science and Industry

This chapter summarizes the outcomes of the thesis from the perspective of their benefits for scientific and industrial environment and their possible utilization.

6.1 Gearbox Test Bench with External Synchronization and Clutch Control

The modifications of the inertia test bench described in Chapter 5.1 greatly expanded the possibilities of testing and research of the gearshift mechanisms, gearboxes, and their behavior during gearshifts under wide range of operational conditions. External synchronization is now independent on the tested gearbox and easily controllable, the effect of the friction clutch on gearshift quality can be tested, the accuracy of the measured data was improved, NVH measurement and analysis is now possible, and sequences of gearshifts with variable inputs can be automatically tested.

All these improvements resulted in a new research project in cooperation with the industrial partner – ŠKODA AUTO, a.s. The research was focused on improving the gearshift quality of an automated hybrid transmission using innovative gearshift strategies. The experimental part of this research was carried out completely at the inertia test bench, and the results were presented at the end of the year 2022.

6.2 Gearshift Mechanism without Angular Backlash

The shape of the dogs of the dog clutch with blocking mechanism is absolutely unique in the field of passenger car gearboxes. Positive angle of the sides guarantees minimal angular backlash in the engaged state, approximately one to two orders of magnitude smaller compared to conventional dog clutches. This improves driving comfort due to much lower shocks when torque direction changes.

Even though this design can be found in specific applications (e.g., differential locks as mentioned in Chapter 2.1.3.1), so far it must have generally been accompanied by a strong detent system and correspondingly strong and heavy actuation system. This does not apply to the new dog clutch with blocking mechanism – the gearshift force required for its engagement and disengagement is comparable to other conventional gearshift mechanisms and approximately two orders of magnitude lower than the axial force it can withstand under full load in the engaged state.

Furthermore, the clutch can always be disengaged even under load. The gearshift force is independent of the load and stays constant under all conditions. This property would solve the issues and limitations of Porsche and AUDI EV gearbox described in Chapter 2.3.2 due to pre-tensioning of the gearshift clutch. Both companies were approached with an offer including a description of the solution of the problem using the dog clutch with blocking mechanism.

6.3 Gearshift Mechanism for Gearboxes with External Synchronization

The design was thoroughly tested and validated. The dog clutch with blocking mechanism is a reliable solution of gearshifts with external synchronization. Its potential is amplified by the fact that the industrial partner was actively participating in the whole development process. The deployment of this solution in the innovative gearbox described in Chapter 6.1 was considered and researched.

6.4 Tools for Design and Simulation of the Gearshift Mechanism

For those interested in the dog clutch with blocking mechanism, digital tools were prepared to make the consideration and implementation easier. The design program can serve for quick acquisition of approximate packaging dimensions for the intended use supplied by basic strength calculations. A data set of measured gearshifts is prepared to validate future simulation models for gearshift optimization.

7 Conclusion and Future Work

The use of externally synchronized dog clutches can contribute to optimizing the efficiency and costs of future electric and hybrid vehicles. Comfortable and fast gearshifts and noiseless torque transmission are crucial for the acceptance of such powertrain concepts.

The new patented dog clutch with blocking mechanism retains all the advantages of a conventional dog clutch and additionally provides the benefits of minimal angular backlash in the engaged state and the ability to disengage anytime, even under load. It is purely mechanical and compatible with standard gear selector mechanisms, including sequential shifting, without additional modifications.

The angular backlash is less than 0.1° and is ensured by the gearshift dogs with a positive angle of the sides. All operating positions of the clutch (engaged, neutral) are secured by one blocking ring only. Due to this unique ring, the clutch can withstand axial forces due to torque transmission, which are several orders of magnitude higher than the force needed for engagement and disengagement. Unwanted disengagement is prevented.

The design of the dog clutch was optimized for effective serial production using powder metallurgy. Comprehensive strength and service life calculations were performed, and a parametric design program was created. The blocking ring and gearshift dogs were detected as the most critical parts of the clutch and their calculations are described in detail in the thesis. The service life of the blocking ring was evaluated using both analytical approach and simulation to ensure that it can last for 700,000 cycles.

The clutch prototypes were manufactured and assembled into a standard mechanical five-speed gearbox. The possible axial saving for this gearbox when using dog clutches without axial backlash instead of the original synchronizers is up to 30 mm. The prototypes successfully passed the functionality and service life testing at the test bench. Furthermore, testing of the gearshift quality and behavior during torque transmission was carried out – the results and comparison with synchronizer are presented in the thesis.

To make testing possible, the gearbox test bench was thoroughly refined and upgraded. The modifications included especially the addition of external synchronization using an electric motor, friction clutch control, and a new control system for the entire test bench. Now it is possible to test and evaluate any gearshift mechanism assembled into a gearbox. The test bench is also suitable for the research of innovative gearshift strategies that utilize friction clutch control.

In the following steps of the research, it would be suitable to assemble a gearbox with the dog clutches with blocking mechanism into a vehicle and perform tests that focus on gearshift quality and comfort perceived by the driver. Especially the noise data would better reflect real operation than those measured at the test bench. This would help to define more precisely the mismatch speed limitations and accuracy requirements of the external synchronization.

Moreover, for further optimization of the gearshift comfort through the design of the dogs, completion of the multi-body simulation program would be beneficial. The model should

be expanded to include the entire powertrain representation with a focus on the torsional stiffnesses of the components. This would allow for the finding of a suitable geometry for a specific application.

Furthermore, the design of the dog clutch with blocking mechanism could be optimized for even greater axial space savings than that mentioned above for the manufactured prototypes. These were limited by the boundary conditions given by the requirement of easy assembly into the test gearbox. The reduction in axial length will be reflected mainly in the weight savings of the gearbox, including the shafts, the gearbox housing, or the gear selector mechanism. Shortening the axial length of the gearbox also reduces the bearing distance of the shafts, which favorably reduces shaft deflections and improves the quality of the gear mesh.

The design of the clutch and the text of the thesis focused on application in automotive gearboxes. It would be advisable to conduct a search for possible application in the drivetrains of commercial vehicles or heavy industrial vehicles and machines.

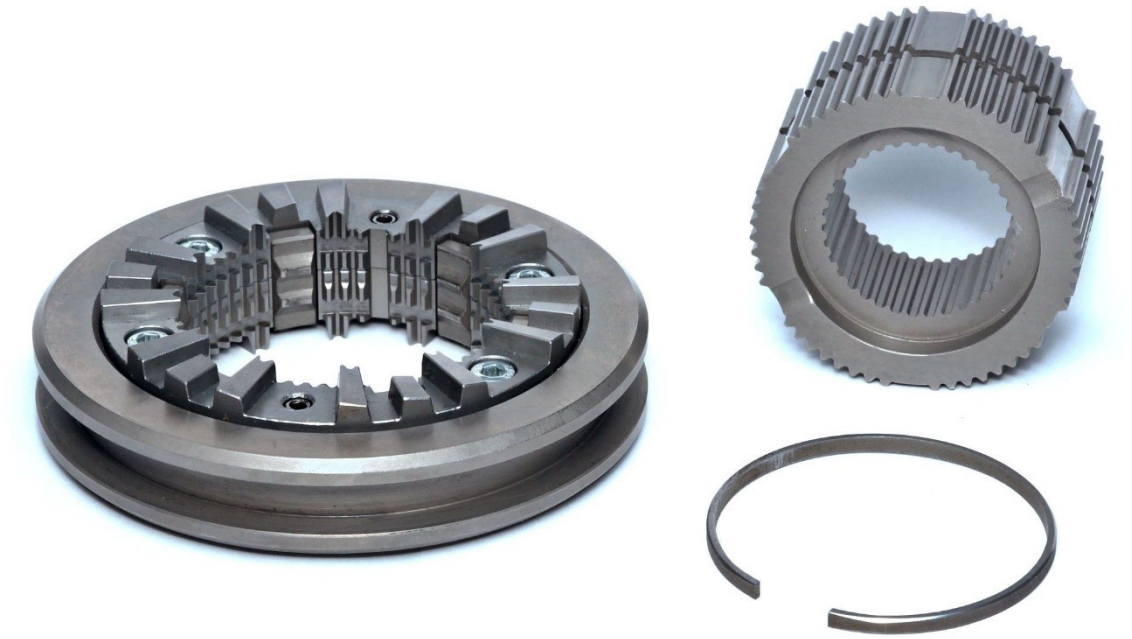

Figure 118: Promotional photo of the dog clutch with blocking mechanism prototype

8 Bibliography

8.1 Sources Cited in the Thesis

[1] **PILLOT, Christophe.** *The Rechargeable Battery Market and Main Trends 2020-2030.* Lyon: Avicenne Energy, 2022.

[2] **FUGEL, M., N. SCHOLZ and F. KÜCÜKAY.** *Anforderungen an die Getriebe in Hybridantrieben.* Düsseldorf: VDI-Verlag, 2006. ISBN 3-18-091943-4. ISSN 0083-5560.

[3] **FISCHER, Robert et al.** *The Automotive Transmission Book.* Switzerland: Springer International Publishing, 2015. ISBN 978-3-319-05262-5.

[4] **HOFMANN, Peter.** *Hybridfahrzeuge – Ein alternatives Antriebssystem für die Zukunft.* Switzerland: Springer, 2014. Second edition. ISBN: 978-3-7091-1780-4.

[5] **NAUNHEIMER, Harald et al.** *Automotive Transmissions: Fundamentals, Selection, Design and Application.* Berlin: Springer-Verlag, 2011. ISBN 978-3-642-16216-8.

[6] **HELLENBROICH, G. and V. ROSENBURG.** *FEV's new parallel hybrid transmission with single dry clutch and electric torque support.* [Online] 2009. [Cited: 25. March 2017] http://www.fev.com/fileadmin/user_upload/Media/TechnicalPublications/Transmission/IV_4_FEVs_new_parallel_hybrid_transmission_with_single_dry_clutch_and_electric_torque_support.pdf.

[7] **POLLAK, B. and U. KNÖDEL.** *How Much Transmission Is Needed for Electrification and Hybridization?* Düsseldorf: IRR Verlag, 2009. 8th International CTI Symposium Innovative Fahrzeug-Getriebe. Conference Paper.

[8] **MEHRGOU, Mehdi et al.** *NVH Aspects of Electric Drives-Integration of Electric Machine, Gearbox and Inverter.* 2018. SAE Technical Paper 2018-01-1556. doi:10.4271/2018-01-1556. ISSN 0148-7191.

[9] **MORGAN, Harald R.** *Improved Clutch Mechanism.* United Kingdom, 11. September 1930. Patent No. 334,649.

[10] **TŮMA, Jiří.** *Vehicle Gearbox Noise and Vibration.* New Delhi: John Wiley & Sons, Ltd., 2014. ISBN 978-1-118-35941-9.

[11] **FISCHER, Robert.** *Dedizierte Hybridantriebe (DHT) – eine neue Getriebekategorie.* Berlin: 14th International CTI Symposium, 2015.

[12] **HEISLER, Heinz.** *Advanced Vehicle Technology.* Oxford: Elsevier Ltd., 2002. Second edition. ISBN 0-7506-5131-8.

[13] **ACHTENOVÁ, Gabriela.** Převodová ústrojí motorových vozidel. *Synchronizační spojky a řadicí mechanismus.* Praha: České vysoké učení technické v Praze, 2014. Lecture slides.

[14] **SOCIN, R. J and, L. K. WALTERS.** *Manual transmission Synchronizers.* 1968. In: SAE 1968 Transactions-V77-A. doi:10.4271/680008. SAE Technical Paper 680008.

[15] **RAZZACKI, Syed T.** *Synchronizer Design: A Mathematical and Dimensional Treatise.* Detroit: SAE International, 2004. SAE Technical Paper 2004-01-1230. doi:10.4271/2004-01-1230. ISBN 0-7680-1319-4.

[16] **MURATA, Shigeo et al.** *Synchronizer and Shift System Optimization for Improved Manual Transmission Shiftability.* 1989. SAE paper 891998. In: SAE Transactions, 1989, Vol. 98, Section 6: JOURNAL OF PASSENGER CARS, pp. 1547-1558.

[17] **OLDTIMER MARKT.** *Porsche-Synchronisierung: Die Spitze.* [Online] 27. June 2012. https://www.oldtimer-markt.de/ratgeber/technik-lexikon/porsche-synchronisierung-die-spitze.

[18] **KERN, M., M. WUNDER and CH. STIFTER.** *Mehrganggetriebe mit Klauenkupplung für Hybridantriebe.* 2014. In: ATZ – Automobiltechnische Zeitschrift, Ed. 16, Vol. 5, pp. 44-47.

[19] **BÓKA, Gergely.** *Shifting Optimization of Face Dog Clutches in Heavy Duty Automated Mechanical Transmissions.* Budapest: Budapest University of Technology and Economics, 2011. Dissertation thesis.

[20] **KAPS TRANSMISSIONS.** *Full Sequentional Gearbox.* [Online] [Cited: 25. March 2017] http://eng.kaps-transmissions.com/products-si-full-sequential-gearbox.html.

[21] **ŠIMEK, Dušan.** *Spojka převodové skříně.* 2012. File No. MPT F 16 H 57/02. Patent No. 303222. 30. May 2022. Czech Office of Industrial Property.

[22] **ČERVENKA, Filip.** *Bezsynchronní převodovky motorových vozidel.* Brno: Vysoké učení technické v Brně, 2013. Bachelors thesis.

[23] **SUCHÝ, M. and L. PŮR.** *Dvoustranná řaditelná zubová spojka, zvláště pro převodová ústrojí.* File No. MPT B 60 K 17/02. Patent No. 148862. 15. May 1973.

[24] **ANDREEV, A. F., V. I. KABANAU and V. V. VANTSEVICH.** *Driveline Systems of Ground Vehicles.* Boca Raton: CRC Press, 2010. ISBN: 978-1-4398-1727-8.

[25] **DUAN, Chengwu.** *Analytical Study of a Dog Clutch in Automatic Transmission Application.* 2014. Int. J. Passeng. Cars-Mech. Syst. 7(3):2014, doi:10.4271/2014-01-1775.

[26] **BÓKA, Gergely et al.** Periodica Polytechnica. *Face Dog Clutch Engagement at Low Mismatch Speed.* 2010. Pages 29-35. doi:10.3311/pp.tr.2010-1.06.

[27] **ACHTENOVÁ, Gabriela.** *Gearbox automation – past and future.* Prague: Czech Technical University in Prague, Faculty of Mechanical Engineering, 2007.

[28] **SCOOTER CENTER.** *Gearbox (gear cogs only) - BGM PRO - Vespa PX.* [Online] [Cited: 27. April 2022.] https://www.scooter-center.com/.

[29] **PARKER, James.** *Honda RC212V: Transmission Patent | Drawing the Line.* [Online] 20. May 2011. https://www.motorcyclistonline.com/blogs/honda-rc212v-transmission-patent-drawing-line/.

[30] **MATSUMOTO, Shinya.** *Multistage transmission.* United States of America, 25. March 2010. Patent No. US 20100071492 A1.

[31] **MOORE, Adrian et al.** *Gearbox.* United States od America, 30. September 2008. Patent No. US 7428854 B2.

[32] **SAITOH, Tetsushi.** *Constant Mesh Type Transmission for Straddled Vehicle with Ratchet Mechanism.* United States of America, 2. August 2018. Patent No. US 2018/0216708 A1.

[33] **BRADFORD, Thomas E.** *Freewheeling Synchronizer.* United States of America, 14. July 2015. Patent No. US 9080621 B2.

[34] **IWATA, Takashi et al.** *Development of the Synchronizer-Less System for HV-AMT.* 2016. SAE Technical Paper 2016-01-1172. doi:10.4271/2016-01-1172.

[35] **MARTIN, Wesley William.** *Transmission system.* Great Britain, 5. May 2003. Patent No. WO 2004/099654 A1.

[36] **GARNIER, Nicolas.** *Device and method for sliding gear and clutch-type coupling for gearbox.* France, 17. September 2015. Patent No. WO 2015/136174 A1.

[37] **VOLKSWAGEN AG.** Manual Gearbox 02T. *Self-Study Programme 237.* Wolfsburg: VOLKSWAGEN AG, 2000.

[38] **MILLER, Pavel.** *Náhrada synchronizačních spojek.* Praha: České vysoké učení technické v Praze, 2007. Dipoma thesis.

[39] **EL MORSY, M., G. ACHTENOVÁ and J. PAKOSTA.** *Smoothness of Maybach dog clutch shift in the automotive gearbox.* Berlin: 17th International CTI Symposium, 2014.

[40] **SIKORA, Martin.** *Nestandardní mechanismus řazení.* Praha: České vysoké učení technické v Praze, 2011. Diploma thesis.

[41] **LIPČAK, Dmitrij.** *Úprava vnitřního mechanismu řazení pro následnou automatizaci.* Praha: České vysoké učení technické v Praze, 2016. Diploma thesis.

[42] **PAKOSTA, Jiří.** *Návrh náhrady synchronizační spojky.* Praha: České vysoké učení technické v Praze, 2016. Dissertation thesis.

[43] **JASNÝ, Michal.** *Návrh nového kompaktního řadicího mechanismu.* Praha: České vysoké učení technické v Praze, 2017. Diploma thesis.

[44] **BOUS, Marek.** *Design of shifting mechanism for automotive gearbox.* Prague: Czech Technical University in Prague, 2019. Diploma thesis.

[45] **FISCHER, Robert et al.** *Four are enough.* Berlin: 11th International CTI Symposium, 2011.

[46] **KÖNIG, Ruben.** *Gang- und Moduswechsel in elektrischen und hybrid-elektrischen Antriebssträngen mit aktiv synchronisierten Klauenkupplungen.* Darmstadt: TU Darmstadt, 2018. Dissertation thesis. ISBN 978-3-8440-6731-6. ISSN 2198-8536.

[47] **KÖNIG, Ruben.** *Gear Shifts and Mode Changes in Electric and Hybrid-Electric Powertrains with Dog Clutches.* Berlin: 17th International CTI Symposium, 2018. Young Drive Expert Award Poster.

[48] **CAUMON, P., D. GILBERTAS and H. MUKUNDAN.** *Renault New Plug-in Hybrid Drivetrain for B Segment Vehicle.* 2019. 28th Aachen Colloquium Automobile and Engine Technology. Conference paper.

[49] **YOLGA, M. and M. BACHINGER.** *Novel Shift Control without Clutch Slip in Hybrid Transmissions.* 2017. SAE Technical Paper 2017-01-1110. doi:10.4271/2017-01-1110.

[50] **KANĚRA, Jaroslav.** *Planetový dělič pro pohon hybridního vozidla.* Praha: České vysoké učení technické v Praze, 2018. Diploma thesis.

[51] **AUDI AG.** Audi e-tron GT (type F8). *Self-study programme SSP 684.* Ingolstadt: AUDI AG, 2021.

[52] **LAIRD, M. P. B. et al.** *Dog Clutches for Rapid Gear Changes in Automotive Gearboxes.* IMechE Proceedings of the Institution of Mechanical Engineers, 1st International Conference, Gearbox Noise and Vibrations, 1990, pp. 103-112.

[53] **GAERTNER, L. and M. EBENHOCH.** *The ZF Automatic Transmission 9HP48 Transmission System, Design and Mechanical Parts.* 2013. SAE Technical Paper 2013-01-1276. doi:10.4271/2013-01-1276.

[54] **SHIOTSU, Isamu et al.** *Development of High Efficiency Dog Clutch with One-Way Mechanism for Stepped Automatic Transmissions.* 2019. In: International Journal of Automotive Engineering, Vol. 10, No. 2, pp. 156-161.

[55] **WINKLER, Johannes.** *Dog shift systems – hype or real potential.* Berlin: 17th International CTI Symposium, 2018. Conference Paper.

[56] **ALZUWAYER, Bashar et al.** *An Advanced Automatic Transmission with Interlocking Dog Clutches: High-Fidelity Modeling, Simulation and Validation.* 2017. SAE Technical Paper 2017-01-1141. doi:10.4271/2017-01-1141.

[57] **ROTOR CLIP COMPANY, INC.** *Product Specifications.* [Online] 2015. [Cited: 25. March 2017] https://www.rotorclip.com/downloads/english_catflip/index.html.

[58] **HENKEL.** *LOCTITE® 638™.* [Online] June 2016. [Cited: 25. March 2017] Technical Data Sheet. http://tds.henkel.com/tds5/search.asp?t=638.

[59] **FLODIN, Anders.** *Evaluation of Wear in an Automotive Transmission using Powder Metal (PM) Gears.* Berlin: 17th International CTI Symposium, 2018.

[60] **HÖGANÄS AB.** *Höganäs Handbooks for Sintered Components.* [Online] 2013-2017. https://www.hoganas.com/en/services/handbooks/. ISBN 978-91-983614-0-7.

[61] **GERMAN, Randall M.** *A-Z of Powder Metallurgy.* Oxford: Elsevier, 2005. ISBN 9781856174299.

[62] **CHANG., I. and Y. ZHAO.** *Advances in Powder Metallurgy.* Sawston: Woodhead Publishing Ltd., 2013. ISBN 9780857094209.

[63] **HANKA, Dalibor.** *Design of the Shift Fork.* Prague: Czech Technical University in Prague, 2019. Diploma thesis.

[64] **ÚŘAD PRO NORMALIZACI A MĚŘENÍ.** ČSN 01 4686. *Pevnostní výpočet čelních a kuželových ozubených kol.* Praha: Vydavatelství Úřadu pro normalizaci a měření, 1989.

[65] **MORAVEC, Vladimír et al.** *Čelní ozubená kola v převodovkách automobilů.* Ostrava: VŠB-TU Ostrava, 2009. ISBN 978-80-7225-304-3.

[66] **DRASTÍK, František et al.** *Strojnické tabulky pro konstrukci i dílnu.* Ostrava: Montanex, 2002. ISBN 80-85780-95-X.

[67] **MORAVEC, Vladimír.** *Konstrukce strojů a zařízení II. – Čelní ozubená kola.* Ostrava: Montanex a.s., 2001. ISBN 80-7225-051-5.

[68] **RŮŽIČKA, M., M. HANKE and M. ROST.** *Dynamická pevnost a životnost.* Praha: České vysoké učení technické v Praze, 1987.

[69] **AMERICAN SOCIETY FOR TESTING AND MATERIALS.** ASTM E 1049-85. *Standard practices for cycle counting in fatigue analysis.* Philadelphia: ASTM, 1999. Annual Book of ASTM Standards, Vol. 03.01.

[70] **US DEPARTMENT OF DEFENSE.** MIL-HDBK-5J. *Metallic Materials and Elements for Aerospace Vehicle Structure.* 2003. Military Standardisation Handbook.

[71] **RŮŽIČKA, M. a PAPUGA, J.** New Concept of a Local Elastic Stress Approach for Fatigue Life Calculation. 2004.

[72] **DANG VAN, K. and I. V. PAPADOPOULOS.** *High-Cycle Metal Fatigue.* Udine: Springer-Verlag, 1999. ISBN 3-211-83144-4.

[73] **MAREŠ, Tomáš.** Bulletin of Applied Mechanics. *Circular Rings for Students.* Prague: Czech Technical University in Prague, Faculty of Mechanical Engineering, 2005.

[74] **VIJAY, Kumar et al.** *C-Shaped Synchronizer Spring-theoretical Analysis and Validation.* USA: SAE International, 2012. doi:10.4271/2012-01-2002. ISSN 0148-7191.

[75] **NOVOTNÝ, Pavel.** *Základy výpočtového modelování pístní skupiny.* Brno: Brno University of Technology, 2016. Lecture slides.

[76] **MACEK, K. and P. ZUNA.** *Nauka o materiálu.* Praha: Vydavatelství ČVUT, 1996. ISBN 80-01-01507-6.

[77] **PUŠKÁR, A. and S. GOLOVIN.** *Kumulácia poškodenia v procese únavy.* Bratislava: VEDA vydavatelstvo Slovenskej akadémie vied, 1981.

[78] **SHABANA, Ahmed A.** *Dynamics of Multibody Systems.* Fifth edition. London: Cambridge University Press, 2013. ISBN 9781108485647.

[79] **BULÍN, R. and M. HAJŽMAN.** Manufacturing Technology 14. *On the Modelling of Contact Forces in the Framework of Rigid Body Motion.* 2014, 136-141.

[80] **VLČEK, Jan.** *Optimalizace řazení soutěžního vozu.* Plzeň: Západočeská univerzita v Plzni, 2014. Dissertation thesis.

[81] **LEITNER, Josef.** *Transmission Simulation with ADAMS.* Rome: 15th International ADAMS User Conference, 2000.

[82] **PAKOSTA, J. and G. ACHTENOVÁ.** *Návrh setrvačníkového zkušebního stavu pro zkoušky řazení převodovek.* Liberec: Technická universita v Liberci, 2015. In: Mezinárodní konference kateder dopravních, manipulačních, stavebních a zemědělských strojů. ISBN 978-80-7494-196-2.

[83] **BRÜEL & KJÆR SOUND & VIBRATION MEASUREMENT A/S.** *Cubic Triaxial CCLD Accelerometer Types 4524, 4524-B and 4524-B-001.* September 2018. Product datasheet.

[84] **BRÜEL & KJÆR.** *Mechanical Vibration and Shock Measurements.* Copenhagen: Nærum, 1984. ISBN 87 87355 34 5.

[85] **PROSIG LTD.** Noise and Vibration Measurement Handbook. 2019. Sixth edition.

[86] **FRADEN, Jacob.** *Handbook of Modern Sensors.* Switzerland: Springer International Publishing AG, 2016. ISBN 978-3-319-19302-1.

[87] **BRANDT, Anders.** *Noise and Vibration Analysis: Signal Analysis and Experimental Procedures.* New Delhi: John Wiley & Sons, Ltd., 2011. ISBN: 978-0-470-74644-8.

8.2 Author's Patents and Publications Cited in the Thesis

[I.] **ČESKÉ VYSOKÉ UČENÍ TECHNICKÉ V PRAZE, FAKULTA STROJNÍ.** *Řadící spojka.* Inventors: JASNÝ, M., G. ACHTENOVÁ and J. PAKOSTA. File No. MPT F 16 D 11/10. Patent No. 307443. 22. August 2018. Czech Office of Industrial Property. Patent.

[II.] **TSCHECHISCHE TECHNISCHE UNIVERSITÄT IN PRAG, FAKULTÄT FÜR MASCHINENBAU.** *Schaltungskupplung.* Inventors: JASNÝ, M., G. ACHTENOVÁ and J. PAKOSTA. IPC-Class F16D 11/00 (2006.01). File No. DE: 20 2018 103 633.5. 26. June 2018. Deutsches Patent- und Markenamt. Utility model.

[III.] **ACHTENOVÁ, G., M. JASNÝ and J. PAKOSTA.** *Dog Clutch Without Circular Backlash.* Warrendale, PE: SAE International, 2018. Vol. 2018-April. doi:10.4271/2018-01-1299. SAE Technical Paper 2018-01-1299. ISSN 0148-7191.

[IV.] **JASNÝ, M., G. ACHTENOVÁ and J. PAKOSTA.** *Zubová spojka bez obvodové vůle.* Kurdějov: Vysoké učení technické v Brně, Fakulta strojního inženýrství, 2018. In. 44. Mezinárodní vědecká konference kateder dopravních, manipulačních, stavebních a zemědělských strojů. Conference paper. ISBN 978-80-214-5644-0.

[V.] **JASNÝ, M. and G. ACHTENOVÁ.** *Gearshift Clutches – New Design and Approach.* Roztoky u Prahy: Česká automobilová společnost, 2018. Autosympo 2018 – Emise, Kolokvium J. Božka. Invited unpublished scientific lecture.

[VI.] **JASNÝ, M., M. HAJŽMAN and G. ACHTENOVÁ.** *Multi-body Simulation of Dog Clutch Engagement.* Plzeň: Západočeská univerzita v Plzni, Fakulta strojní, 2019. In: 45. mezinárodní vědecká konference kateder dopravních, manipulačních, stavebních a zemědělských strojů. Conference paper. ISBN 978-80-261-0884-9.6.

[VII.] **JASNÝ, M. and J. PAKOSTA.** *External Synchronization for Gearbox Test Bench.* Žilina: VTS pri ŽU, 2020. In: Proceedings of the 46th International Scientific Conference of the Departments of Transports, Handling, Construction and Agricultural Machinery. Conference paper. ISBN 978-80-89276-60-8.7.

[VIII.] **JASNÝ, M., M. HAJŽMAN and R. BULÍN.** *Dog Clutch Without Circular Backlash – Design Optimization Using Multi-Body Simulation.* London: FISITA – International Federation of Automotive Engineering Societies, 2020. In FISITA Web Congress 2020 – Technical Papers. ISBN 978-1-9160259-1-2.

[IX.] **JASNÝ, M., G. ACHTENOVÁ and J. PAKOSTA.** *Zubová spojka bez obvodové vůle.* 2021. In: Strojárstvo. 2021, XXV(4), pp. 58-59. ISSN 1335-2938.

[X.] **JASNÝ, M., M. HAJŽMAN and R. BULÍN.** *Dog Clutch without Circular Backlash – Sequential Shifting Adaptation.* Praha: Česká zemědělská univerzita v Praze, Technická fakulta, 2021. In: 52. Mezinárodní vědecká konference českých a slovenských univerzit a institucí zaměřená na výzkumné a výukové metody spojené se spalovacími motory, alternativními pohony a dopravou. Conference paper. ISBN 978-80-213-3132-7.

[XI.] **JASNÝ, M. and J. PAKOSTA.** *Addition of Clutch to Gearbox Test Bench.* Liberec: Technická univerzita v Liberci, 2022. In: 48. Mezinárodní konference kateder dopravních, manipulačních, stavebních a zemědělských strojů. Conference paper. ISBN 978-80-7494-606-6.

8.3 Other Author's Publications

[XII.] **PAKOSTA, J., G. ACHTENOVÁ and M. JASNÝ.** *Stanoviště pro testování synchronizačních spojek.* Kurdějov: Vysoké učení technické v Brně, Fakulta strojního inženýrství, 2018. In: 44. Mezinárodní vědecká konference kateder dopravních, manipulačních, stavebních a zemědělských strojů. Conference paper. ISBN 978-80-214-5644-0.

[XIII.] **KANĚRA, J. and M. JASNÝ.** *Automation and Hybridization of a Manual Gearbox for Passenger Vehicles.* Roztoky u Prahy: Česká automobilová společnost, 2019. Autosympo 2019, Kolokvium J. Božka. Invited unpublished scientific lecture.

[XIV.] **JASNÝ, M and G. ACHTENOVÁ.** *Gearshift Parameter Map for P0 Hybrid Powertrain.* Roztoky u Prahy: Česká automobilová společnost, 2022. MobilitySympo 2022. Invited unpublished scientific lecture.

List of Figures

Figure 1: EV sales forecasts regarding to international organizations (2021 data) [1] 1
Figure 2: Sliding gear mechanism [5] 3
Figure 3: Borg-Warner single-cone synchronizer (ZF-B) [5] 4
Figure 4: The synchronizing process of Borg-Warner synchronizer [5] 5
Figure 5: Double-cone synchronizer (ZF-D) [5] 6
Figure 6: Porsche synchronizer [5], [17] 7
Figure 7: Six-speed sequential gearbox with dog clutches of a Subaru racing car [20] 8
Figure 8: Face dog clutch components [21] 9
Figure 9: Sliding dog used in Formula 1 gearbox [22] 9
Figure 10: Types of face dog dogs regarding to the side angle of the dogs 10
Figure 11: Engagement process of a face dog clutch with rectangular dogs [19] 10
Figure 12: Possible gearshift scenarios of sliding dog [26] 11
Figure 13: Prototype of a ball shift mechanism for a 3+R-speed automotive gearbox [27] ... 13
Figure 14: Internals of Vespa motorcycle gearbox with cruciform gearshift element [28] 13
Figure 15: Honda RC212V ratchet gearshift mechanism [30] 14
Figure 16: Dog clutch patented in 1930 – bolts C1 minimize the angular backlash [9] 15
Figure 17: Dog clutch patented in 1930 – bolts C3 minimize the angular backlash [9] 15
Figure 18: Dog clutch without backlash regarding to 1930 patent [9] 15
Figure 19: Aisin dog clutch – exploded view [34] 16
Figure 20: Negative side angle visible at the inner dogs of the sleeve [34] 16
Figure 21: Zeroshift – exploded view [20] 17
Figure 22: Zeroshift – detailed view of the gearshift process [35] 17
Figure 23: Dog clutch with rectangular dogs – exploded and detailed view [21] 18
Figure 24: Dog clutch with cradles – exploded view [36] 19
Figure 25: Section view of the 5-speed MQ200 gearbox [37] 20
Figure 26: Maybach dog clutch – exploded view [38] 21
Figure 27: Geometry of the Maybach dogs [38] 21

Figure 28: Sliding dog neutral blocking mechanism [38] 21
Figure 29: Dog clutch with cylindrical dogs [40] 22
Figure 30: Geometry of the cylindrical dogs [40] 23
Figure 31: Pakoshift – exploded view [41] 23
Figure 32: Engagement process of face dogs and blocking dogs [41] 24
Figure 33: Backlash during engagement [41] 25
Figure 34: Geometry of blocking dogs [41] 25
Figure 35: Example of Pakoshift behavior during gearshift [41] 25
Figure 36: Dog clutch with blocking mechanism – exploded view [43] 26
Figure 37: Dog clutch with blocking mechanism mounted into the MQ200 gearbox [43] 27
Figure 38: Axial force flow in the engaged state [43] 28
Figure 39: Bous clutch – exploded view [44] 29
Figure 40: DE-REX transmission diagram [47] 30
Figure 41: Electric power-on upshift at 50% drive pedal in the DE-REX vehicle [46] 30
Figure 42: Renault E-tech DHT – schematics of the powertrain [48] 31
Figure 43: Length comparison of mechanical gearbox (left) and E-tech DHT (right) [48] 31
Figure 44: Aisin HAMT – schematics of the powertrain [34] 31
Figure 45: AUDI/Porsche 2-speed EV transmission equipped with a dog clutch [51] 32
Figure 46: Pre-tensioned dog clutch in the 2-speed AUDI/Porsche EV transmission [51] 33
Figure 47: Scheme of ZF 9HP48 equipped with two dog clutches at positions A and F [53] 33
Figure 48: First manufactured prototype of the dog clutch with blocking mechanism 35
Figure 49: Heights of the blocking ring in the initial design 36
Figure 50: Three stages in a powder compaction cycle during die pressing [60] 37
Figure 51: Final dog clutch with blocking mechanism design 38
Figure 52: Cross-section of the final dog clutch design in neutral position 39
Figure 53: Gearshift process of the dog clutch with blocking mechanism 40
Figure 54: Dog clutch assembled between a pair of shifted gear wheels 41
Figure 55: Contact height on the side of the dog as shown by the design program 43
Figure 56: Trapezoidal dogs geometry design diagram [24] 43
Figure 57: Detail of the dogs at the sliding gear 44
Figure 58: Width and medium thickness of the dog 44
Figure 59: S-N curve (logarithmic scale) showing basic fatigue characteristics [65] 45
Figure 60: Schematics of bending an encastered beam 46
Figure 61: Load at the 3rd gear clutch during the drive cycle 47
Figure 62: Load spectrum of equivalent torques for 3rd gear 48
Figure 63: Schematics of Haibach hypothesis (logarithmic scale) [65] 49
Figure 64: Rounded edge of the Maybach dog after ca. 500 gearshifts [39] 51
Figure 65: Cross-section of blocking ring in engaged position 52
Figure 66: Diagram for calculating the bending stress in a quarter of a circular beam [73] 53
Figure 67: Piston ring gap [75] 54
Figure 68: Maximum stress at the blocking ring during simulated gearshift 55

Figure 69: Stress at the blocking ring during the simulated gearshift 56
Figure 70: Axial force flow in the engaged state 57
Figure 71: Force decomposition on the side of the dog during torque transmission 57
Figure 72: Angle β at the inner sleeve surface 58
Figure 73: Prototypes of the clutch for the 1st, 2nd, 3rd and 4th gear 59
Figure 74: Possible axial length saving for 1st gear dog clutch compared to synchronizer 60
Figure 75: Kinematical scheme of the created multi-body model 61
Figure 76: ADAMS multi-body model of the Input shaft with the dog clutch 61
Figure 77: Example of simulated gearshift results 62
Figure 78: Gear selector drum of Subaru Impreza R4 [44] 63
Figure 79: Gear selector drum with gearshift trajectories for individual gears [80] 63
Figure 80: Operating range of the additional spring 64
Figure 81: Dog clutch with additional disc springs – cut section 65
Figure 82: Comparison of disc springs stacking 65
Figure 83: Reaction force of the disc spring stack during deformation. 65
Figure 84: Comparison of engagement with nominal gearshift sleeve displ. (6.25 mm) 66
Figure 85: Initial state of the test bench with major measurement locations 68
Figure 86: Updated test bench with major measurement locations 69
Figure 87: Input assembly – section cut 70
Figure 88: External synchronization assembly at the test bench 71
Figure 89: Front panel of new control system 73
Figure 90: Assembly of the dog clutch with blocking mechanism 74
Figure 91: Gearshift force verification on the scales 75
Figure 92: Gearshift verification using video inspection probe 76
Figure 93: Gearbox with clutch prototypes at the inertia test bench 77
Figure 94: Shifting 3rd gear; mismatch speed 30 min^{-1} 77
Figure 95: Schematic of an open gearbox test bench 78
Figure 96: Gearbox with clutch prototypes at the dynamometer test bench 78
Figure 97: Ring after service life test 80
Figure 98: Ring after service life test – detail 80
Figure 99: Sliding gear after service life test 81
Figure 100: Sliding gear after service life test – detail 81
Figure 101: Hub after service life test 81
Figure 102: Hub after service life test – detail 81
Figure 103: Synchronizer ring after the removal of locking toothing 82
Figure 104: Engagement phases of the friction clutch regarding the position of eClutch 83
Figure 105: Available accelerometer positions 1 to 3 and orientations on the gearbox case 85
Figure 106: B&K accelerometer in position 2 85
Figure 107: Gearshift of variant 1 – synchronizers 87
Figure 108: Gearshift of variant 2 – blocking rings removed 88
Figure 109: Gearshift of variant 3 – dog clutch with blocking mechanism 89

Figure 110: Input range of eClutch and mismatch speed for the dog clutch testing.....90
Figure 111: Vibrations (RMS) during gearshift of the dog clutch with blocking mechanism...90
Figure 112: Torque max. during gearshift of the dog clutch with blocking mechanism.....91
Figure 113: Gearshift time of the dog clutch with blocking mechanism 91
Figure 114: Comparison – vibrations (RMS).....92
Figure 115: Comparison – maximum torque.....92
Figure 116: Comparison – noise (RMS) 92
Figure 117: Comparison – noise (SPL) 92
Figure 118: Promotional photo of the dog clutch with blocking mechanism prototype.....97

List of Tables

Table 1: Abbreviations used in the thesis.....VIII
Table 2: Latin nomenclature used In the thesis VIII
Table 3: Greek nomenclature used In the thesis VIII
Table 4: Dimensions of the dogs 44
Table 5: Basic material characteristics of 14140 steel 45
Table 6: Input parameters affecting the load of the dogs 45
Table 7: Static strength results.....46
Table 8: Moments of inertia of the input components.....50
Table 9: Blocking ring dimensions 52
Table 10: Basic material characteristics of blocking ring spring steel.....52
Table 11: Bending stress in the blocking ring according to different methodologies 56
Table 12: Increase based on the mismatch speed (dog clutch compared to synchronizer)....93

List of Attachments

1) Patent full text.
2) Animation of gearshift process and dog clutch functionality.
3) Videos of gearshift simulation in Abaqus.
4) Production drawings and 3D models of the dog clutch prototypes.
5) LabVIEW control program.
6) Videos of gearshift force and blocking functionality verification on the scales.
7) Videos of gearshifts recorded inside of the gearbox by the video inspection probe.
8) Video of service life testing.

List of Used Software

- Adobe Acrobat DC
- Autodesk AutoCAD
- Dassault Systèmes Abaqus
- GeoGebra
- MathWorks MATLAB
- Microsoft 365
- MSC ADAMS
- NI DIAdem
- NI LabVIEW
- NI MAX
- OpenShot Video Editor
- PTC Creo Parametric
- Zoner Photo Studio

Download Links

Thesis full text in PDF

Thesis attachments